

**Topological Defects And Phase Transition  
in the Early Universe**

by

David Richard Haws

A thesis presented for the Degree of Doctor of Philosophy  
of the University of London and for the Diploma of  
Membership of Imperial College.

Theoretical Particle Physics Group,  
Blackett Laboratory,  
Imperial College,  
London. SW7 2BZ

July 1988

## ABSTRACT

Several of the implications of the presence of topological defects in the early universe are considered.

Chapter one provides a brief introduction to the subject.

In chapter two a three dimensional model for the formation of monopoles connected by strings is presented. The length distribution of the strings has been found using a Monte Carlo simulation of the phase transition. The result is that long strings connecting monopoles are exponentially suppressed. The implications of the results for the monopole problem are discussed.

In chapter three the dynamics of, and radiation from, superconducting strings are studied. An approximate local action for a current carrying string is derived and some exact solutions to its equation of motion given. The radiation from one of these solutions is calculated exactly and is found to be finite (unlike the results of previous work). It is shown that loop shrinkage can lead to current loss rather than gain and the astrophysical implications of the work are discussed.

In chapter four the parameter space for theories of the type which produce bosonic strings is investigated. The tunnelling rate for current loss from the string is also estimated.

Chapter five presents the results of a study of the nature of phase transitions leading to the production of cosmic strings. The statistical properties of the strings are derived and the implications of the results for the cosmic string scenario of galaxy formation discussed.

## PREFACE

The work presented in this thesis was carried out in the Department of Physics, Imperial College, London between June 1986 and October 1987 and in the astrophysics group at Fermilab between October 1987 and May 1988 under the supervision of Professor T.W.B. Kibble and Doctor N.G. Turok, with the financial support of an SERC Research Studentship.

Unless otherwise stated, the work is original, and it has not been submitted before for a degree of this or any other university. Chapter 2 is based on work with E.Copeland, T.W.B Kibble, D.Mitchell and N.Turok published in Nucl. Phys. B298, 445(1988); Chapter 3 on work with E.Copeland, M.Hindmarsh and N.Turok to appear in Nucl. Phys. B in 1988; Chapter 4 on work with M.Hindmarsh and N.Turok to appear in Phys. Lett. B in 1988 and Chapter 5 on work with E.Copeland and R.Rivers released as a Fermilab preprint and submitted to Nucl. Phys. B.

I am deeply indebted to Prof. T.W.B.Kibble for his constant interest in, and help with, my research. I would like to thank all my friends at Fermilab and Imperial College and especially A.Albrecht, E.Copeland, T.Evans, M.Hindmarsh, H.Hodges, D.Levy, D.Mitchell and R.Rivers for the many useful discussions.

Finally, I would especially like to thank Helen Popham and Neil Turok; Neil for his guidance, friendship and the many ideas he has shared with me, Helen for the love and support she gave me during my two years of research and during the production of this thesis.

To my parents

-Thank You!-

## CONTENTS

	page
<u>Chapter 1: Introduction</u>	15
<u>Chapter 2: Monopoles-connected by strings and the monopole problem</u>	22
2.1 The causality arguments	24
2.2 The model	30
2.3 The Monte Carlo simulation	35
2.4 Discussion	43
<u>Chapter 3: Dynamics of and radiation from superconducting strings and springs</u>	48
3.1 The superconducting string action	51
3.2 Solutions of the equations, springs and their stability	62
3.3 Electromagnetic radiation from a kinky loop	71
3.4 The effect of non-local self interactions on a kink	80
3.5 Loop shrinkage leads to current loss	89
3.6 Discussion	91
3.7 Appendix	96
<u>Chapter 4: Superconducting strings or springs?</u>	100

	page
<u>Chapter 5: The effect of Topological defects on</u>	119
<u>phase transitions in the early universe</u>	
5.1 The partition function for a real scalar field theory	122
5.2 The partition function for a U(1) scalar gauge theory	133
5.3 The statistical properties of strings around the phase transition	140
5.4 Discussion	152
5.5 Appendix A	158
<u>References</u>	163



FIGURE CAPTIONS

	page
<u>Chapter 2</u>	
2.1 Our local evolution rule for $\Phi$ which demonstrates the falsity of the causality bounds. On the left is our tetrahedral approximation to the vacuum manifold. On a triangulated surface each triangle carries a net flux, 0, +1/4, or -1/4 (as shown). Each triangle is evolved as described in the text.	29
2.2a A diagram showing how the body centred cubic lattice was divided into tetrahedra. Each vertex of the tetrahedron is common to 24 others.	36
2.2b The tetrakaidekehedral lattice associated with the body centred cubic lattice. The points of the lattice correspond to the centres of the tetrahedra shown in figure 2a. For example, the point A could be associated with the centre of the tetrahedron shown in figure 2a.	37
2.3 A tetrahedron containing a monopole and for which 2 string segments and 1 antistring segment enter it. The computer decided at	39

random which string segment was connected to the monopole.

2.4 A tetrahedron for which 2 string segments and 2 antistring segments enter it. The computer decided at random which string segment was connected to which antistring segment. 39

2.5 A plot of  $\log(N_{\text{open}})$  vs.  $\lambda$  in units in which  $\xi = 1$  for a typical run using a lattice size of  $(80\sqrt{2})^3$  41

2.6 A plot of a) (squares)  $\log(N_{\text{closed}})$  vs.  $\lambda$  for a lattice size of  $(80\sqrt{2})^3$  42

b) (circles)  $\log(N_{\text{acc}})$  vs.  $\lambda$  where  $N_{\text{acc}}$  is defined by

$$N_{\text{acc}}(\lambda') = \sum_{\lambda=\lambda'}^{44} A \lambda^{-5/2} \exp(-\alpha\lambda)$$

$$\alpha = 0.087$$

$$A = 0.0345$$

2.7 The same as 5 except using a lattice size of  $(40\sqrt{2})^3$  44

	page
2.8 The same as 6 except using a lattice size of $(40\sqrt{2})^3$	45

Chapter 3.

3.1 The sphere on which the curves $\underline{a}'^2 = \underline{b}'^2 = \xi^2$ lie. The oscillating square solution has $\underline{a}'$ being two points, the north and south pole, and $\underline{b}'$ being any two antipodal points on the equator.	69
3.2 The $\underline{a}'$ , $\underline{b}'$ trajectories for a more general 'kinky' loop solution.	70
3.3 Diagram showing how the $\sigma$ - $\tau$ integral (3.3.3) is split up into different regions. The ++, +- etc. denote the direction of $\underline{a}'\underline{b}'$ .	74
3.4 A plot of the integrand of $\int d\Omega \frac{dP}{d\Omega}$ for small $j$ . The spike corresponds to $\Theta=\pi/2$ , $\phi=0$ .	79
3.5 A right moving $90^\circ$ kink moving with a velocity $v_k \sim 1$ on an otherwise straight string which carries a current $J$ . The straight string segments move with velocity $1/\sqrt{2}$ .	81

	page
3.6 A diagram showing the locus of the points of intersection of the backward light cone of two different points (A,B) on the string with the string (dotted lines). The labels A, A', B,... are explained in the text.	85
3.7 The locus of the points of intersection of the backward light cone of the point B with the string after we have performed our 'renormalisation'.	86
3.8 A plot of $\frac{dj}{dt}$ versus j	92

#### Chapter 4.

4.1 A diagram showing the region of parameter space in which a string will be superconducting.	105
4.2 The field profiles for a string with $\mu=1$ ; 'f' and 's' are $\phi$ and $\chi$ scaled by $\eta$ , while b is the azimuthal component of the gauge field scaled by $\eta$ and multiplied by $e\rho$ .	117

<u>Chapter 5.</u>	page
5.1 Diagrammatic representation of the lowest order mass correction. (Here dashed lines denote the heavy modes and the solid lines the light modes).	130
5.2 Feynman graphs for the tadpole corrections to the scalar mass. (Here again dashed lines denote the heavy modes, solid lines the light mode and wavy lines refer to heavy gauge field modes.)	135
5.3 Feynman graph for the tadpole correction to the gauge field mass.	136
5.4 The remaining Feynman graphs of $O(e^2)$ .	138
5.5 An example of the field configurations for a vortex solution at a temperature $T$ .	143

$$\xi = O(m_S^{-1}) \quad \lambda = O(m_V^{-1})$$

Table Captions

	Page
1.1: Possible topologically stable defects.	19
1.2: The mass per unit length of a string formed at an energy scale $\mu$ .	19
4.1: Some results from the numerical solutions of the string field equations.	112

CHAPTER 1: INTRODUCTION

## CHAPTER 1. Introduction

The hypothesis that the universe was once very hot has led to the development of a close relationship between particle physics and cosmology. Particle physics enables us to understand our hot past, whilst cosmology has proved a useful testing ground on which to try out new and speculative ideas in particle physics. Astrophysical observations have also been useful in placing strong restrictions on some of the parameters of the more standard physics models.

The standard cosmological model [1.1] begins shortly after the Planck time and is based on the premise of a homogeneous isotropic universe in a state of thermal equilibrium. Using nothing but well established physics, the model has been highly successful in providing a rationale for many hitherto unexplained observations. It has for example, led to a clear understanding of nucleosynthesis and in particular accounts for the relative primordial abundances of hydrogen, helium and lithium [1.2]. The theoretical predictions of these abundances are however, sensitive to the number of types of particles of various species. Astrophysical observations have therefore been able to constrain our standard particle physics model.

For many years the homogeneity of the 3K background radiation made it difficult to understand the formation of galaxies. Recently however, thanks to some of the more speculative ideas of particle physics two plausible



scenarios have been suggested - inflation [1.3] and cosmic strings [1.4].

I would like to explain in a little more detail some of the ideas leading to the second of these pictures. The idea that the electromagnetic and strong interactions are all united at extremely high energies in a grand unified theory [1.5] described by a simple group is an attractive hypothesis. At lower energies the unified symmetry has to be spontaneously broken by, for example, the Higgs-Kibble-Brout-Englert mechanism [1.5]. In this mechanism the symmetry is broken by the acquisition of a non-zero expectation value by a scalar field  $\Phi$ . The magnitude of this expectation value is constrained (at the tree level) to minimise the potential  $U(\Phi)$  of our theory. In general, this constraint is not enough to specify  $\langle\Phi\rangle$  uniquely. For example, if the grand unified group  $G$  is reduced to a subgroup  $H$ , the value of  $\langle\Phi\rangle$  is constrained only to lie on  $M=G/H$ , the minimum surface of  $U$  [1.7].

Spontaneous symmetry breaking at finite temperature has been studied by Weinberg and others [1.8]. Their work had very interesting implications for cosmology. They discovered that symmetry may be restored at high temperatures. At early times the universe was very hot and we therefore expect that the full symmetry was manifest. As the universe expanded and cooled a series of phase transitions would have occurred as the symmetry was successively broken.

$$G \rightarrow H \rightarrow \dots \rightarrow SU(3) \times SU(2) \times U(1) \rightarrow SU(3) \times U(1)_{em}$$
$$T_{ph} = T_G \sim 10^{16} \text{ GeV} \qquad T_{EW} = 10^3 \text{ GeV}$$

$T_{ph}$  is the temperature at which the phase transition occurred.

Let us consider the first of these phase transitions where  $G$  is broken to  $H$ . As  $T$  falls below  $T_G$ ,  $\Phi$  will tend to acquire a vacuum expectation value. But, as we have already seen, its direction is arbitrary, any point on  $M$  is equally probable. Different regions in space may choose different points. As the universe continues to expand and cool  $\langle \Phi \rangle$  will, for energetic reasons, tend to spatial uniformity, unless of course it is prevented from doing so by trapped singularities of some kind [1.9]. The possible types of singularities are determined by the topology of  $M$ . If, for example,  $M$  has disconnected pieces, domain walls may be formed. In the language of homotopy theory this corresponds to  $\pi_0(M)$  being non trivial. In table 1.1 some of the possible types of singular structure have been listed [1.9].

The presence of such singularities in the early universe would have interesting consequences.

Domain walls, because of their great mass, have tremendous gravitational effects [1.10]. So much so that we can be sure that they do not exist in our present day universe - at least within our field of view.

Table 1.1 Possible topologically stable defects.

Structure	Dimension of singularity	Non trivial homotopy group
domain walls	2	$\pi_0(M)$
strings	1	$\pi_1(M)$
monopoles	0	$\pi_2(M)$
texture	-	$\pi_3(M)$

Strings have less dramatic effects. A string formed at an energy scale  $\mu$  has mass per unit length [1.9]

$$M/L \sim \mu$$

In table 1.2 some typical values have been listed.

Table 1.2 The mass per unit length of a string formed at an energy scale  $\mu$ .

$\mu$	M/L (gm/cm)
$10^3$ GeV (electroweak scale)	$10^{-4}$
$10^{10}$ GeV	$10^{10}$
$10^{16}$ GeV (GUT scale)	$10^{22}$
$10^{19}$ GeV (Planck scale)	$10^{28}$

Those strings formed at energy scales close to the Planck scale have too large a mass to be consistent with

astrophysical observations [1.11]. The lensing angle [1.12] for such strings is  $O(\pi)$  and, as Witten [1.11] pointed out, the presence of a few of these strings would make our universe appear kaleidoscopic. There would be many images of the same object and gigantic jumps in the microwave background [1.13] etc.

Strings formed at GUT scales have intriguing astrophysical consequences. They might have provided the inhomogeneities around which galaxies form [1.14]. They also may have been observed as gravitational lenses for example (some recent candidate double images have been suggested by Cowie and Hu [1.15]).

Strings formed at much lower energy scales would have negligible gravitational effects. Does this mean they are of no interest to astrophysics? By no means! It is possible that in some particle physics models these strings behave like superconducting wires [1.16]. Several observational consequences of the presence of such strings have been suggested [1.17-1.19]. For example, they might produce high energy cosmic rays [1.18] or explain quasars [1.19]. In chapters 3 and 4 such strings are discussed in detail.

The third possible type of structure, monopoles, are particularly interesting in that essentially all grand unified theories would predict their formation [1.20]. Grand unified monopoles are massive, have large magnetic charges and may catalyse nucleon decay [1.21]. These properties have enabled stringent bounds to be placed on

their present day number density [1.22,1.23]. For example, let us assume that they catalyse proton decay. Not only is the cross-section large for processes such as



but the energy released is enormous. Only about  $10^{30}$  monopoles in the sun would account for the total solar luminosity. By looking at low luminosity stars such as white dwarfs and neutron stars, an upper limit on the number of monopoles in these objects can be determined. This can then be translated into a bound on the monopole flux [1.23]. The stringent bounds people have obtained has lead many people to believe that we have a 'monopole problem'; that is, too copious a number of monopoles would be formed in the early universe to be consistent with these bounds [1.24]. This belief is questioned in chapter 2.

The final type of defect listed in table 1.1, texture, is slightly different to the others in that no singularity is present. Instead the whole universe is characterized by a given element of  $\pi_3(M)$ . Texture can also have interesting consequences and anyone interested is referred to [1.25].

The final chapter of this thesis is devoted to a detailed study of the nature of the phase transition producing these topologically stable defects.

CHAPTER 2: MONOPOLES CONNECTED BY STRINGS  
AND THE MONOPOLE PROBLEM

## CHAPTER 2. Monopoles Connected by Strings and the 'Monopole Problem'

The aim of this chapter is to clarify the status of proposed 'causality' arguments limiting the annihilation rate of monopoles in the early universe.

Two years ago, Everett, Vachaspati and Vilenkin[2.4] (EVV) suggested that these arguments were wrong. They presented the results of a two-dimensional model of 'monopoles' connected by 'strings', from which they argued that the rate of annihilation of monopoles in their model would be faster than allowed by the causality arguments. There were however two shortcomings to their model; it was limited to two dimensions and it allowed monopoles of the same topological charge to be joined by strings. These monopoles therefore did not annihilate but formed stable, doubly charged monopoles.

In this chapter we present the results of a study of a three-dimensional model of monopoles connected by strings to antimonopoles. We shall show that an annihilation process exists that would result in the monopole density rapidly falling far below the minimum allowed by the causality arguments.

The model is described in section 2 and the results of a Monte Carlo simulation are presented in section 3.

Before turning to the model, however, we review in section 1 the causality arguments. Our conclusions are discussed in section 5.

Section 1. THE CAUSALITY ARGUMENTS

Two distinct types of causality arguments have been proposed, that we shall refer to as A and B respectively.

The first [2.4] is based on the observation that the direction of the Higgs field cannot become correlated on scales larger than the horizon size (unless the correlations were present initially). The argument asserts that as a result, following the production of monopoles at a phase transition, there must always be at least of order one monopole per horizon volume, i.e. the monopole number density  $n$  is always larger than

$$n_{\min} \sim t^{-3} .$$

The second argument B was proposed by Weinberg [2.2, 2.3]. He argued that magnetic charge density fluctuations, once formed, could not be erased on scales greater than the horizon size. This means that the monopole density could not decrease faster than a power law. For example, in a radiation dominated universe, one would have

$$n_{\min} \propto t^{-5/2} .$$



These arguments are very plausible, in part because the analogue of argument A in the case of domain walls is valid. If there is a broken discrete symmetry and the sign of the Higgs field in far separated regions is uncorrelated there must be domain walls. Each horizon volume  $\sim t^3$  must contain an area of wall of order  $t^2$ .

For a continuous symmetry, however, the situation is more subtle. Both arguments A and B are in fact wrong for the same reason: they neglect the cumulative effect that local processes can have.

To illustrate this let us start by recalling the arguments of EVV concerning their two dimensional model of broken U(1) symmetry. In this there are two complex Higgs fields  $\Phi$  and  $\chi$  with U(1) charges 2 and 1 respectively. In the first stage of symmetry breaking  $\Phi$  acquires a non-zero expectation value and the U(1) is broken down to  $Z_2$ ; monopoles are produced. In the second stage  $\chi$  also becomes non-zero. At the minimum of the potential  $\Phi = \chi^2$ , so there are two values of  $\chi$  for any given  $\Phi$ . The  $Z_2$  symmetry is broken and strings are produced joining the monopoles.

The subsequent evolution is governed by local dynamics. The tendency will be for the strings to shorten, eventually leading to annihilation or merger of the monopoles. It is entirely consistent with causality to assume that the evolution of the strings is highly

irreversible, so that strings shorten but almost never lengthen. As EVV showed, the strings are on average quite short, so that after a brief time they will disappear. In this final state there will be doubly-charged monopoles (around which the phase of  $\chi$  changes by  $2\pi$ ) but no remaining singly-charged monopoles.

It is interesting to examine the causality arguments to see where they break down. Consider how the phase of  $\Phi$  varies around a circle of radius much larger than the horizon size. Since the phase is uncorrelated, it appears to follow a random walk and one might therefore expect that the total phase change around the circle could be  $2\pi$  times any integer (up to some limit). In fact, because of the relation  $\Phi = \chi^2$ , as long as  $\chi$  is in its vacuum everywhere (i.e. there are no strings), it can only be any even integer. This has been achieved by entirely local processes, and without introducing any correlations between the phases in far separated regions.

Even without explicitly introducing  $\chi$  it is quite possible to define a local evolutionary rule that will achieve this result for the phase of  $\Phi$ . Suppose for example that following EVV (see also [2.5]) we approximate  $U(1)$  by  $Z_3$  and discretize  $R^2$  into a planar lattice. At each lattice point the phase of  $\Phi$  is represented by 0, 1 or 2, initially chosen at random. (A smooth interpolation between the points is assumed, following the shortest available path.)

Consider the phase change around a large loop and the effect of the following local rule. At each intervening site, whenever the two neighbours have different phases, change  $\phi$  so that its phase is different from both. This ensures that the total phase change must be even. (This rule is roughly speaking, the effect of requiring that  $\phi = \chi^2$ , since if the phase of  $\chi$  varies by  $2\pi/3$  that of  $\phi$  must vary by  $4\pi/3$ .)

This example should make us cautious about accepting the causality arguments, but in three dimensions it is perhaps harder to see how they could fail. Consider for example an SU(2) model with a triplet Higgs field  $\phi$  that breaks the symmetry to U(1) and induces monopoles. The topological charge within some large sphere can be expressed in the usual way as a surface integral in terms of  $\phi$ . Initially the direction of  $\phi$  is random and the topological charge will in general be non-zero.

As in the previous example, let us also introduce a doublet Higgs field  $\chi$  that breaks the remaining U(1) completely, joining the monopoles with strings.

Once again, if the field  $\chi$  evolves to its vacuum everywhere by the strings shrinking and disappearing there can be no monopoles. If we parameterise a sphere  $S^2$  in space as a disc with boundary identified then the group element producing the  $\chi$ ,  $\phi$  configuration on the sphere provides a loop in the U(1) little group of  $\phi$  on the

boundary of the disc. The  $\Phi$  configuration has non-zero topological charge if and only if the  $U(1)$  group element is non-contractable, which means that the  $\chi$  field is not in vacuo everywhere.

In this case we can also invent local dynamics for the  $\Phi$  field which will rapidly reduce the net topological charge to zero in any closed surface.

On a triangulated surface (such as that used in our simulation described in the next section) each triangle has a value of  $\Phi$  at each of its vertices. If these are all different then the triangle can be mapped onto a tetrahedral approximation to the vacuum manifold  $S^2$ . The magnetic flux through a triangle is  $+1/4$  if the orientation matches that in the vacuum manifold and  $-1/4$  otherwise. Then in any closed surface the net flux must be an integer, and we must have  $4m$  triangles with  $+1/4$  flux, and  $4n$  with  $-1/4$ . The net charge (number of monopoles minus antimonopoles) is  $m-n$ .

The local rule for  $\Phi$  is to draw an extra point inside each triangle and assign a new value of  $\Phi$  there. Thus each triangle becomes 3 triangles (see figure 2.1). If  $\Phi$  takes 3 different values on the original vertices (i.e. there is a net flux  $f$ ) assign the fourth value at the new point. Now the net flux is changed to  $-3f$ , in effect we have pulled a monopole through the triangle. If  $\Phi$  does not take 3 different values on the original vertices then it makes no difference how one assigns the new point. Now our local

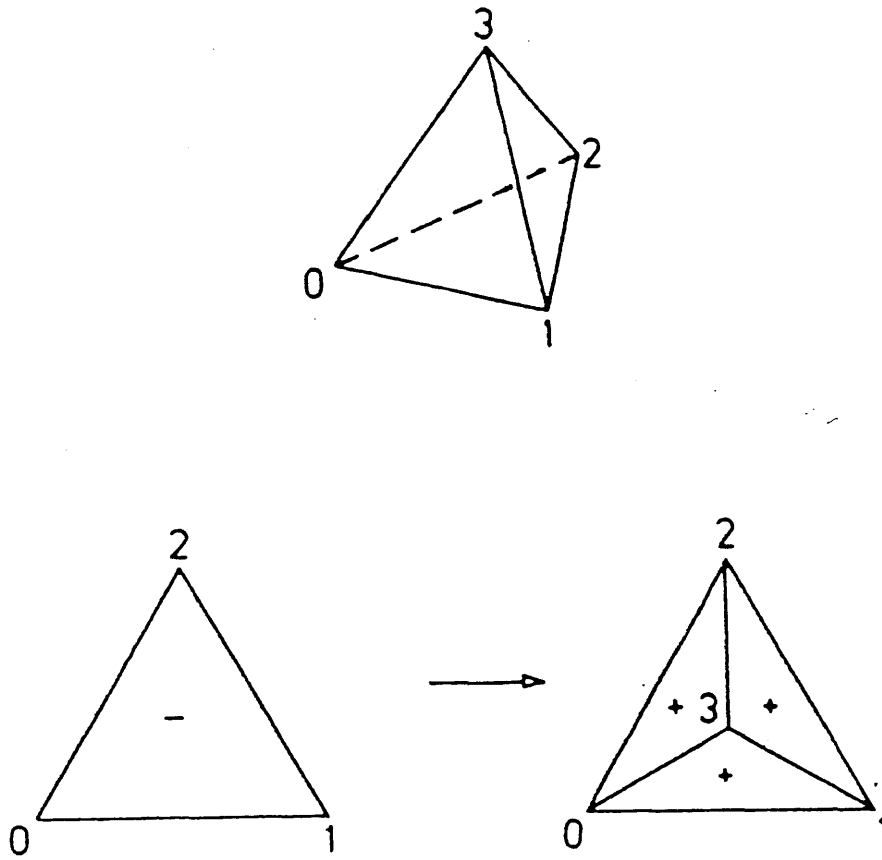


Figure 2.1 Our local evolution rule for  $\Phi$  which demonstrates the falsity of the causality bounds. On the left is our tetrahedral approximation to the vacuum manifold. On a triangulated surface each triangle carries a net flux, 0,  $+\frac{1}{4}$ , or  $-\frac{1}{4}$  (as shown). Each triangle is evolved as described in the text.

rule is to make such a change in a probabilistic way with a probability of  $1/4$  on each face with flux through it. Our  $4m$  triangles with  $+1/4$  flux become  $3m$  with  $+1/4$  and  $3m$  with  $-1/4$  flux. The net charge is zero. Due to randomness in our choice at each face we expect a net error (or net charge) after one timestep of  $\sqrt{(n+m)}$ . Nevertheless in one timestep we have decreased the net charge far below the causality bound (under which we could at most halve the net flux.)

Note that both our local evolution rules can be followed simultaneously in two dimensions (three dimensions) on all links (faces) with the same result for any closed loop (surface) in space.

Just because it is theoretically possible for local processes to reduce the total charge to zero it does not mean it actually happens. The dynamics above are certainly rather strange and only a detailed study of realistic dynamics can answer this question. In this chapter we try to answer it, so far as one model of monopoles connected by strings is concerned.

## Section 2. THE MODEL

We now turn to our specific model, which is based on a system possessing an  $SU(2)$  symmetry that undergoes two symmetry breaking phase transitions at roughly the same temperature. At the first,  $SU(2)$  is broken to  $U(1)$ . In this process 't Hooft-Polyakov monopoles [2.6] are formed

[2.7]. At the second transition the U(1) symmetry is completely broken. This causes the magnetic field to be squeezed into flux tubes (strings) connecting monopoles with antimonopoles [2.8]. Also closed and infinite strings are formed.

The strings connecting monopoles with antimonopoles, being regions of false vacuum, tend to contract to minimise their energy. The monopole-antimonopole pairs are pulled together and then annihilate into the vacuum. The life-time of these pairs will be roughly the time it takes to dissipate the energy of the string [2.9, 2.10, 2.11]. The monopole number density at any time after the phase transition can thus be related to the initial distribution of string lengths.

The above sequence of symmetry breakings can be achieved using two Higgs fields,  $\Phi$  and  $\Psi$ , which transform according to the 3 and 2 of SU(2) respectively. It is convenient to regard  $\Phi$  as a 2x2 traceless hermitian matrix;  $\Psi$  is a two-component doublet.

If the symmetry group is SU(2), the potential must contain interaction terms between the  $\Phi$  and  $\Psi$  fields such as

$$\Psi^\dagger \Phi \Psi, \Psi^\dagger \Phi^2 \Psi, \Psi^\dagger \Psi \text{tr}(\Phi^2) .$$

By suitable normalisation of the  $\Phi$  and  $\Psi$  fields the

potential can be chosen so that at its minimum

$$\Phi^2 = 1, \Psi^\dagger \Psi = 1, \Phi \Psi = \Psi$$

After the first transition,  $\Phi$  acquires a nonzero expectation value and the symmetry is broken to  $U(1)$ . After the second,  $\Psi$  also acquires a nonzero expectation value and the symmetry is reduced to  $\{1\}$ . The standard vacuum solution may be chosen to be

$$\Phi_0 = \sigma_3, \quad \Psi_0 = \begin{pmatrix} 1 \\ 0 \end{pmatrix}$$

A monopole at the origin with a string along the  $-z$  axis is represented by

$$\Phi = \hat{\underline{r}} \cdot \underline{\sigma} = \begin{pmatrix} \cos \theta & \sin \theta e^{-i\phi} \\ \sin \theta e^{i\phi} & -\cos \theta \end{pmatrix}$$

$$\Psi = \begin{pmatrix} \cos \frac{1}{2} \theta \\ \sin \frac{1}{2} \theta e^{i\phi} \end{pmatrix}$$

To perform the Monte Carlo simulation it is convenient to approximate the space of  $\Phi$  ( $S^2$ ) by four points forming a tetrahedron[3.12], say

$$\begin{aligned} \Phi_0 &= \sigma_3 \\ \Phi_1 &= -1/3 \sigma_3 + 2\sqrt{2}/3 \sigma_1 \\ \Phi_2 &= -1/3 \sigma_3 - \sqrt{2}/3 \sigma_1 + \sqrt{(2/3)} \sigma_2 \\ \Phi_3 &= -1/3 \sigma_3 - \sqrt{2}/3 \sigma_1 - \sqrt{(2/3)} \sigma_2 \end{aligned}$$



Having chosen a discrete approximation for the manifold  $S^2$  we need to know what phase the  $\Psi$  field picks up on transforming it from a point  $(\Phi_i)$  to another  $(\Phi_j)$ . The smallest angle rotations taking one  $\Phi_k$  into another are :

$$U_{10} = 1/\sqrt{3} - i \sqrt{2/3} \sigma_2$$

$$U_{20} = 1/\sqrt{3} + i 1/\sqrt{2} \sigma_1 + i 1/\sqrt{6} \sigma_2$$

$$U_{30} = 1/\sqrt{3} - i 1/\sqrt{2} \sigma_1 + i 1/\sqrt{6} \sigma_2$$

$$U_{32} = 1/\sqrt{3} + i \sqrt{2/3} \sigma_1 - i 2/3 \sigma_3$$

$$U_{13} = 1/\sqrt{3} - i 1/(3\sqrt{2}) \sigma_1 + i 1/\sqrt{6} \sigma_2 - i 2/3 \sigma_3$$

$$U_{21} = 1/\sqrt{3} - i 1/(3\sqrt{2}) \sigma_1 - i 1/\sqrt{6} \sigma_2 - i 2/3 \sigma_3$$

for example,  $U_{10} \Phi_0 U_{10}^+ = \Phi_1$  .

We can now choose standard phases at each of the  $\Phi_j$  values

$$\Psi_0 = \begin{pmatrix} 1 \\ 0 \end{pmatrix}$$

$$\Psi_1 = U_{10} \Psi_0 = \begin{pmatrix} 1/\sqrt{3} \\ \sqrt{2/3} \end{pmatrix}$$

$$\Psi_2 = U_{20} \Psi_0 = \begin{pmatrix} 1/\sqrt{3} \\ i/\sqrt{2} - 1/\sqrt{6} \end{pmatrix}$$

$$\Psi_3 = U_{30} \Psi_0 = \begin{pmatrix} 1/\sqrt{3} \\ -i/\sqrt{2} - 1/\sqrt{6} \end{pmatrix}$$

A general value of  $\Psi$  may be specified by its phase  $\alpha$  relative to these standards. For example if  $\Phi = \Phi_q$ , then  $\Psi = \Psi_q e^{i\alpha}$ . Having allotted standard phases we can consider transforming  $\Psi_2$  by the rotation that carries  $\Phi_2$

to  $\Phi_3$ . The result is

$$U_{32} \Psi_2 = -i \Psi_3$$

similarly

$$U_{13} \Psi_3 = -i \Psi_1, \quad U_{21} \Psi_1 = -i \Psi_2 \quad .$$

We see that if we wish to compare the phases of the  $\Psi$  field at two neighbouring points where  $\Phi$  has the values  $\Phi_i$  and  $\Phi_j$  we must include a phase correction factor  $A_{ij}$ . As an example, suppose that at the first point

$$\Phi = \Phi_2, \quad \Psi = \Psi_2 e^{i\alpha_2}$$

Applying to these fields the transformation  $U_{32}$  we arrive at

$$\Phi = \Phi_3, \quad \Psi = -i \Psi_2 e^{i\alpha_2}$$

which is to be compared with the field at the second point, say

$$\Phi = \Phi_3, \quad \Psi = \Psi_3 e^{i\alpha_3}$$

The difference in phase is thus  $\alpha_2 - \alpha_3 - \pi/2$ . In general it is

$$\Delta\alpha = \alpha_i - \alpha_j + A_{ij}$$

where

$$A = \begin{pmatrix} 0 & 0 & 0 & 0 \\ 0 & 0 & -\pi/2 & \pi/2 \\ 0 & \pi/2 & 0 & -\pi/2 \\ 0 & -\pi/2 & \pi/2 & 0 \end{pmatrix}$$

### Section 3. THE MONTE CARLO SIMULATION

We considered an  $n \times n \times n$  body centered cubic lattice. At each vertex of this lattice one of the four values of  $\Phi$ , namely  $\Phi_0, \Phi_1, \Phi_2, \Phi_3$  was chosen at random along with a value of  $\alpha$  between  $-\pi$  and  $\pi$ . The lattice may be regarded as made up of irregular tetrahedral cells, the vertices of which are the lattice points (Figure 2.2a). The centres of the tetrahedra form a regular lattice (the tetrakaidekahedral lattice, Figure 2.2b). A monopole was considered to lie at the centre of a given tetrahedron if the four vertices had values for the  $\Phi$  field of  $\Phi_0, \Phi_1, \Phi_2, \Phi_3$  or an even permutation thereof (an antimonopole if an odd permutation). A string was considered to pass through a face of the tetrahedron if the net phase change was less than  $-\pi$  and an antistring if it was greater than  $\pi$ .

For a tetrahedron containing a monopole/antimonopole, there were two possibilities in our simulation; they may have been a single string/antistring entering it or two strings/antistrings and one antistring/string. This latter

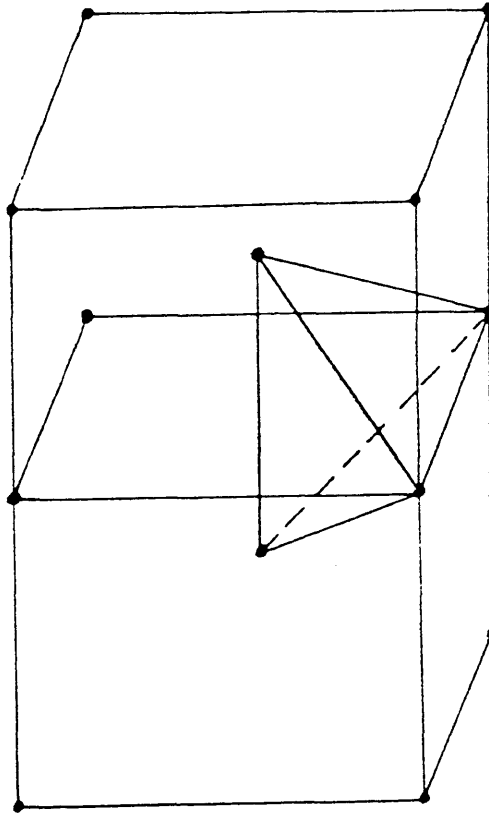


Figure 2.2a A diagram showing how the body centered cubic lattice was divided into tetrahedra. Each vertex of the tetrahedron is common to 24 others.

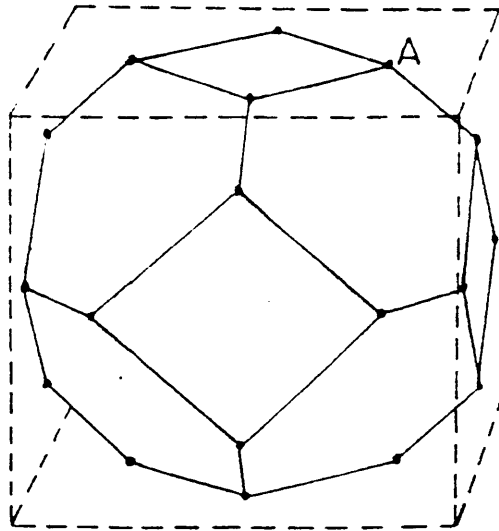


Figure 2.2b The tetrakaidecahedral lattice associated with the body-centered cubic lattice. The points of the lattice correspond to the centres of the tetrahedra shown in figure 2.2a. For example, the point A could be associated with the centre of the tetrahedron shown in figure 2.2a.

case represents a string entering the tetrahedron through one face and leaving it through a second, in addition to a string segment terminating on the monopole. Similarly, it is easy to see that for tetrahedra which do not contain a monopole or an antimonopole, our algorithm always gives an equal number of string and antistring segments entering it. The monopoles were taken to lie at the centres of the tetrahedra and the strings along lines joining them (all of which are of equal length), namely along the edges of the tetrakaidekahedra. From the above considerations it follows that string segments either formed closed loops or start or end on monopoles or antimonopoles. Periodic boundary conditions were used to prevent strings leaving the lattice.

Having determined the positions of the monopoles and antimonopoles the computer followed the string leaving a monopole, determining its length, until it terminated on an antimonopole. This was done for all the monopoles before proceeding to follow the string segments in loops evaluating their lengths. In the case of configurations like that in Figure 2.3 the computer decided at random which string/antistring segment was connected to the monopole/antimonopole. Similarly, for configurations like the one shown in Figure 2.4, the computer decided at random which pair of string and antistring segments were connected with each other.

The largest sized body centered cubic lattice we used was  $(40)^3$ . In a typical run we found the number of

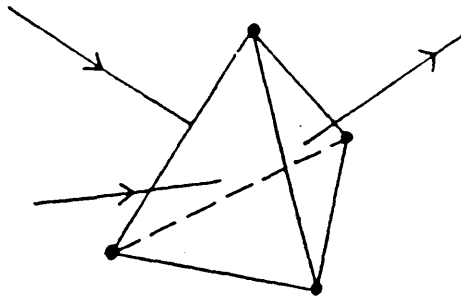


Figure 2.3 A tetrahedron containing a monopole and for which 2 string segments and 1 antistring segment enter it. The computer decided at random which string segment was connected to the monopole.

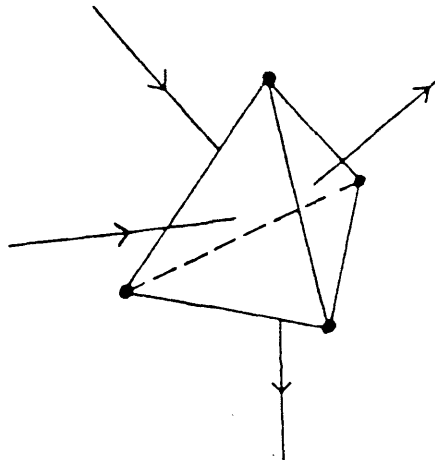


Figure 2.4 A tetrahedron for which 2 string segments and 2 antistring segments enter it. The computer decided at random which string segment was connected to which antistring segment.

monopole/antimonopole pairs produced was 35930. This is consistent with our algorithm which gives a probability of  $3/64$  of finding a monopole in any given tetrahedron. The number of string segments produced was 419216 which is again consistent with our algorithm (the mean probability of a string passing through a given face of a tetrahedron is  $35/128$ ) The percentage of string segments in loops was approximately 9%. In units in which the correlation length  $\xi$  of the Higgs field at the phase transition is taken to be one, the length of the largest open string segment was 141 and that of the largest loop was 41 (note in these units the lattice size would be  $(40 \times 2\sqrt{2})^3$ ). Let  $n_{\text{open}}(\lambda)$  and  $n_{\text{closed}}(\lambda)$  be the number density of open and closed strings of length greater than or equal to  $\lambda$  respectively. In Figures 2.5 and 2.6 we show plots of  $\ln[n(\lambda)]$  versus  $\lambda$ . Figure 2.5 is consistent with

$$n_{\text{open}}(\lambda) = n_0 \exp(-\lambda\beta)$$

and Figure 2.6 is consistent with

$$n_{\text{closed}}(\lambda) = A \int_{\lambda}^{\infty} d\lambda' \lambda'^{-5/2} \exp(-\zeta\lambda')$$

in agreement with the theoretical predictions of Mitchell and Turok and Copeland, Haws and Rivers [2.1, 2.14]. A fit to the curve of Figure 2.5 gave

$$\begin{aligned} \beta &= 7.4 \pm 0.6 \times 10^{-2} \\ n_0 &= 1.9 \pm 0.5 \times 10^{-2} \end{aligned}$$



Figure 2.5 A plot of  $\log(N_{\text{open}})$  vs.  $\lambda$  in units in which  $\xi = 1$  for a typical run using a lattice size of  $(80/2)^3$

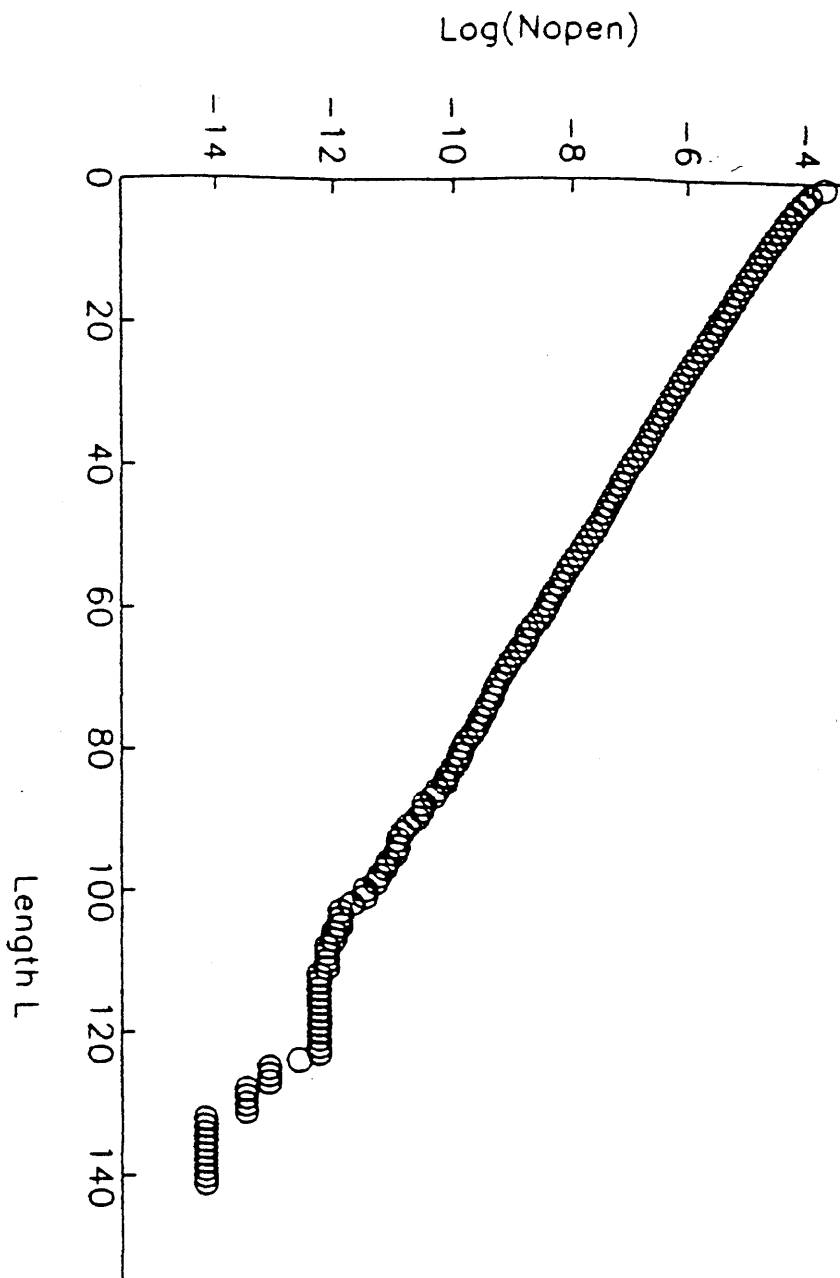


Figure 2.6 A plot of

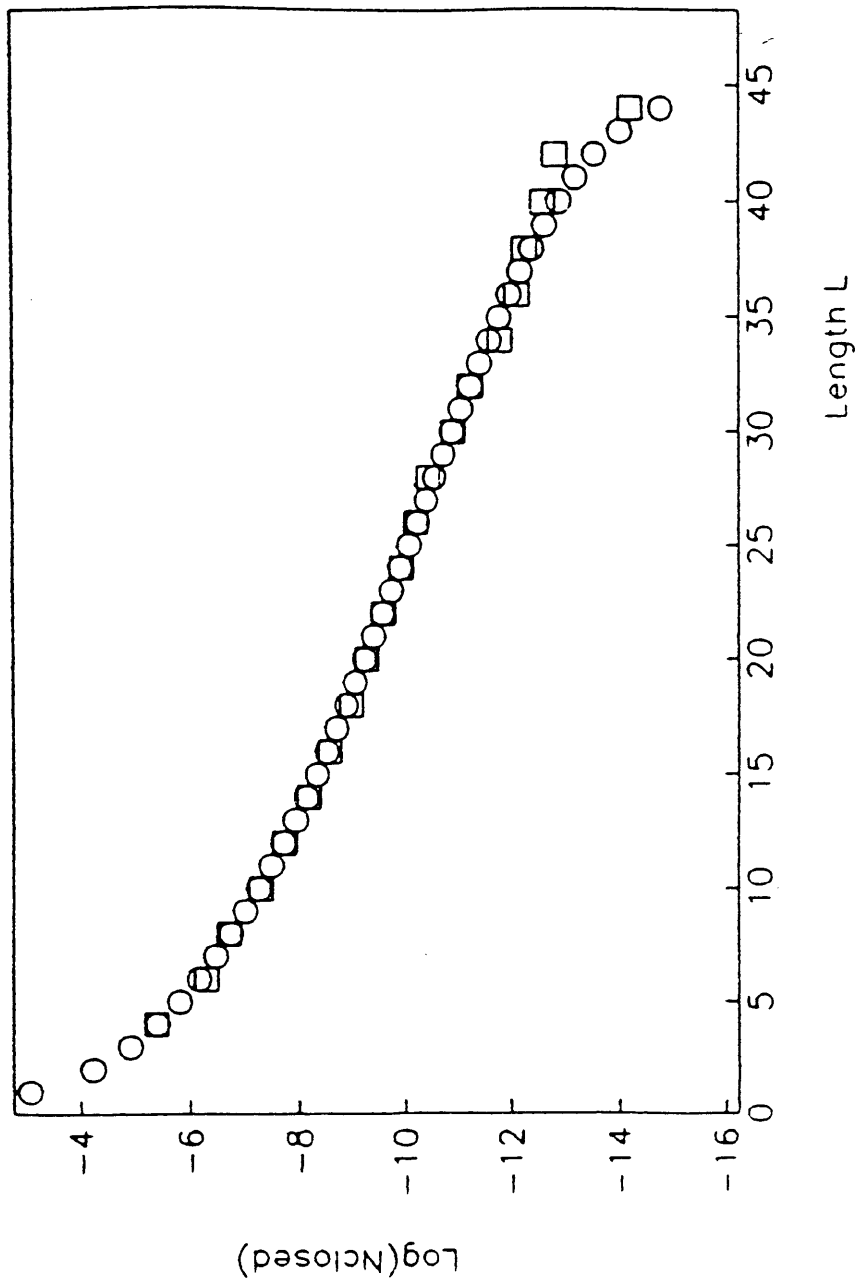
a) (squares)  $\log(N_{\text{closed}})$  vs.  $\lambda$   
for a lattice size of  $(80/2)^3$

b) (circles)  $\log(N_{\text{acc}})$  vs.  $\lambda$  where  
 $N_{\text{acc}}$  is defined by

$$N_{\text{acc}}(\lambda') = \sum_{\lambda=\lambda'}^{\lambda_4} A \lambda^{-5/2} \exp(-\alpha\lambda)$$

$$\alpha = 0.087$$

$$A = 0.0345$$



The value  $1/\beta \ll 80/2$  (the size of the lattice) and since the vast majority of the strings are much smaller than  $80/2$  the finite size of the lattice does not affect our results. As a further check on the effect of the finite lattice size a run was made using a body centered cubic lattice size of  $(20)^3$  ( $(40/2)^3$  in units where  $\xi=1$ ). These results are shown in Figures 2.7 and 2.8. A fit to the curve of Figure 2.7 gave

$$\begin{aligned}\beta &= 7.0 \pm 0.6 \times 10^{-2} \\ n_0 &= 1.6 \pm 0.5 \times 10^{-2}\end{aligned}$$

insignificantly different from those of the  $(40)^3$  lattice results.

#### Section 4. DISCUSSION

In this chapter we have shown that the length distribution of strings exhibits an exponential suppression of long strings:

$$n_{\text{open}} \propto \exp(-\kappa \ell/\xi)$$

The lifetime of any monopole-antimonopole pair will depend on the time it takes to dissipate the string's energy. Since the string lengths are predominately microscopic ( $\ell \sim \xi$ ) the whole system rapidly decays. In a very short time the monopole number density will therefore become much less than one per horizon volume, contrary to the causality arguments. Causality alone does not impose any

Figure 2.7 The same as 5 except using a lattice size of  $(40\sqrt{2})^3$

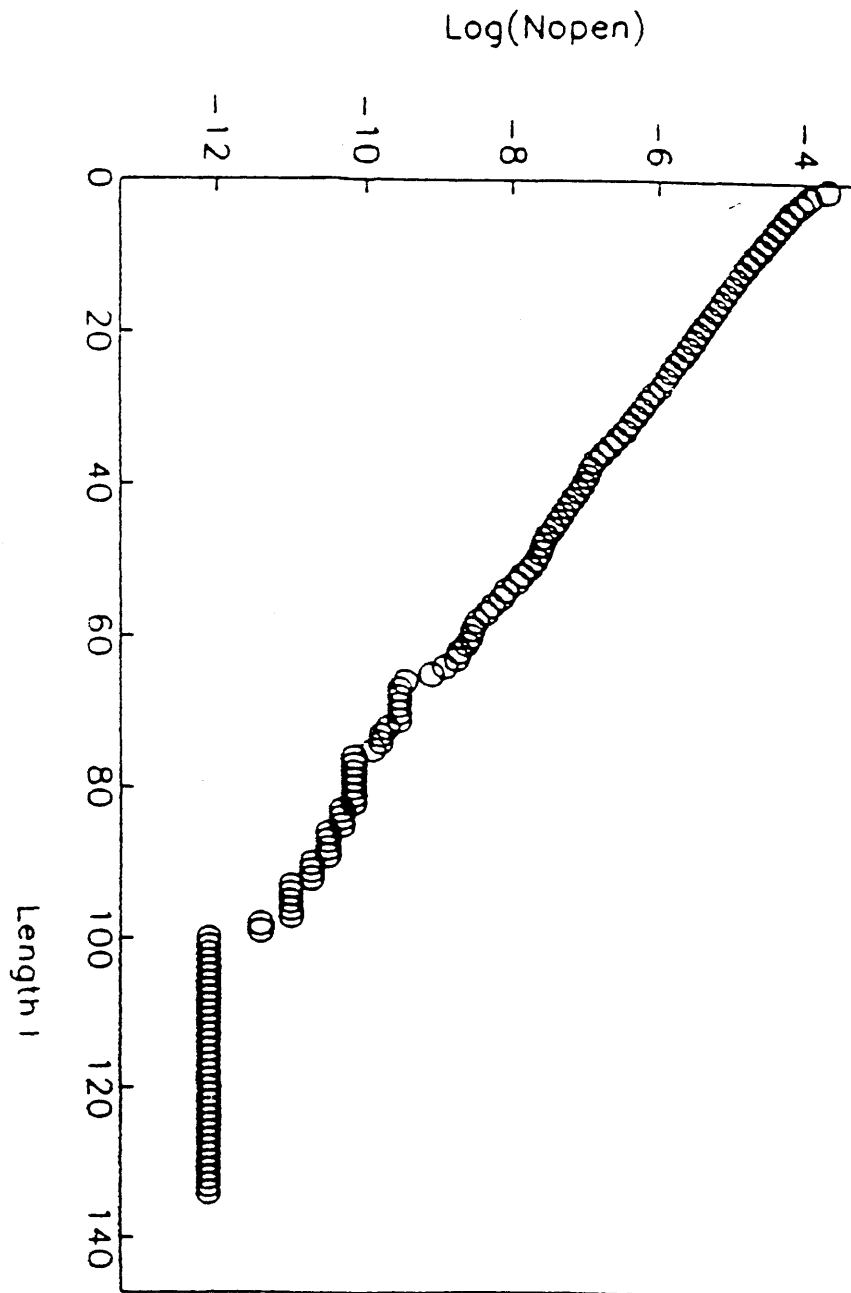
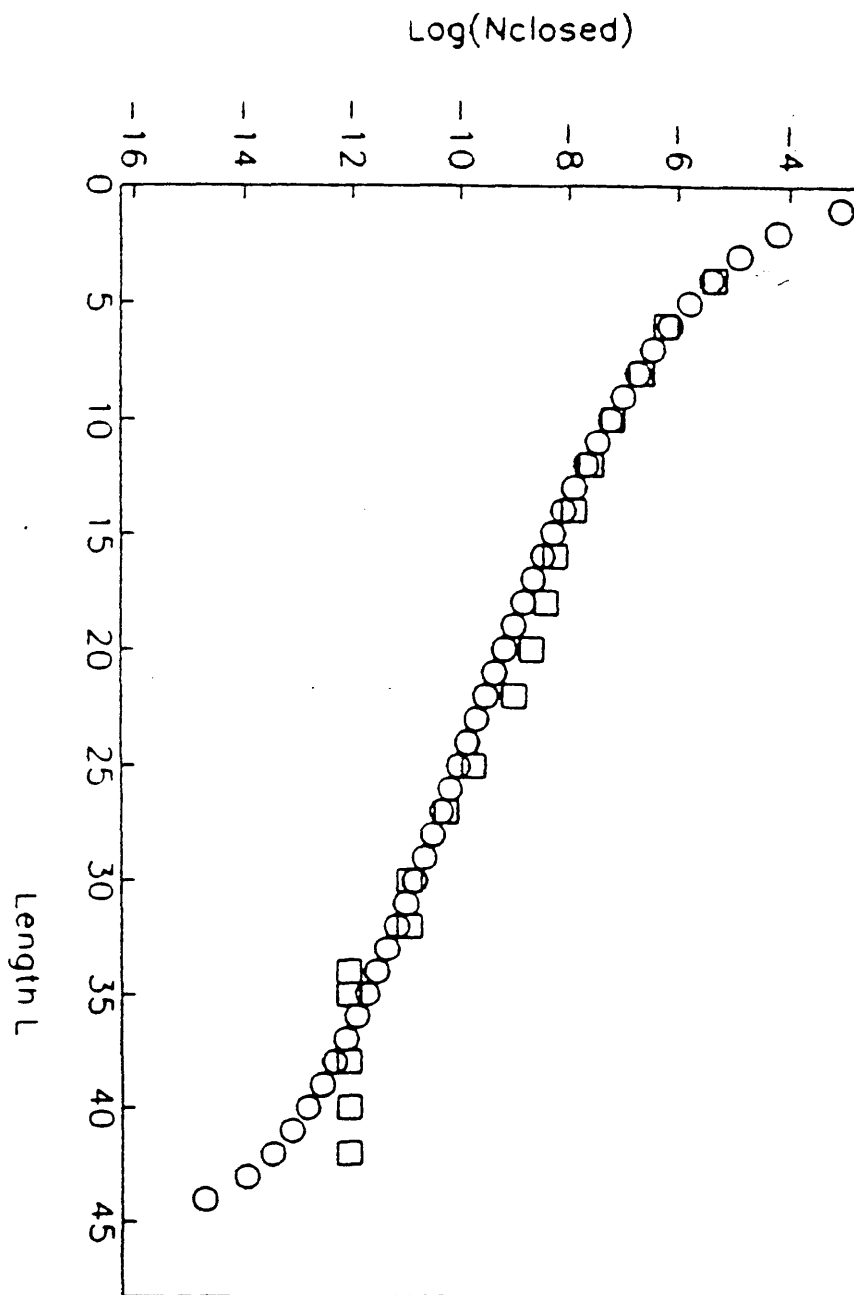


Figure 2.8 The same as 6 except using a lattice size of  $(40/2)^3$



interesting constraints on monopole annihilation. To determine the rate of annihilation the dynamics of the monopoles in the primordial plasma must be studied in detail.

In our simulations, as EVV did, we have used the same lattice spacing to simulate both phase transitions. As they pointed out, this amounts to the assumption that if the phase transition is second order, then both transitions occurred at roughly the same temperature. Let us suppose now that this is not the case. We still would expect qualitatively the same conclusion, i.e. that the monopole density rapidly falls away. Even if the string distribution was not initially exponential, in a short time we would expect it to become so. This is because, as EVV emphasized, the strings can break with the formation of a monopole-antimonopole pair. Fragmentation would rapidly establish an exponential distribution unless the transitions occurred at such widely different temperatures that the breaking probability was negligible.

This study has only answered the question of monopole evolution for the special case of monopoles connected by strings. What happens when the monopoles are not connected by strings or flux tubes? At temperatures less than the Ginsburg temperature  $T_G$  the monopoles may effectively only disappear by annihilation with antimonopoles. This process has been discussed by Preskill [2.14] and Zel'dovich and Khlopov [2.15]. Their work studied the diffusion of

monopoles towards antimonopoles followed by capture in Bohr orbits and final annihilation. The results of their work suggests that, if we accept the standard monopole density at  $T_G$ , we have a 'monopole problem'. The work of this chapter however questions the validity of the standard estimate of the monopole density at  $T_G$ . Whether or not we do have a monopole problem in the standard cosmological model would therefore still seem to be open to question.

CHAPTER 3: THE DYNAMICS OF, AND RADIATION  
FROM, SUPERCONDUCTING STRINGS



### CHAPTER 3 The dynamics of and radiation from superconducting strings

In the next few chapters superconducting cosmic strings are discussed. These are a particularly interesting type of topological defect predicted to occur by some unified theories [3.1]. Like 'ordinary' cosmic strings [3.2], they are line-like defects which may be formed at a phase transition in the early universe. The observational situation is, however, much brighter for superconducting strings - the large currents they are capable of carrying could lead to a variety of interesting astrophysical phenomena [3.3 - 3.7]. For example, they have been invoked as the energy sources for an explosive scenario of galaxy formation by Ostriker, Thompson and Witten (OTW) [3.3]. Chudnovsky et al. [3.4] have considered their effect on plasma, estimating synchrotron emission and radiation from shock heating. While Field and Vilenkin [3.5] have suggested that electromagnetic radiation beamed from cusps on strings might provide an explanation for quasars.

In order to test these scenarios it is important to understand the motion of, and radiation from, superconducting strings. In this chapter we continue the work of Copeland et al. [3.8] who showed that the Nambu action acquires an extra local correction term due to the current on the string.

Depending on the value of the critical current on the

string [3.1], this correction may be large enough to cancel the string tension completely forming 'springs' [3.8]. In this case the large currents initially present on the string at formation quickly stabilise loops, forming magnetic dipoles which may come to dominate the universe. In chapter 4 we show that typically, in regions of parameter space where the current carrying state is long lived, springs are formed. (Long lived currents are of course essential for the strings to have interesting astrophysical consequences.) As we shall explain, however, it does appear possible to produce current lifetimes long enough to be observable without producing springs.

Even if the critical current is small (as is typically the case for fermionic strings [3.1]) the effect of current is still important in correctly calculating the radiation from the superconducting strings. Calculations [3.10, 3.16] using Nambu trajectories give infinite answers. In this chapter we calculate the radiation from an exact solution to our corrected action and find it is perfectly finite.

Also if the critical current is small, current loss processes will occur on the string [3.8]. For small critical current the Nambu action is in general a reasonable approximation and generically produces 'cusps' in closed loops where the current density becomes very large [3.11]. At these points we show that current will be lost, so that loop 'shrinkage' due to radiation results in the net loss rather than gain in current as other authors

had assumed [3.3, 3.5]. Thus for example, we show that the OTW scenerio can only work for very large primordial fields.

This chapter is divided into six sections. In section 1 we derive the corrected action describing the motion of current-carrying strings. In section 2 we discuss some exact solutions to the corrected equations of motion including springs and kinky loops. Springs are shown to be stable to small perturbations, and the local effect of the current is shown to decrease the velocity of propagation of waves on the strings. In section 3 we calculate the electromagnetic radiation from a kinky loop and in section 4 we show that kinks, although not 'rounded' off by the local corrections to the equations in our action, are 'rounded' off by the higher order effects of the nonlocal current self-interactions. This is important in section 5 where we see how the 'cusps' formed in this process quickly lead to the loss of current from loops. The final section summarises our results and discusses their cosmological implications.

### Section 1. The Superconducting String Action

In this section we explain how the current flowing along a superconducting string affects its motion. We begin by recalling the derivation of the Nambu action for an ordinary string in a broken U(1) gauge theory [3.12].

The field theory action is

$$S = \int d^4y \left( -\frac{1}{4} F^2 + |D_a \Phi|^2 - V(\Phi) \right) \quad (3.1.1)$$

$$V(\Phi) = \frac{\lambda}{4} (|\Phi|^2 - \eta^2)^2$$

with  $\Phi$  a complex scalar and  $F_{ab} = \partial_a A_b - \partial_b A_a$ ,  $a, b = 0, 1, 2, 3$  as usual. We look for an approximate solution to the equations of motion of (3.1.1) which locally take the form of the static cylindrically symmetric string or vortex line solution [3.12]. These are given by

$$\Phi(\rho, \theta) = f(\rho) e^{i\theta} \quad A_\theta = \frac{1}{e \rho} (a(\rho) - 1) \quad (3.1.2)$$

in cylindrical coordinates, with  $f(0) = 0$ ,  $a(0) = 1$  and 'f' and 'a' tending exponentially to  $\eta$  and 0 respectively on a length scale given by the inverse masses of  $\Phi$  and  $A_a$ .

Our solutions are constructed around an arbitrarily curved worldsheet with spacetime coordinates  $x^a(\sigma^\alpha)$ , where  $\sigma^\alpha = (\tau, \sigma)$  are the two worldsheet coordinates. Given such a worldsheet we may construct two space-like normal vectors  $n_A^a(\sigma)$  ( $A = 1, 2$ ), which everywhere obey  $n_A^a X_{a, \alpha} = 0$ . We can also choose them to be orthonormal i.e.  $n_A^a n_{aB} = -\delta_{AB}$ . For any point  $y$  in spacetime closer to the string than its radius of curvature we can associate two worldsheet coordinates  $\sigma^\alpha$  and two radial coordinates  $\rho^A$ :

$$y^a = x^a(\sigma) + n_A^a(\sigma) \rho^A \quad (3.1.3)$$

Our ansatz for the fields is then  $\Phi = \Phi_S(\rho)$  for the scalar field and  $A^a(y) = n_A^a(\sigma) A_S^A(\rho)$  where the subscript 's' stands for the static cylindrically symmetric solutions. Now we change coordinates in (3.1.1) from  $y^a$  to  $\zeta^\mu = (\sigma^\alpha, \rho^A)$  to obtain

$$S = -\int d^2\sigma d^2\rho \sqrt{-M} \left( \frac{1}{2} B_S^2(\rho) + |D_A \Phi_S(\rho)|^2 + V(\Phi_S(\rho)) \right) \quad (3.1.4)$$

where

$$M_{\mu\nu} = \frac{\partial y^a}{\partial \zeta^\mu} \frac{\partial y^b}{\partial \zeta^\nu} g_{ab} = \begin{bmatrix} \gamma_{\alpha\beta} \\ -\delta_{AB} \end{bmatrix} + O(\rho) \quad (3.1.5)$$

comes from the Jacobian and  $\gamma_{\alpha\beta} = \partial_\alpha x^a \cdot \partial_\beta x_a$  is the induced metric on the string worldsheet.

Performing the transverse integration we note that terms of  $O(\rho)$  will, when integrated against the energy density, be down by  $O(W/R)$  where  $W$  is the width of the string and  $R$  its radius of curvature. Hence we find

$$S = -\mu \int d^2\sigma \sqrt{-\gamma} + O(W/R) \quad (3.1.6)$$

where  $\mu$  is the energy per unit length of a static straight string. Except in regions of high curvature (such as cusps or kinks) the equations of motion derived from (3.1.6) should be a good approximation for strings of radius  $R \gg W$ . Note that in the case of global strings the energy density of the string only decays like a power law away from the string - this leads to an extra non-local interaction term in the action (3.1.6) [3.13, Appendix].

For superconducting strings the above derivation breaks down when there is a current on the string because the static configuration is no longer independent of the  $z$  coordinate - fields vary along the string. This means that the Lorentz invariance of the string under boosts in the  $z$  direction is broken and the relativistic string begins to behave more like an ordinary non-relativistic string.

Let us briefly recall how bosonic superconducting strings arise. The simplest theory in which they occur is a  $U(1)' \times U(1)_{em}$  gauge theory which has two complex scalars  $\chi$  and  $\phi$  carrying  $U(1)_{em}$  and  $U(1)'$  charges respectively. The  $\phi$  Higgs field breaks  $U(1)'$  forming strings and couplings are then arranged so the condensate field  $\chi$  acquires a non-zero value in the string core where  $\phi \sim 0$ . Spatial variations of the phase of  $\chi$  along the string produces an electromagnetic current which is topologically conserved as long as  $\chi$  remains non-zero on the string.

In more detail, the Lagrangian used is

$$\begin{aligned}
 L = & |D_\mu \phi|^2 + |D_\mu \chi|^2 - \frac{1}{4} F_{\mu\nu} F^{\mu\nu} - \frac{1}{2} \lambda_1 (|\Phi|^2 - \eta^2)^2 \\
 & - \frac{1}{2} \lambda_2 |\chi|^4 - \lambda_3 (|\Phi|^2 - m^2) |\chi|^2 \quad (3.1.7) \\
 & - \frac{1}{4} R_{\mu\nu} R^{\mu\nu}
 \end{aligned}$$

To ensure electromagnetism is not broken outside the string we take :

$$\frac{m^2}{\eta^2} < 1, \quad \frac{\lambda_1 \lambda_2}{\lambda_3^2} > \frac{m^4}{\eta^4} .$$

$|\chi|$  is zero at the global minimum, but if  $\Phi$  is zero, as it is in the string core, the potential for  $\chi$  has the symmetry-breaking form and forces  $|\chi|$  to be non-zero, of order  $\sqrt{(\lambda_3/\lambda_2)} m$ . For some range of the couplings a  $\chi$  condensate does indeed exist on the string [chapter 4, ref. 3.9, 3.14]. Let us call it  $\chi_0(\rho)$ . The condensate does not carry any current if its phase is constant. If we set  $\chi = \chi_0(\rho) e^{i\theta(z,t)}$  in the static straight string solution we find an extra contribution to the string action :

$$\begin{aligned}
 \Delta S = & \int d^2\sigma \int d^2\rho \sqrt{-\gamma} |D_\alpha \chi|^2 \\
 = & \kappa \int d^2\sigma \sqrt{-\gamma} \gamma^{\alpha\beta} (\partial_\alpha \theta + eA_\alpha)(\partial_\beta \theta + eA_\beta) \quad (3.1.8)
 \end{aligned}$$

where  $\kappa = \int d^2\rho (\chi_0(\rho))^2$ . Here we used

$$\eta^{ab} D_a \chi D_b \chi = M^{\mu\nu} D_\mu \chi D_\nu \chi$$

with the inverse of  $M^{\mu\nu}$ ,  $M_{\mu\nu}$  given in (3.1.5). We include the term  $- \left| D^A \chi_0(\rho) \right|^2$  in our definition of  $\mu$  and, to order  $\rho$ , are left with the  $|D_\alpha \chi|^2$  term in (3.1.8). We also have

$$A_\alpha(\sigma) = x^a_{,\alpha} A_a(x(\sigma))$$

and we assumed that the electromagnetic gauge field  $A_a$  varied slowly across the string in performing the integral in (3.1.8). This will be justified later. In the next chapter we will show that for the current to last for a significant period of time one requires  $\kappa \gg 20$  [3.9].

From (3.1.8) we find the electromagnetic current

$$J_\alpha = - \frac{\delta(\Delta S)}{\delta A^\alpha} = -2 e\kappa (\partial_\alpha \theta + eA_\alpha) \quad (3.1.9)$$

and so

$$\Delta S = \frac{1}{4e^2\kappa} \int d^2\sigma \sqrt{(-\gamma)} \gamma^{\alpha\beta} J_\alpha J_\beta \quad (3.1.10)$$

The current carried by such a string persists because the total change in  $\theta$  around a loop is conserved as long as  $|\chi|$  does not go to zero (i.e. does not 'hop' over the potential barrier) at the core of the string. The winding



of  $\theta$  may change through tunnelling of the  $\chi$  field so the current carrying state is actually metastable [chapter 4, ref. 3.1, 3.9].

In fact, the gauge field  $A_\alpha$  is determined in terms of  $\partial_\alpha \theta$  by Maxwell's equations. In the Lorentz gauge,  $\partial_a A^a = 0$ , these read

$$\begin{aligned} \partial^2 A^a(y) &= \int d^2\sigma \sqrt{-\gamma} \delta^4(\mathbf{x}(\sigma) - y) J^\alpha \partial_\alpha x^a \\ &\equiv J^a(y) \end{aligned} \quad (3.1.11)$$

obtained by setting

$$\begin{aligned} A_\alpha(\sigma) &= \partial_\alpha x^a A_a(\mathbf{x}(\sigma, \tau)) \\ &= \int d^4y \delta^4(\mathbf{x}(\sigma, \tau) - y) \partial_\alpha x^a A_a(y) \end{aligned}$$

in (3.1.10). This has the solution

$$\begin{aligned} A^a(y) &= \int d^4y' G^{\text{ret}}(y - y') J^a(y') \\ &= \int d^2\sigma' \sqrt{-\gamma} G^{\text{ret}}(y - \mathbf{x}(\sigma', \tau')) J^\alpha \partial_\alpha x^a \end{aligned} \quad (3.1.12)$$

where

$$G^{\text{ret}}(y) = (1/2\pi) \delta(y^2) \theta(y^0)$$

is the retarded Green function. From (3.1.12)  $A_\alpha$  is determined in terms of  $J_\alpha$  which depends on  $A_\alpha$  as well as  $\partial_\alpha \theta$ . We evaluate (3.1.12) on the string world sheet as follows. Letting  $y^a = x^a(\sigma, \tau)$ , we perform the  $\tau'$  integral by expanding the argument of the delta function in  $\tau' - \tau$  and  $\sigma' - \sigma$ , since the integral is dominated by  $\tau' = \tau$  and  $\sigma = \sigma'$ .

$$\begin{aligned}
 & \theta(x^0(\sigma, \tau) - x^0(\sigma', \tau')) \delta[(x(\sigma, \tau) - x(\sigma', \tau'))^2] \\
 & \approx \delta((\tau' - \tau)^2 \dot{x}^2 + 2(\tau' - \tau)(\sigma' - \sigma)\dot{x} \cdot x' + (\sigma' - \sigma)^2 x'^2) \theta(\tau - \tau') \\
 & = \frac{\delta[\tau' - \tau + \{(\dot{x} \cdot x'(\sigma' - \sigma) + \sqrt{((\dot{x} \cdot x')^2 - \dot{x}^2 x'^2)}|\sigma' - \sigma|)/(\dot{x}^2)\}]}{2 \sqrt{((\dot{x} \cdot x')^2 - \dot{x}^2 x'^2)}|\sigma' - \sigma|}
 \end{aligned}
 \tag{3.1.13}$$

Performing the  $\tau'$  integral and noting that the square root in (3.1.13) is  $\sqrt{-\gamma}$  we find

$$A^a(x(\sigma, \tau)) \approx \frac{1}{4\pi} \int d\sigma' \frac{1}{|\sigma' - \sigma|} (J^\alpha \partial_\alpha x^a(\sigma) + O(\sigma' - \sigma))
 \tag{3.1.14}$$

the first term of which diverges logarithmically.

For a loop of radius of curvature  $R$  and string width  $W$ , we know that the formula (3.1.12) must break down for  $|\underline{y} - \underline{x}(\sigma, \tau)| \sim W$  so (3.1.14) gives

$$A^a(x(\sigma)) \approx (1/2\pi) \ln(R/W) J^\alpha \partial_\alpha x^a(\sigma) \quad (3.1.15)$$

as the leading term. For a wire of width  $W$  carrying a uniformly distributed current  $J$ , the gauge field interior to the surface  $A_I = A_0 + (J/2\pi) (\rho/W)^2$  (in 'SI' units with  $\epsilon_0=\mu_0=c=1$ ) where  $A_0$  is the value of the gauge field at the centre; so the variation of  $A$  across the string is indeed negligible as previously assumed. Putting (3.1.15) into (3.1.9) we find that on the string

$$\left. \begin{aligned} J_\alpha &= -2e\kappa_{\text{eff}} \partial_\alpha \theta \\ A_\alpha &= -e \ln(R/W) (\kappa_{\text{eff}}/\pi) \partial_\alpha \theta \\ \kappa_{\text{eff}} &= \kappa / (1 + e^2 (\kappa/\pi) \ln(R/W)) \end{aligned} \right\} \quad (3.1.16)$$

These formulae were derived by Witten [3.1] for a straight string.

For  $\kappa \gg 1$ , which is required in order for the current to last a reasonable time,

$$\kappa_{\text{eff}} \sim 1/(4\alpha_{\text{EM}} \ln(R/W)) \sim 1/4$$

when  $\alpha_{\text{EM}}=1/137$  and  $\ln(R/W)\sim 100$ .

We may similarly calculate the electromagnetic contribution to the superconducting string action by substituting (3.1.12) into

$$\int d^4y \left( -\frac{1}{4} F^2 \right) = \frac{1}{2} \int d^4y A_a \partial^2 A^a \quad (3.1.17)$$

in the Lorentz gauge. We find using (3.1.11) and (3.1.12)

$$\begin{aligned} \Delta S_{EM} = (1/4\pi) \int d^2\sigma d^2\sigma' \sqrt{(-\gamma(\sigma))} \sqrt{(-\gamma(\sigma'))} & \theta(\mathbf{x}^0(\sigma) - \mathbf{x}^0(\sigma')) \\ & \delta((\mathbf{x}(\sigma) - \mathbf{x}(\sigma'))^2) J^\alpha(\sigma) J^\beta(\sigma') \\ & \partial_\alpha \mathbf{x}^a(\sigma) \partial_\beta \mathbf{x}_a(\sigma') \end{aligned}$$

Performing the same steps leading to (3.1.15) we find

$$\Delta S_{EM} = (1/4\pi) \ln(R/W) \int d^2\sigma \sqrt{(-\gamma)} \gamma_{\alpha\beta} J^\alpha J^\beta \quad (3.1.18)$$

as the leading local contribution to the string action. There are also non-local terms in the expansion but these do not include the logarithm which is typically  $\sim 100$  for macroscopic strings. Adding (3.1.10) to (3.1.18) and rescaling  $J_\alpha$  we find the action for a superconducting string in the absence of external electromagnetic fields to be [3.8]

$$S = -\mu \int d^2\sigma \sqrt{(-\gamma)} \left( 1 - \gamma^{\alpha\beta} j_\alpha j_\beta \right) \quad (3.1.19)$$

which is the main result of this section. Here,  $j_\alpha$  is dimensionless and is the current in units of  $J_s = 2e \sqrt{(\kappa_{eff}\mu)}$ . We shall discover in the next section the reason for the subscript. The dimensionless current  $j_\alpha$  is given in terms of the field  $\theta$  from (3.1.16) by

$$j_{\alpha} = - \sqrt{(\kappa_{\text{eff}}/\mu)} \partial_{\alpha} \theta \quad (3.1.20)$$

Thus (3.1.19) describes a string with a massless field  $\theta$  propagating along it. We shall discuss solutions to the equations of motion stemming from (3.1.19) in the next section.

Before doing so, however, we should discuss under what conditions the action is valid. It is obviously not a good approximation in regions where the string is curved on scales approaching its width, like kinks or cusps. It also ignores the non-local self-interaction of the string with itself by radiation from one part affecting another part of the string. These effects were dropped because they are down by  $(1/(\ln(R/W))) \sim 1/100$  (for large loops) relative to the terms we retained. In principle they can be determined by continuing the expansion in (3.1.13). The derivation of the action is also incorrect in the case of infinite strings. In writing down equation (3.1.17) we have dropped surface terms which are non-zero for an infinite string.

Finally the existence of the current on the string was assumed not to effect  $\chi_0(\rho)$  which was taken to be independent of  $J$ . This is actually a very good approximation in regions of parameter space where  $\kappa$  is large and the current carrying state has an astrophysically interesting lifetime. Thus our action (3.1.19) is not just valid to order  $j^2$  but to all orders

in  $j$  in 'interesting' regions of parameter space [3.9]. Our action agrees to order  $j^2$  with that proposed by Nielsen and Olesen [3.15] based on a Kaluza-Klein construction. Thus we believe their action is only a valid description of the type of superconducting strings we are discussing for small  $j$ . As we shall see however, one of the most interesting phenomena occurs when  $j \sim 1$ .

## Section 2. Solutions of the equations, springs and their stability

We now look for solutions to the equations of motion of superconducting strings derived from (3.1.19) and (3.1.20). Varying with respect to  $\theta$  and  $x^a$  we find

$$\partial_\alpha ( \sqrt{-\gamma} \gamma^{\alpha\beta} j_\beta ) = 0 \quad (3.2.1a)$$

$$\partial_\alpha ( \sqrt{-\gamma} ( \gamma^{\alpha\beta} + \theta^{\alpha\beta} ) \partial_\beta x^a ) = 0 \quad (3.2.1b)$$

where we have defined a world sheet energy momentum tensor

$$\theta^{\alpha\beta} = \frac{2}{\sqrt{-\gamma}} \frac{\delta \Delta S}{\delta \gamma_{\alpha\beta}} = 2j^\alpha j^\beta - \gamma^{\alpha\beta} ( j^\gamma j_\gamma ) \quad (3.2.2)$$

which is covariantly conserved and traceless.

As usual we can choose the orthonormal gauge  $\gamma_{\sigma\tau} = 0$ ,  $\gamma_{\tau\tau} + \gamma_{\sigma\sigma} = 0$ , so using (3.1.20), (3.2.1a) becomes

$$(\partial_{\tau}^2 - \partial_{\sigma}^2)\theta = 0 \quad (3.2.3)$$

$$\theta = f(\sigma + \tau) + g(\sigma - \tau) \quad (3.2.4)$$

with  $f$  and  $g$  arbitrary functions. Now the orthonormal gauge is invariant under the coordinate transformation

$$\sigma + \tau \rightarrow \tilde{\sigma} + \tilde{\tau} = \frac{2}{A} f(\sigma + \tau)$$

$$\sigma - \tau \rightarrow \tilde{\sigma} - \tilde{\tau} = \frac{2}{A} g(\sigma - \tau)$$

and in these coordinates  $\theta = A \tilde{\sigma}$ . We can always choose these coordinates provided the current is space-like everywhere (the case of time-like currents is discussed in [3.19]). If the current vanishes at some point however, we may need several patches to cover the loop. In these coordinates we have, using (3.1.20)

$$j_0 = 0, \quad j_1 = -A/(\kappa_{\text{eff}}/\mu) = -j, \quad \sqrt{(-\gamma)\theta^{\alpha\beta}} = -\gamma^{11} j^2 \delta^{\alpha\beta} \quad (3.2.5)$$

and the equation of motion (3.2.1b) becomes

$$\partial_{\tau}((1-\gamma^{11}j^2)\partial_{\tau}x^a) = \partial_{\sigma}((1+\gamma^{11}j^2)\partial_{\sigma}x^a) \quad (3.2.6)$$

$$\gamma^{11} = 1/(\partial_\sigma \underline{x})^2$$

Note that only  $\gamma^{11}j^2$ , which is invariant under rescaling  $\sigma$ , enters these equations and therefore they are independent of  $A$ .

Our first set of solutions comes from noticing that if  $(\partial_\sigma \underline{x})^2 + j^2 = 0$  (remember  $\partial_\sigma \underline{x}^a$  is a space-like vector) then the right hand side of (3.2.6) vanishes. We then have the solution  $x^0 = j\tau$  (the factor  $j$  being necessary to satisfy the orthonormal gauge conditions) and  $\underline{x} = \underline{x}(\sigma)$ , an arbitrary function subject to  $(\partial_\sigma \underline{x})^2 = j^2$  (i.e.  $\gamma^{11}j^2 = -1$ ). These solutions are arbitrary static curves in 3 dimensions and are called 'springs' [3.8]. What is happening is that the positive pressure contributed by the current cancels the string tension.

This may be seen by computing the stress-energy tensor from (3.1.19). In Minkowski spacetime this is

$$\begin{aligned} T^{ab} &= -2 \frac{\delta S}{\delta \eta_{ab}} \\ &= \mu \int d^2\sigma \sqrt{(-\gamma)} (\gamma^{\alpha\beta} + \theta^{\alpha\beta}) \partial_\alpha x^a \partial_\beta x^b \delta^4(x^a - x^a(\sigma)) \end{aligned} \tag{3.2.7}$$

which in the gauge described above becomes



$$T^{ab} = \mu \int d^2\sigma \left( (1 - \gamma^{11}j^2) \partial_\tau x^a \partial_\tau x^b - (1 + \gamma^{11}j^2) \partial_\sigma x^a \partial_\sigma x^b \right) \delta^4(x^a - x^a(\sigma)) \quad (3.2.8)$$

For example, for a loop of radius of curvature large enough for us to approximate it to a straight line in the z direction say (i.e.  $x^a \approx (\tau, 0, 0, \sigma)$ ) we have

$$T^a_b = \mu \delta^2(x) \text{diag}((1+j^2), 0, 0, (1-j^2)) \quad (3.2.9)$$

and we see that as the dimensionless current  $j$  increases to 1 the energy density  $T^0_0$  increases whilst the tension  $T^3_3$  decreases. If  $j=1$  the energy momentum tensor is just that of a line of pressureless dust.

An interesting difference between superconducting string solutions and ordinary string solutions is that if the current density is non-zero we cannot have 'cusps'. These occur generically in ordinary strings [3.11] and may be defined as points on the worldsheet where the determinant of the metric  $\gamma$  vanishes. At such points all directions on the worldsheet are null. For superconducting strings however, the energy density (3.2.8) becomes infinite if  $\gamma_{11}$  vanishes since then  $\gamma^{11}$  is infinite. This

is because if a cusp were to form, the current density there would be infinite.

Now we would like to check the stability of our 'spring' solutions to small perturbations. Naively we expect that a perturbed spring solution can be moved at zero energy cost into another spring. Any other perturbation either compresses the string, in which case the pressure becomes dominant, or extends it so the tension becomes dominant. Thus one expects stability.

In our gauge, (3.2.5),  $\delta j_\alpha = 0$ , so from (3.2.6) we find

$$j^2 \delta \ddot{\underline{x}} = \partial_\sigma (\underline{x}'_\sigma \cdot \delta \underline{x}'_\sigma) \underline{x}'_\sigma \quad (3.2.10a)$$

$$j \delta \dot{\underline{x}}^0 = \partial_\tau (\underline{x}'_\tau \cdot \delta \underline{x}'_\tau) \quad (3.2.10b)$$

where  $\dot{\underline{x}} = \partial_\tau \underline{x}$ ,  $\underline{x}' = \partial_\sigma \underline{x}$ . Setting  $\delta \underline{x}(\tau, \sigma) = \delta \underline{x}(\sigma) e^{i\omega t}$  we multiply (3.2.10a) by  $\delta \underline{x}$  and integrate around the loop to obtain, upon integration by parts,

$$-\omega^2 \int d\sigma (\delta \underline{x})^2 = - \int d\sigma (\underline{x}'_\sigma \cdot \delta \underline{x}'_\sigma)^2 / \underline{x}'_\sigma{}^2 \quad (3.2.11)$$

Thus  $\omega^2 > 0$  with  $\omega=0$  iff  $\delta \underline{x}' \cdot \underline{x}' = 0$  everywhere. Now we impose the perturbed gauge conditions. Equation (3.2.10b) is just the  $\tau$  derivative of  $\delta \gamma_{\tau\tau} + \delta \gamma_{\sigma\sigma} = 0$ . Using this and  $\delta \gamma_{\sigma\tau} = 0$  one gets  $j \delta \dot{\underline{x}}^0 = \underline{x}'_\sigma \cdot \delta \underline{x}'_\sigma$ ,  $j \delta \underline{x}^0 = \underline{x}'_\sigma \cdot \delta \underline{x}$ . These can be integrated using the gauge conditions for  $\underline{x}_\sigma$  and (3.2.10a)

to show that  $\delta x^0$  is purely oscillatory. Thus we have shown stability. There is a whole family of zero modes corresponding to deformations of springs into other springs, those for which  $\delta \underline{x}' \cdot \underline{x}'_S = 0$ .

One should also bear in mind that we have neglected the non-local electromagnetic self-interaction of a loop which would act to reduce the electromagnetic field energy, presumably slowly bringing a loop to a more circular form.

The second class of solutions we present are oscillating loops which are nevertheless solutions to (3.2.6). We suppose that  $\underline{x}'^2 = \text{constant}$ ,  $x^0 = \tau$  and then (3.2.6) becomes

$$\begin{aligned} \ddot{\underline{x}} &= v^2 \underline{x}'' \\ v^2 &= \frac{1 - j^2 / \underline{x}'^2}{1 + j^2 / \underline{x}'^2} \end{aligned} \quad (3.2.12)$$

which has the general solution

$$\underline{x}(\sigma, \tau) = (1/2) [ \underline{a}(\sigma + v\tau) + \underline{b}(\sigma - v\tau) ] \quad (3.2.13)$$

However we must also satisfy the orthonormal gauge conditions  $\dot{\underline{x}} \cdot \underline{x}' = 0$ ,  $\dot{\underline{x}}^2 + \underline{x}'^2 = 1$ . These imply

$$\underline{a}'^2 = \underline{b}'^2 = 2/(1 + v^2) \equiv \xi^2 \quad (3.2.14)$$

if we impose the extra condition  $\underline{a}' \cdot \underline{b}' = 0$ . Equation (3.2.14) says that  $\underline{a}'$  and  $\underline{b}'$  are curves lying on a sphere of radius  $\xi$ . They are periodic and have centre of mass zero, i.e.  $\int d\sigma \underline{a}'(\sigma) = 0$ , in the loops centre of mass frame. Solutions of this type for ordinary strings were discussed by Garfinkle and Vachaspati [3.16]. They have kinks - places where the derivative  $\underline{x}'$  is discontinuous, but this is expected to be a generic feature for loops chopped off long strings in an expanding universe. The simplest kinky loop has  $\underline{a}'$  being simply two points, the north and south pole, and  $\underline{b}'$  any two antipodal points on the equator (Figure 3.1). More generally  $\underline{b}'$  can be any arc or collection of arcs on the equator (Figure 3.2).

We can explicitly evaluate  $v$  in terms of  $j$ . From (3.2.13) and (3.2.14) we find  $\underline{x}'^2 = 1 / (1 + v^2)$  and from (3.2.12) we have

$$v^2 = \frac{\sqrt{(1 + 8j^2)} - (1 + 2j^2)}{2j^2} \quad (3.2.15)$$

Note that the effect of the current has simply been to reduce the velocity of wave propagation on the string to  $v^2 < 1$ . As the current is increased we see the velocity decreases until we reach  $j^2 = 1$  where  $v^2 = 0$  and we are back in the realm of springs. To lowest order the current does not therefore 'round off' kinks on strings, it just slows them down. This effect is nevertheless enough to

Figure 3.1 The sphere on which the curves  $a^2 = b^2 = \xi^2$  lie. The oscillating square solution has  $a$  being two points, the north and south pole, and  $b$  being any two antipodal points on the equator.

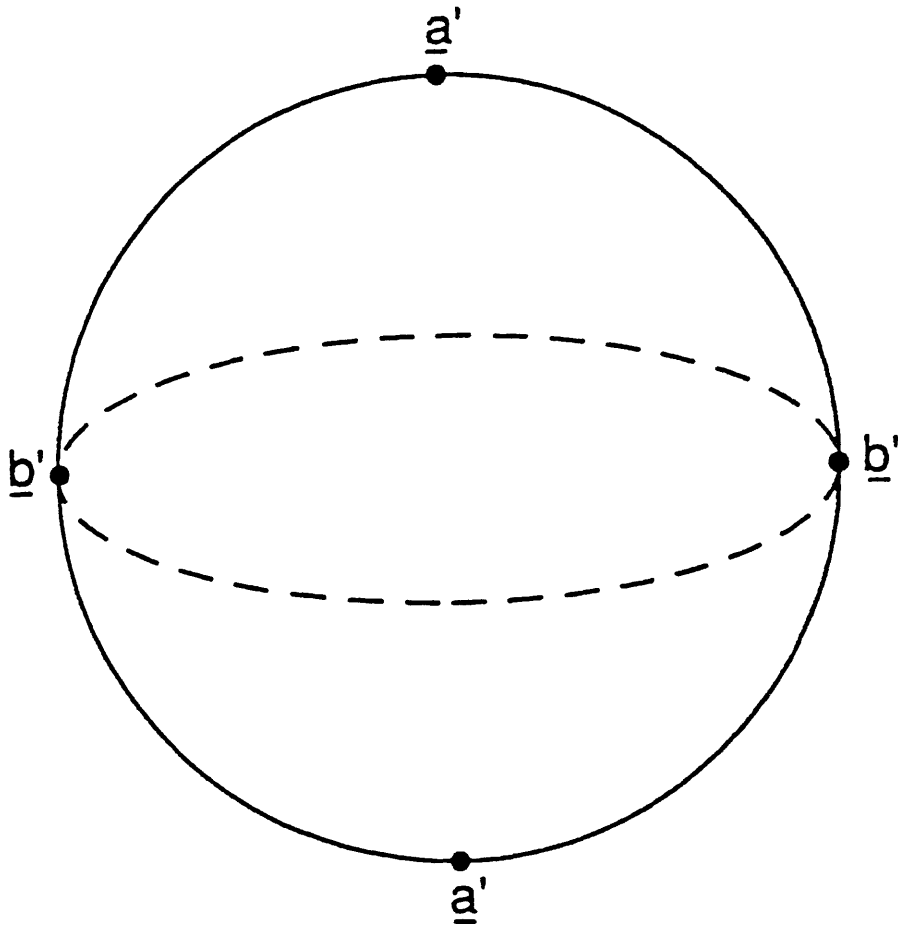
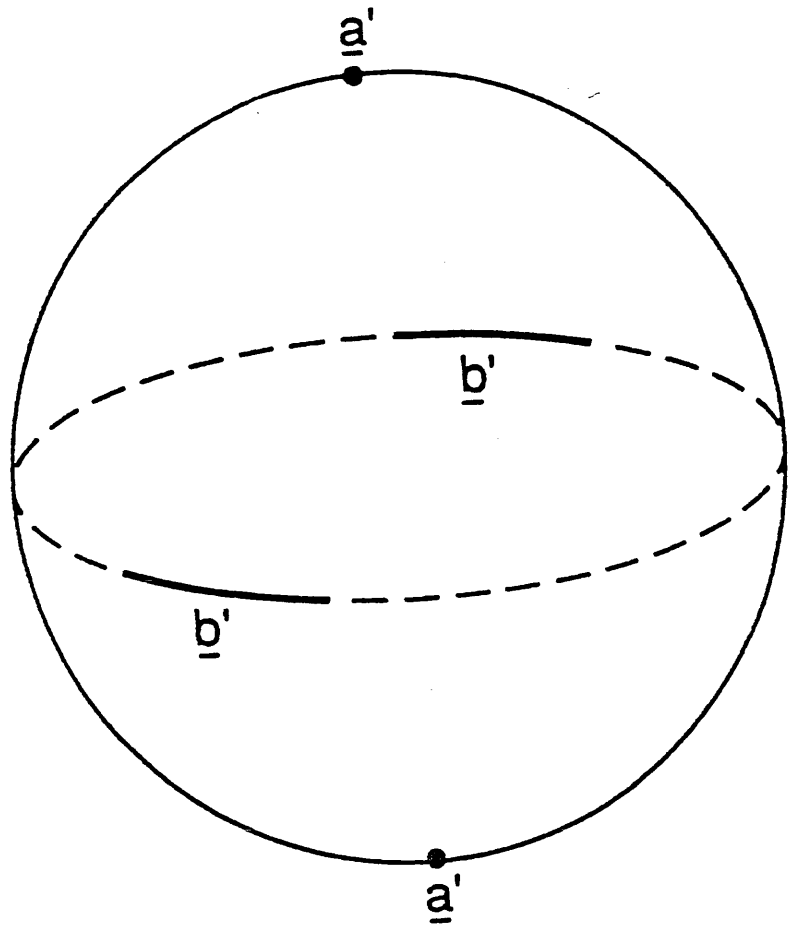


Figure 3.2 The a , b trajectories for a more general 'kinky' loop solution.



make the radiated power calculated from such an oscillating loop finite as we show in the next section. In the section after that we discuss how the non-local self-interaction of the loop does actually 'round off' the kinks.

### Section 3. Electromagnetic Radiation from a Kinky Loop

Superconducting strings radiate electromagnetically as well as gravitationally, and this effect has been evoked by many authors to produce explosions [3.3], quasar jets [3.5] and other astrophysical phenomena [3.6, 3.7]. Previous calculations have however produced very crude estimates of the total power radiated since the naive calculation of the total radiation from a 'Nambu' trajectory gives an infinite result [3.10, 3.16].

In this section we calculate the radiation from the simplest kinky loop and find it is perfectly finite if we include the local effect of the current on the string's motion.

The solution we use is given by (3.2.13) and (3.2.14) where

$$\begin{aligned} \underline{a}'(x) &= \xi (1,0,0) ; \underline{a}(x) = \xi (x,0,0) & 0 < x < L/2 \\ &= \xi (-1,0,0) & = \xi (L-x,0,0) & L/2 < x < L \end{aligned}$$

$$\underline{b}'(x) = \xi (0,1,0) ; \underline{b}(x) = \xi (0,x,0) \quad 0 < x < L/2$$

$$= \xi (0, -1, 0) \quad = \xi (0, L-x, 0) \quad L/2 < x < L$$

and  $L$  is the length of the loop. The trajectory is shown in Figure 3.1.

For a periodic source, the power radiated per unit solid angle is given by [3.10]

$$\frac{dP}{d\Omega} = \sum_n \frac{dP_n}{d\Omega}$$

$$\frac{dP_n}{d\Omega} = - \frac{\omega_n^2}{2\pi} J_a^*(\omega_n, \underline{k}) J^a(\omega_n, \underline{k}) \quad (3.3.2)$$

$$|\underline{k}| = \omega_n = \frac{2\pi n}{T} = \frac{4 \pi n v}{L}$$

where  $T = L/2v$  is the period of the source and  $J^a$  the Fourier transform of the current density. In our case from (3.1.16, 3.1.20) and with

$$J^a = \int d^2\sigma \sqrt{(-\gamma)} x_{,\alpha}^a J^\alpha \delta^4(x - x(\sigma, \tau)),$$

$$J^\alpha = (0, J_{\text{eff}}),$$

$$\underline{J}(\omega_n, \underline{k}) = (2v/L) J_{\text{eff}} \int_0^{L/2v} dt \int_0^L d\sigma \exp(i(\omega_n t - \underline{k} \cdot \underline{x}(\sigma))) \underline{x}'(\sigma)$$

$$J_{\text{eff}} = j (4e^2 \kappa_{\text{eff}} \mu)^{1/2} \quad (3.3.3)$$



It is convenient to split the integral (3.3.3) up into several regions in the  $\sigma$ - $t$  plane. Thus

$$\underline{J} = \frac{2vJ_{\text{eff}}}{L} [ \underline{J}_{++} + \underline{J}_{+-} + \underline{J}_{-+} + \underline{J}_{--} ] \quad (3.3.4)$$

where the subscripts  $\pm\pm$  correspond to regions where

$$\underline{a}' = \xi (\pm 1, 0, 0), \quad \underline{b}' = \xi (0, \pm 1, 0)$$

(Figure 3.3). Changing variables to  $\sigma_{\pm} = \sigma \pm vt$  the Fourier transforms are easily evaluated. For example

$$\begin{aligned} \underline{J}_{++} = (\xi/v) (1, 1, 0) & \left[ \frac{e^{i(L/4)((\omega_n/v) - k_1\xi)} - 1}{((\omega_n/v) - k_1\xi)((\omega_n/v) + k_2\xi)} \right] \\ & \times \left[ e^{-iL/4((\omega_n/v) + k_2\xi)} - 1 \right] \end{aligned} \quad (3.3.5)$$

(here,  $k_1$  and  $k_2$  are the  $x$  and  $y$  components of the Fourier Transform variable). Now using  $\underline{a}' \cdot \underline{b}' = 0$  we have

$$L^2/(4v^2J_{\text{eff}}^2) |\underline{J}|^2 = |\underline{J}_{++} + \underline{J}_{--}|^2 + |\underline{J}_{+-} + \underline{J}_{-+}|^2$$

and writing

$$A = |\underline{J}_{++} + \underline{J}_{--}|^2 \quad ; \quad B = |\underline{J}_{+-} + \underline{J}_{-+}|^2$$

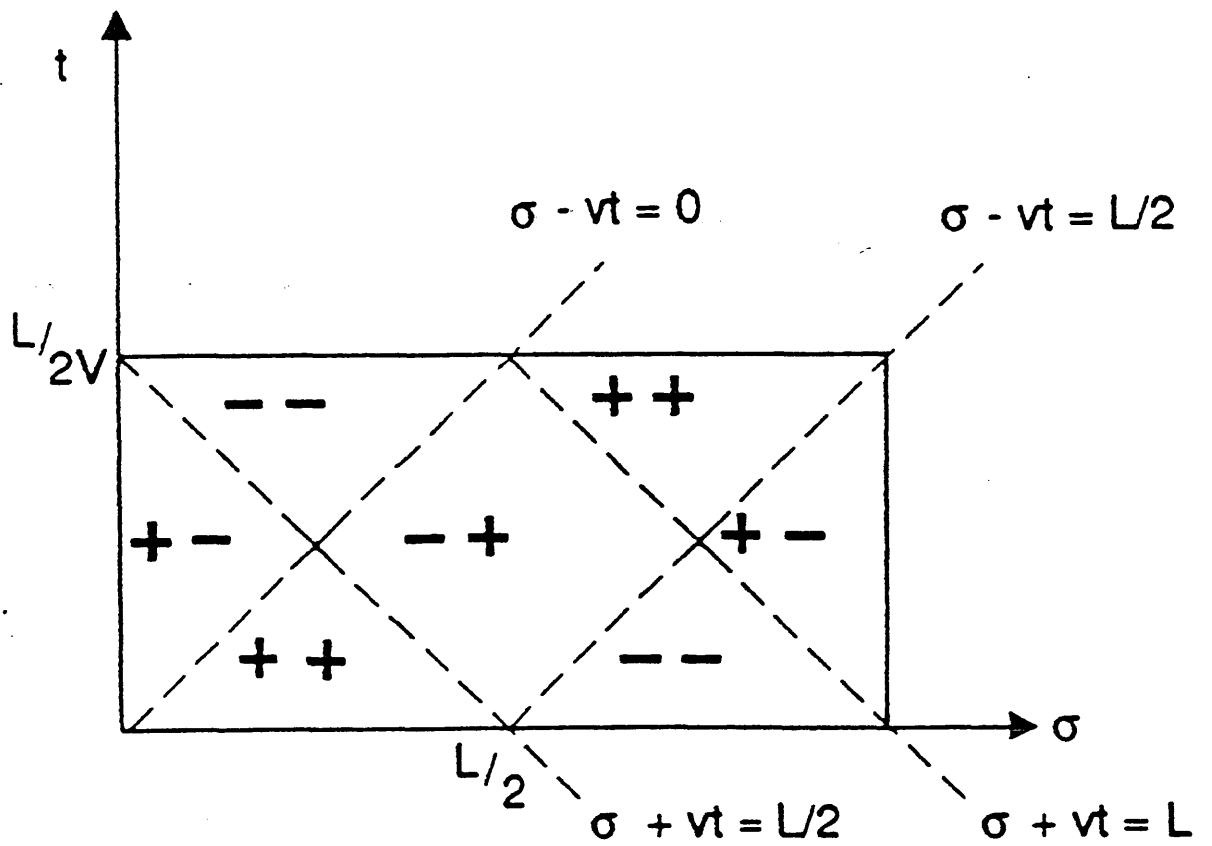


Figure 3.3 Diagram showing how the  $\sigma - \tau$  integral (3.3.3) is split up into different regions. The  $++$ ,  $+-$  etc. denote the direction of  $\underline{a}'$   $\underline{b}'$ .

it follows that

$$\begin{aligned}
 A &= (32/v^2) \xi^2 \left[ \frac{\sin(L\omega_-^1/8)\sin(L\omega_+^2/8)}{\omega_-^1 \omega_+^2} - \right. \\
 &\quad \left. \frac{\sin(L\omega_+^1/8)\sin(L\omega_-^2/8)}{\omega_+^1 \omega_-^2} \right]^2 \\
 B &= (32/v^2) \xi^2 \left[ \frac{\sin(L\omega_-^1/8)\sin(L\omega_-^2/8)}{\omega_-^1 \omega_-^2} - \right. \\
 &\quad \left. \frac{\sin(L\omega_+^1/8)\sin(L\omega_+^2/8)}{\omega_+^1 \omega_+^2} \right]^2
 \end{aligned}
 \tag{3.3.7}$$

where  $\omega_{\pm}^1 = (\omega_n/v) \pm k_1 \xi$  and  $\omega_{\pm}^2 = (\omega_n/v) \pm k_2 \xi$ . Changing to polar coordinates we write

$$k_1 = \omega_n \sin\theta \cos\phi \equiv \omega_n \alpha$$

$$k_2 = \omega_n \sin\theta \sin\phi \equiv \omega_n \beta$$

Re-expressing  $\omega_{\pm}^1, \omega_{\pm}^2$  we have

$$\omega_{\pm}^1 = (4\pi n/L) (1 \pm \xi v \alpha) = (4\pi n/L) \delta_{\pm} \quad (3.3.8)$$

$$\omega_{\pm}^2 = (4\pi n/L) (1 \pm \xi v \beta) = (4\pi n/L) \gamma_{\pm}$$

Substituting (3.3.7), (3.3.8) into (3.3.2) we obtain

$$\begin{aligned} \frac{dP}{d\Omega} &= \frac{16\pi^2 v^2}{L^2} \frac{128\xi^2 J_{\text{eff}}^2}{(2\pi)L^2} \sum_n \frac{n^2}{\left(\frac{4\pi n}{L}\right)^4} \\ &\left\{ \left( \frac{\sin(\frac{\pi n \delta_-}{2}) \sin(\frac{\pi n \gamma_+}{2})}{\delta_- \gamma_+} - \frac{\sin(\frac{\pi n \delta_+}{2}) \sin(\frac{\pi n \gamma_-}{2})}{\delta_+ \gamma_-} \right)^2 \right. \\ &+ \left. \left( \frac{\sin(\frac{\pi n \delta_+}{2}) \sin(\frac{\pi n \gamma_+}{2})}{\delta_+ \gamma_+} - \frac{\sin(\frac{\pi n \delta_-}{2}) \sin(\frac{\pi n \gamma_-}{2})}{\delta_- \gamma_-} \right)^2 \right\} \quad (3.3.9) \end{aligned}$$

$$= \frac{4J_{\text{eff}}^2 \xi^2 v^2}{\pi^3} \sum_n \frac{1}{n^2} \left\{ \quad \right\}$$

After some algebra and using the relation [3.17]

$$\sum_{n=1}^{\infty} (1/n^2) \cos n\alpha = \frac{(\alpha - \pi)^2}{4} - \frac{\pi^2}{12} \quad 0 < \alpha < 2\pi$$

we arrive at the result for  $\alpha > \beta > 0$  (i.e. in the first octant  $0 < \phi < \pi/4$ )

$$\frac{dP}{d\Omega} = (32/\pi) J_{\text{eff}}^2 \xi v^2 \times \frac{(\alpha'^2 + \beta'^2)}{(1 - \beta'^2)^2 (1 - \alpha'^2) (1 + \alpha')}$$

where  $\alpha' = \xi v \alpha$  ,  $\beta' = \xi v \beta$ . In terms of polar coordinates  $\theta, \phi$  we have

$$\begin{aligned} \frac{dP}{d\Omega} &= \frac{32 J_{\text{eff}}^2 \xi^4 v^4}{\pi} \\ &\times \frac{\sin^2 \theta}{(1 - \xi^2 v^2 \sin^2 \theta \sin^2 \phi)^2 (1 - \xi^2 v^2 \sin^2 \theta \cos^2 \phi)} \\ &\times \frac{1}{(1 + \xi v \sin \theta \cos \phi)} \quad (3.3.10) \end{aligned}$$

The appropriate expression for other values of  $\theta$  and  $\phi$  can be obtained by symmetry.

Note that if we had used a Nambu trajectory we would have  $\xi v = 1$  and (3.3.10) would diverge at  $\theta = \pi/2$ ,  $\phi = 0$ . Here however we have from (3.2.14), (3.2.15) that  $v < 1$ ,  $\xi v < 1$  and so (3.3.10) is finite everywhere. Also note that as 'j' approaches 1 'v' goes to zero and so does the power radiated.

The total power radiated, the integral of (3.3.10), is hard to calculate exactly but we can obtain a good approximation of it for small j by extracting the dominant contribution, around  $\theta = \pi/2$ ,  $\phi = 0$  (Figure 3.4). We find (setting  $\theta = \pi/2 + \chi$  and  $\xi^2 v^2 = 1 - j^2 (1 + v^2) \approx 1 - 2j^2$ ) the

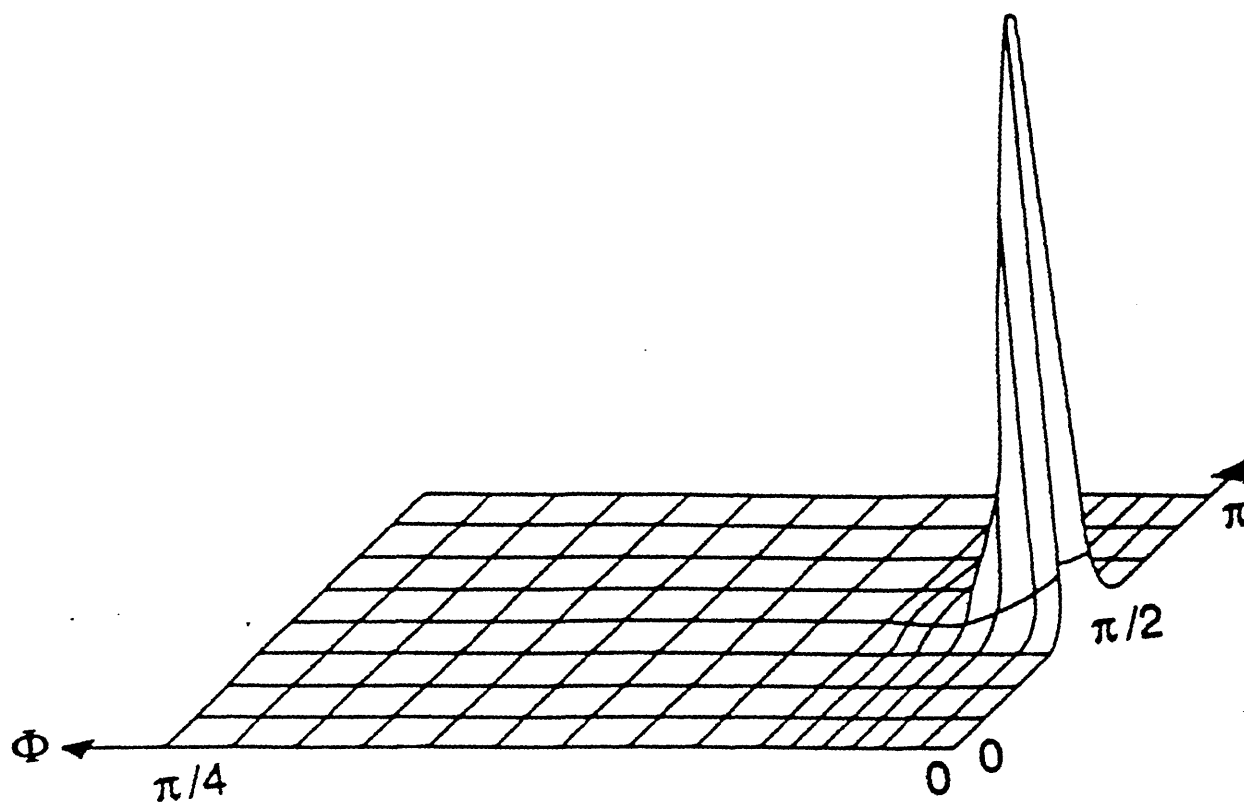


Figure 3.4 A plot of the integrand of  $\int d\Omega \frac{dp}{d\Omega}$  for small

j. The spike corresponds to  $\theta = \pi/2, \phi = 0$ .

integral

$$I = \int_0^{\pi/4} d\phi \int_{-\pi/2}^{\pi/2} d\chi \frac{1}{(2j^2 + \chi^2 + \phi^2)} \quad (3.3.11)$$

which may be performed by first doing the  $\chi$  integral, then setting  $\phi = \sqrt{2} j \sinh z$  and integrating by parts to obtain at small  $j$

$$I = 2 \ln(\pi/(2\sqrt{2} j)) \arctan 2 + O(j^0) \quad (3.3.12)$$

and thus (multiplying by 8 for each of the eight octants) from (3.3.10)

$$\begin{aligned} P &= (512/\pi) J_{\text{eff}}^2 [ \ln(\pi/(2\sqrt{2}j)) \arctan 2 + O(j^0) ] \\ &= (512/\pi) J_{\text{eff}}^2 [ \ln(e\pi/(\kappa_{\text{eff}}\mu)/(\sqrt{2}J_{\text{eff}})) \arctan 2 \\ &\quad + O(J_{\text{eff}}^0) ] \end{aligned} \quad (3.3.13)$$

where  $J_{\text{eff}}$  is the true electromagnetic current including the gauge field contribution. We repeat that (3.3.13) is valid for  $J_{\text{eff}} \ll e/(\kappa_{\text{eff}}\mu)$ . Rewriting (3.3.13) in dimensionless units of current,  $J = -2e/(\kappa_{\text{eff}}\mu) j$ , we find

$$P \approx \Gamma_{\text{EM}} j^2 \mu \quad (3.3.14)$$

with  $\Gamma_{\text{EM}} \approx 15 \ln(1/j) \approx 100$  for  $j \sim 10^{-3}$ , using  $\kappa_{\text{eff}} \sim 1/4$ . For small  $j$  this is smaller than previous estimates

[3.10] obtained by cutting off the infinite result obtained from Nambu trajectories. We argue in Section 6 that large  $j$  is only possible if we have large primordial magnetic fields. This looks to be a problem for example, for Vilenkin and Field's [3.11] quasar scenario.

In the opposite limit, as  $j$  approaches 1 or the magnitude of the electromagnetic current  $J_{\text{eff}}$  approaches  $2e \sqrt{(\kappa_{\text{eff}} \mu)}$  the string turns into a 'spring', and the velocity of propagation goes to zero, and so does the radiated power. In fact  $P$  goes to zero like  $(1 - j^2)^2$ .

We emphasise that (3.3.13) is perfectly finite unlike previous calculations of the radiated power which used Nambu trajectories and were infinite [3.10].

#### Section 4. The Effect of Non-Local Self-Interactions on a Kink

In this section we use a simple model for a kink to estimate the rate at which it departs from its original shape due to electromagnetic back reaction. This force is the result of the current on the string moving through a field whose source is another part of the string. We shall calculate this force for a right moving ninety degree kink on an otherwise straight string carrying a current  $J$  starting at time  $t=0$  [Figure 3.5].

For small currents, the kink moves almost at the



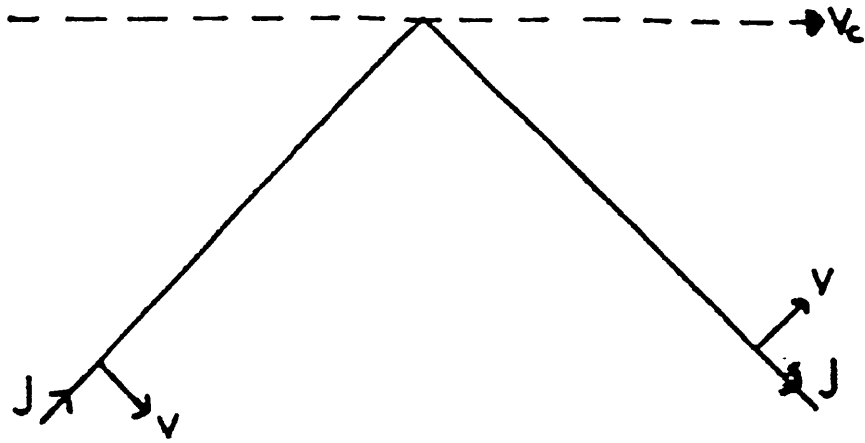


Figure 3.5 A right moving  $90^\circ$  kink moving with a velocity  $v_k \sim 1$  on an otherwise straight string which carries a current  $J$ . The straight string segments move with velocity  $1/\sqrt{2}$ .

speed of light. Our calculation will not be sensitive to us taking the velocity to be 1 and  $v$  to be  $1/\sqrt{2}$ .

The field  $\underline{B}$  at any point in space close to the string is, by the Biot-Savart law, given by

$$\underline{B}(t, \underline{x}) = (1/4\pi) \int d\sigma' (d\underline{J}(\sigma', t_{\text{ret}}) \wedge \underline{r}) / r^3 \quad (3.4.1)$$

where  $\underline{r} = \underline{x}(\sigma', t_{\text{ret}}) - \underline{x}$  and the retarded time  $t_{\text{ret}} = t - r$ . Thus at any point on the string the self force per unit length is

$$\underline{F} = \underline{J}(\sigma, t) \wedge \underline{B}(\underline{x}(\sigma, t), t)$$

The magnetic field  $\underline{B}$  is that due to an integral over all the infinitesimal current elements intersecting the backward light cone from  $\underline{x}(\sigma, t)$ .

Of course, all self-force calculations have ambiguities [3.18]. Here, the problem can be illustrated by calculating the self-force due to a straight wire moving with velocity  $1/\sqrt{2}$  in the  $x$  direction. If our initial conditions are that the string lies along the  $z$ -axis at  $t=0$ , at a later time  $t$  the backward light cone for any point  $(z_0, t_0)$  on the string lies on the lines  $z - z_0 = \pm |x - x_0|$ , and each point interacts with a magnetic field

$$\underline{B}_S(t, \underline{x}) = (J/4\pi) \int_{\sigma'_-}^{\sigma'_+} d\sigma' \frac{\underline{x}'(\sigma', t_{\text{ret}}) \wedge (\underline{x}(\sigma', t_{\text{ret}}) - \underline{x})}{|\underline{x}(\sigma', t_{\text{ret}}) - \underline{x}|^3} \quad (3.4.2)$$

where  $\sigma'_\pm = \sigma \pm (1/\sqrt{2})t$  are the limits of the backward light cone. This is not zero, and we are presented with the nonsensical result that a moving wire experiences an acceleration due to its own magnetic field. However, we know that a wire moving with constant velocity is a solution to the true equations of motion, (just by Lorentz boosting a static wire), so we will 'renormalise' all calculations by subtracting  $\underline{B}_S$  at every point on the string, so that straight wires do indeed move with constant velocity.

Let us now turn to the kink of Figure 3.5. First of all we need to find the locus of the intersection of the backward light cones of points on the string with the string world sheet. It is fairly straightforward to convince oneself that points in front of a kink (like point (A) on Figure 3.6) can only "see" other points that were in front of the kink, so the locus of intersection are two lines at  $45^\circ$  to the string, terminating at points  $A'$ ,  $A''$  such that  $AA' = AA'' = t$ .

The locus for a given point behind the kink, such as a point B, is a little more complicated. Points further away from the kink (which is at  $\sigma = t$ ) than B (ie.  $\sigma < \sigma(B)$ ) again are on a horizontal line  $BB'$  when they are



sources for the field observed at B at time  $t$ . Furthermore, the locus extends upwards to point  $K'$  where the backward light cone from B intersects the trajectory of the kink. For  $\sigma > \sigma(K')$  the point B is running into the field produced by the string which was in front of the kink when the field was produced. The locus of true points is determined by the condition that  $DD'/BD' = 1/\sqrt{2}$  because  $DD'$  is the distance the string moves while the field is travelling from  $D'$  to B. This is a *hyperbola* with its focus at point B, which extends to point  $B''$  where the straight line distance  $BB''$  is equal to  $t$ .

Now we can perform our renormalisation, which for point A is graphically equivalent to eliminating  $A'A$ , and  $AA''$ , leaving nothing, while for point B we eliminate  $B'B$  and  $BK'$ , and add a piece  $K'R$  consisting of current elements pointing in the opposite direction to  $J$  ( $\sigma < \sigma(K)$ ). This is shown in Figure 3.7.

In principle we can now evaluate the field at B exactly. However, this is not really worthwhile because the subsequent evolution of the string changes the geometry of the kink, making the calculation of the locus of the intersection of the light cone with the string world sheet difficult. Instead, we shall content ourselves with estimating the magnetic field at point B. The closest source point to B is point C; because of the  $1/r^2$  in the Biot-Savart formula the source points around C will dominate the integral in (3.4.1). Hence, if we let  $\lambda = BC$ , and approximate the parabola as a straight line,

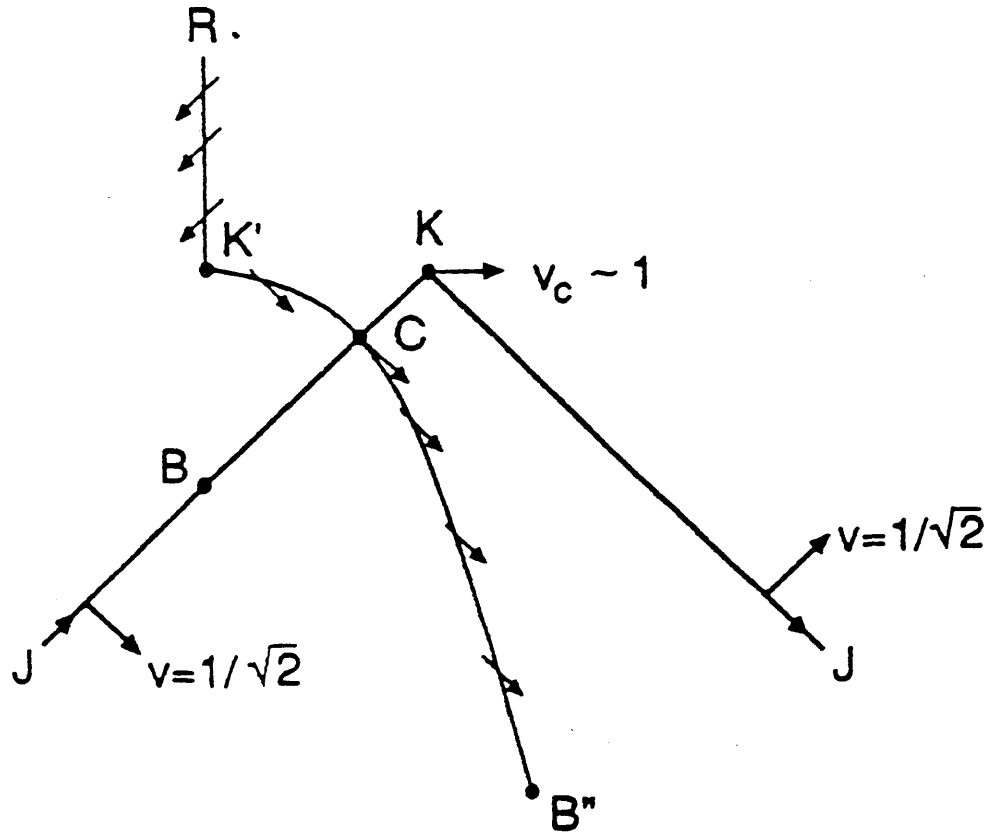


Figure 3.7 The locus of the points of intersection of the backward light cone of the point B with the string after we have performed our 'renormalisation'.

$$| \underline{B}(\sigma(B)) | \sim J \int_{x_{B''}}^{x_R} dx \frac{1}{(\lambda^2 + x^2)} \quad (3.4.3)$$

where  $(x_{B''}, x_R) \sim t$

If  $\lambda < t$ , then  $|\underline{B}| \sim J/\lambda$ , whereas if  $\lambda > t$  (i.e. B is a long way from the kink) then  $|\underline{B}| \sim Jt/\lambda^2$ . Since the sources near C dominate, the direction of  $\underline{B}(\sigma(B))$  is into the page.

Hence the force  $\underline{F} = \underline{J} \wedge \underline{B}$  acts in the opposite direction to the velocity of the string behind the kink, and has the magnitude

$$|\underline{F}| \sim \begin{cases} J^2/\lambda & \lambda < t \\ J^2 t/\lambda^2 & \lambda > t \end{cases}$$

Thus we can estimate the displacement of a piece of string away from its unperturbed position as the kink passes through it from the equation of motion

$$\ddot{\underline{x}} - \underline{x}'' \approx \underline{F}/\mu$$

As the kink catches up with a piece of string it suddenly experiences an acceleration  $j^2/w$  ( $w$  is the width of the string  $j^2 = J^2/\mu$ ) in a direction opposite to its motion behind the kink. After time  $t$  the displacement of the string from its unperturbed position is therefore (for  $t > w$ )

$$\Delta x \sim \int_w^t \int_w^{t'} dt' dt'' j^2/t'' = \int_w^t dt' j^2 \ln(t'/W) \sim j^2 t \ln(t/w) \quad (3.4.6)$$

The kink is not actually removed by this back reaction, because the force always operates behind it. However it seems likely that the kink will tend to straighten out in order to join smoothly with string lagging behind. For  $t \gg w$ , the logarithm in (3.4.6) is large and indicates that the kink actually 'rounds out' faster than the rate of loss of energy from the loop (3.3.14). This will be important in Section 5. The calculations presented in this section have been very crude. The conclusions have however recently been confirmed by Spergal [3.21] who evaluated numerically the trajectory of an oscillating current carrying loop.

### Section 5. Loop Shrinkage Leads to Current Loss

There is a simple argument that the radiation from loops and their consequent shrinkage leads to a build-up of currents. The total winding number of the  $\theta$  field is fixed barring tunnelling events where  $\chi$  goes to zero. The current is however proportional to the gradient of  $\theta$ . Now as a loop loses energy its length decreases. Thus the gradient of  $\theta$  must rise. This growth of current is particularly important in the OTW scenario where it leads to the conclusion that whatever the magnitude of the



primordial magnetic fields, at some point a loop will radiate very large amounts of electromagnetic energy. The electromagnetic radiation  $P_{EM} = \Gamma_{EM} \mu j^2$  dominates the gravitational radiation  $P_{GR} = \Gamma_{GR} G\mu^2$  for  $j > \sqrt{(G\mu)} \sim 10^{-3}$  (recall that  $j$  is the electromagnetic current in terms of the spring current). For any interesting effect one generally requires the critical current  $j_c$  to be this large.

One knows however, that if  $j_c > 1$  then theories predicting superconducting strings are ruled out (see section 6). So we are led to study the range  $10^{-3} < j_c < 1$ . The upper end of this range is hard to investigate: all we can safely say is that the Nambu action will have significant corrections and therefore the naive calculations of [3.3-3.7] may be unreliable.

What if  $10^{-3} < j_c < 10^{-1}$  ?

From (3.1.16) any region where the  $\theta$  field has larger gradient than  $|\underline{\nabla}\theta|_c = J_c / (2e\kappa_{eff})$  (where  $\underline{\nabla}\theta$  is the spatial gradient of  $\theta$  along the string) will turn critical and lose current. Recalling that in the gauge we use

$j_\sigma = -\sqrt{(\kappa_{eff}/\mu)} \partial_\sigma \theta = j$  this translates into

$$|\underline{x}'|_c = j \frac{2e \sqrt{(\kappa_{eff}\mu)}}{J_c} = \frac{j}{J_c}$$

For  $|\underline{x}'|$  smaller than this current will be rapidly lost.

Now for small  $j_c$  the motion of the loop should be 'approximately Nambu'. Thus we expect that 'near-cusps' [3.11] will occur. These are regions where  $|\underline{x}'|$  gets very small. In these regions current will be lost.

It might be objected that the  $\theta$  field is a massless field obeying (to zeroth order in  $j^2$ ) the same equation as  $x^a$  and therefore a 'cusp' in a loop will occur periodically at exactly the same place and so the process of cleaning current off the string ceases after the first cusp.

This may be wrong however. We cannot expect cusps to remain exactly at the same point. The string radiates gravitationally losing length at a rate  $\Delta L \sim \Gamma_{GR} G\mu L$  per period where  $L$  is the length of the loop. Cusps dominate the radiation and so they should precess around the string at this rate or faster. Recalling that it is precisely the process of shrinkage in the loop which gives rise to a growing current, we see that the loss of current at 'cusps' can outweigh the gain due to loop shrinkage. In more detail, the current lost is given roughly by

$\frac{dj}{dt} = -\frac{j}{j_c} \frac{j}{L}$  compared to the gain  $\frac{dj}{dt} = +\Gamma_{GR} G\mu \frac{j}{L} + \Gamma_{EM} \frac{j^3}{L}$  due to the loop shrinking by gravitational and electromagnetic radiation.

In Figure 3.8  $\frac{dj}{dt}$  is plotted versus  $j$ . We assume that

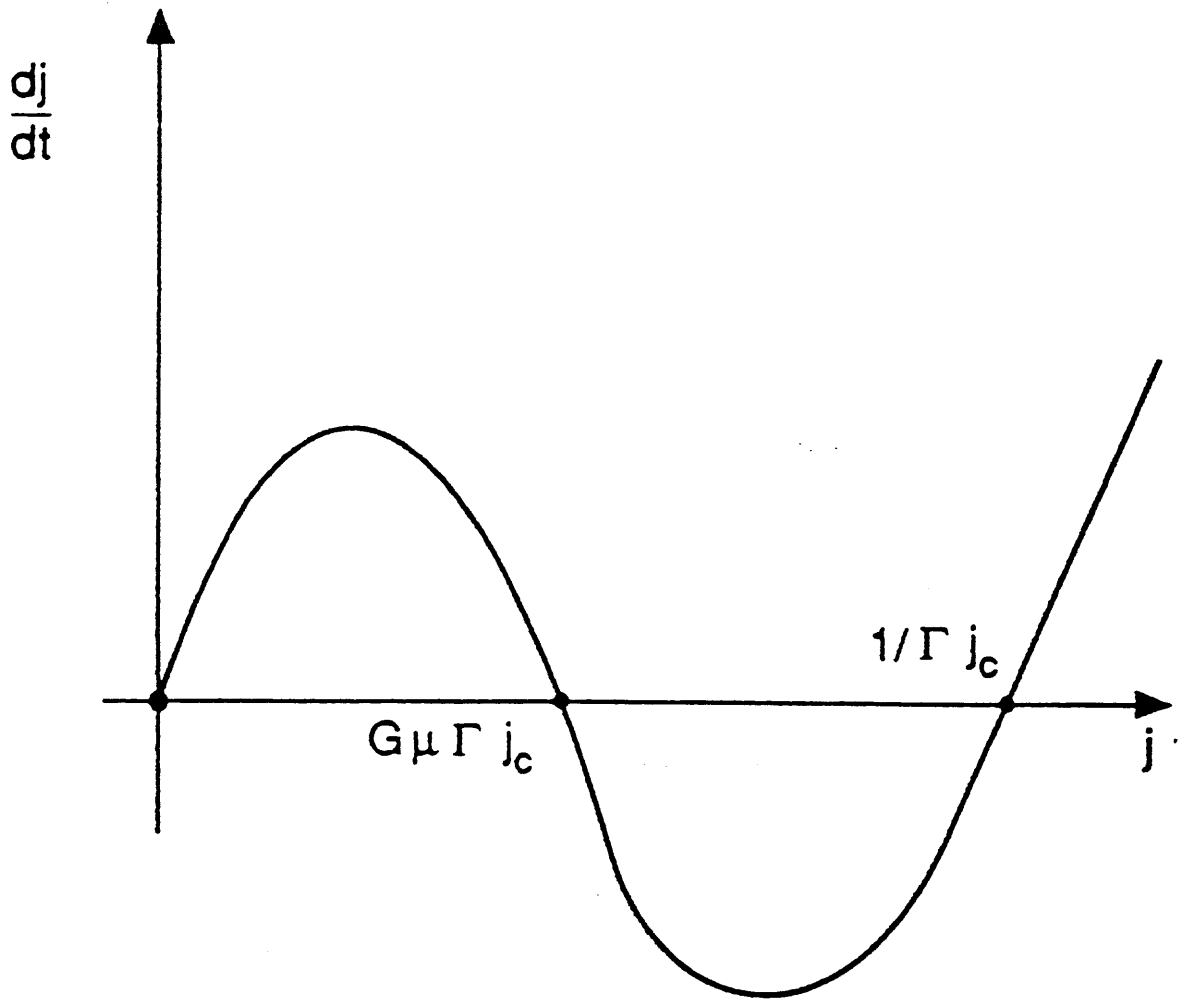


Figure 3.8 A plot of  $\frac{dj}{dt}$  versus  $j$ .

$\Gamma_{EM} \sim \Gamma_{GR}$  and  $\Gamma^2 G_\mu j_c^2 \ll 1$ . For very small initial  $j$  gravitational radiation causes  $j$  to rise until  $j \sim G_\mu \Gamma j_c \sim 10^{-4} j_c$ . This is too small to cause the explosions required by OTW. Now however we have reached a stable fixed point. Any larger initial current, up to  $\sim 1/(\Gamma j_c)$  (which for  $\Gamma \sim 100$ ,  $j_c < 10^{-1}$  is always greater than  $j_c$ ), will cause a negative  $\frac{dj}{d\tau}$  and thus loss of current. The timescale for current loss is  $\tau \sim \frac{L j_c}{j} 10^3$ .

## Section 6. Summary and Discussion

In this chapter we have presented the results of a detailed study of the dynamics of, and the radiation emitted from, superconducting strings. We have derived an approximate local action for a current carrying vortex line and presented some exact solutions to its equations of motion. These included 'static' spring solutions which we showed were stable to small perturbations. The subject of the next chapter will be 'for what values of parameters can springs form?' Here let us assess the cosmological implications of their formation [3.21,3.8].

Even in the absence of primordial magnetic fields current will be present on a loop at its formation. When the  $\chi$  condensate forms the phase of the  $\chi$  field will be uncorrelated on scales  $\epsilon_0 < t_0$  (the time of the phase transition). If we have a loop of size 'l' one might

expect a net phase change of  $O(\sqrt{1/\epsilon_0})$  and therefore (using (3.1.20)) a current  $j_{\text{kibble}} \sim \sqrt{(\kappa_{\text{eff}}/\mu)} \sqrt{1/\epsilon_0 l}$ . Since  $j_{\text{spring}} < j_{\text{critical}}$  cusps are never formed and current will therefore not be lost. Thus as the loop oscillates and radiates the current will build up to  $j=1$  at which time  $l_{\text{spring}} \sim \sqrt{(\kappa_{\text{eff}}/\mu\epsilon_0 l)} l$ . What happens to these springs? They will look like magnetic dipoles. Since the force between dipoles is weaker than that between monopoles we do not expect annihilation to prevent them from dominating the energy density of the universe. The dipoles will eventually decay by tunnelling but, as we will show in chapter 4, the lifetime of the current on the spring when  $j=j_{\text{spring}}$  is similar to that when the current is very small. Thus if we want the current to last an astrophysically interesting time the springs will as well. Neglecting annihilation then, let us estimate the energy density in springs. Roughly speaking we would expect the birth rate of loops of size  $l \sim t$  to be  $t^{-4}$  (the same as for non-superconducting strings [3.21]). Therefore

$$\rho_{\text{springs}}(t') \sim \int_{t_f}^{t_1} dt t^{-4} E_{\text{spring}}(t) (a(t)/a(t'))^3$$

$t_1$  = time at which the latest loops which become springs at  $t'$  are formed

$t_f$  = time when friction effects become negligible so the loops can start to oscillate and therefore radiate freely  
 $\sim (G\mu)^{-2} t_{\text{plank}} [3.23]$

$a(t)$  is the scale factor at time  $t$ .

Estimating  $\epsilon_0 \sim t_0$  we obtain [3.22]

$$\rho_{\text{spring}} \sim \frac{t^{-3/2} \mu^{1/2} T^2}{m_{\text{plank}}^4}$$

Requiring that  $\Omega = (\rho/\rho_{\text{critical}})$  today be less than 2 means that  $\mu < 10^{13}$  GeV. According to OTW the explosive scenario of galaxy formation requires  $\mu \sim 10^{16}$  GeV and so regions of parameter space where springs are formed can be ruled out if we are interested in their scenario.

In the last section we saw that for  $j_c < 10^{-1}$  current loss rather than current gain occurs as a loop with cusps radiates and shrinks. One might say, so what! Kinky loops without cusps are generically formed. In section 4 we showed that kinks are probably rounded out on a time scale faster than the time for significant electromagnetic radiation to occur. Thus kinks are rounded out on a length scale larger than the total length of string lost - leading to the formation of cusps and the loss of current as detailed in section 5.

If current building due to loop shrinkage can be ruled out, what about the possibility of large currents being induced in loops by large primordial magnetic fields as they form? As OTW discussed, a magnetic field will induce a current in loops of order the Hubble radius  $j_i \sim \sqrt{\rho_m} / \sqrt{\rho_{\text{bac}}}$  (where  $\rho_m$  is the magnetic field energy density and  $\rho_{\text{bac}}$  is the background energy density) in a newly formed loop. The electromagnetic radiation will only

be significant compared to the gravitational radiation initially if

$$P_{EM} = \Gamma_{EM} \mu j^2 > P_{GR} = \Gamma_{GR} G \mu^2$$

$$j > \sqrt{(G \mu (\Gamma_{GR} / \Gamma_{EM}))} \sim 10^{-3}$$

This requires a primordial B field with  $\sim 10^{-6}$  of the energy density of the background. This is difficult to rule out at present but may in the future be a problem for their scenario.

There is perhaps another way in which large a/c currents could be produced. It is possible that the coupling of the electromagnetic field between different parts of an oscillating loop could lead to a dynamo effect.

From the above discussion it is clear that, to date, it is far from certain that the explosive scenario of galaxy formation is plausible. Further work is still needed in order to check the scenario is consistent with astronomical observations.

#### Appendix: The Global String Action.

In this Appendix, using the techniques outlined in section 3.1 we derive the action for a global string.

The simplest theory that posses global string solutions is the goldstone model of a self-interacting

scalar field described by the action

$$S = \int d^4y \left( (\partial_\mu \Phi)^\dagger (\partial^\mu \Phi) - \frac{1}{2} \lambda (\Phi^\dagger \Phi - \eta^2)^2 \right) \quad (\text{A.1})$$

Performing the coordinate transformation

$$y^a = x^a(\sigma) + n_A^a(\sigma) \rho^A \quad (\text{3.1.3})$$

and substituting the ansatz  $\Phi = \Phi_S$  (where  $\Phi_S$  was given in (3.1.2)) into the action (A.1) we obtain

$$\begin{aligned} S_{\text{string}} &\approx \int d\sigma d\tau \sqrt{-\gamma} \left( \int_{V_S} d^2\rho L'(\rho) + \int_{V_O} d^2\rho \eta^2 f^2(\rho) \partial_\mu \theta \partial^\mu \theta \right) \\ &\approx -\mu \int d\sigma d\tau \sqrt{-\gamma} + \int_{V_O} d^4x \eta^2 \partial_\mu \theta \partial^\mu \theta \end{aligned} \quad (\text{A.2})$$

where  $V_S$  is the volume of the string and  $V_O$  the remaining volume. In writing these expressions we have assumed that  $\theta$  is a slowly varying function so that the width  $\delta \sim (\sqrt{(\lambda)\eta})^{-1}$  is well defined. The  $\theta$  field must also satisfy the constraint

$$\int dx^\mu \partial_\mu \theta = 2\pi b \quad (\text{A.3})$$

where  $b$  counts the number of times the surface  $S$  bounded by  $C$  cuts the string. This constraint makes the action (A.2) rather difficult to use in studies of the motion and radiation from global strings. We now therefore seek a classically equivalent action (i.e. one with the same



equation of motion and energy momentum tensor) in which the constraint can be written in a local form.

The equation of motion for the  $\theta$  field is

$$\partial_{\mu} \partial^{\mu} \theta = 0 \quad (\text{A.4})$$

which implies that

$$\partial_{\mu} F^{\mu} = 0 \quad \text{where} \quad F^{\mu} = \partial^{\mu} \theta$$

This suggests that we should introduce an antisymmetric tensor field defined by

$$\epsilon^{\mu\nu\rho\sigma} \partial_{\nu} A_{\rho\sigma} = \partial^{\mu} \theta$$

outside the string (note  $\theta$  is not defined in the string, the definition of  $A$  there will be given later). The equation of motion (A.4) is then just an identity for the  $A$  field. The identity

$$\epsilon^{\mu\nu\beta\psi} \partial_{\nu} \partial_{\beta} \theta = 0$$

$$\epsilon^{\mu\nu\beta\psi} \partial_{\nu} (\epsilon_{\beta}^{\kappa\eta\gamma} \partial_{\kappa} A_{\eta\gamma}) = 0$$

for the  $\theta$  field gives the equation of motion for  $A$ . The appropriate action to give this equation of motion is

$$C S = \int d^4y (\epsilon_{\mu\nu\beta\alpha} \partial^\nu A^{\beta\alpha})^2$$

where C is a constant. The global constraint (A.3) can be written as a local constraint for the A field.

$$\int_c dx^\mu (\epsilon_{\mu\nu\beta\alpha} \partial^\nu A^{\beta\alpha}) = \iint_S d\Sigma^{\mu\nu} \partial_\mu (\epsilon_{\nu\beta\alpha\phi} \partial^\beta A^{\alpha\phi}) = 2\pi b n$$

Here we have used Stokes theorem. We now define A in the string by

$$\epsilon^{\mu\nu\beta\alpha} \epsilon_{\beta\alpha\sigma\delta} \partial_x^\alpha \partial^\sigma A^{\delta\delta} = 8\pi n \int_{\text{string}} dy^\mu \wedge dy^\nu \delta^4(x - y(\sigma, \tau))$$

world sheet

W

The local constraint can be incorporated into the action using Lagrange multiplier techniques to obtain

$$C L = (\epsilon^{\mu\nu\beta\alpha} \partial_\nu A_{\beta\alpha})^2 + \lambda_{\alpha\beta} (\epsilon_{\mu\nu\alpha\phi} \epsilon^{\alpha\beta\mu\delta} \partial_\delta \partial^\nu A^{\alpha\phi} - 8\pi n \int_W dy^\alpha \wedge dy^\beta \delta^4(x - y(\sigma, \tau)))$$

The equation of motion for the A field relates A to  $\lambda$ . This relationship may be used to eliminate A from the lagrangian to obtain

$$C L = - (\epsilon^{\mu\nu\beta\alpha} \partial_\nu \lambda_{\beta\alpha})^2 - 8\pi n \int_W dy^\alpha \wedge dy^\beta \delta^4(x - y(\sigma, \tau)) \lambda_{\alpha\beta}$$

In order to fix the constant C we require that the energy

momentum tensor for the two fields  $\theta$  and  $\lambda$  to be the same. After some algebra we find  $C=-(1/4)$ . Thus we finally obtain

$$S = \frac{1}{2} \int d^4y (\epsilon^{\mu\nu\beta\alpha} \partial_\nu \lambda_{\beta\alpha})^2 + 2\pi\eta \int d\sigma^{\alpha\sigma} \lambda_{\alpha\sigma} - \mu \int d^2\sigma$$

This is the same as the action proposed by Lund and Regge [3.13] to describe global strings and that used by Vilenkin and Vachaspati [3.24] when they estimated the radiation emitted by global strings.

CHAPTER 4: SUPERCONDUCTING STRINGS OR  
SPRINGS

#### Chapter 4. Superconducting Strings or Springs?

For a cosmic string [4.2] to become a bosonic superconductor, an electromagnetically charged field has to develop a vacuum expectation value (VEV) in a localised region around the string [4.1]. Whether it does so or not depends on the details of the dynamics - we have to arrange for it to happen by carefully choosing the relative magnitude of the coupling constants in the potential. How careful do we have to be? In this chapter we answer this question for the simplest theory in which bosonic superconducting strings arise, that defined by equation (3.1.7).

The current carrying state is only metastable. Tunnelling processes exist whereby current is lost. We evaluate the tunnelling rate so we can find the regions of parameter space where the current lasts long enough for interesting astrophysical consequences. Finally we discover what regions of parameter space can be ruled out as cosmologically unacceptable for GUT strings because of the formation of springs.

The Lagrangian we use is

$$\begin{aligned}
 L = & |D_\mu \Phi|^2 + |D_\mu \chi|^2 + \frac{1}{2} (\underline{E}^2 - \underline{B}^2) - \frac{1}{2} \lambda_1 (|\Phi|^2 - \eta^2)^2 \\
 & - \frac{1}{2} \lambda_2 |\chi|^4 - \lambda_3 (|\Phi|^2 - m^2) |\chi|^2 \quad (3.1.7) \\
 & - \frac{1}{4} R^{\mu\nu} R_{\mu\nu}
 \end{aligned}$$

which has the global vacuum manifold  $\Phi = \eta, \chi = 0$  as long as [chapter 3, 4.1, 4.8]

$$m^2 < \eta^2 \quad \lambda_1 \lambda_2 > \lambda_3^2 (m/\eta)^4 \quad (4.1)$$

For simplicity, in this chapter we shall set the gauge couplings to be equal and then explore parameter space for the dimensionless quantities  $\lambda_1, \lambda_2, \lambda_3$  and  $\mu=m/\eta$ . We shall understand the region of parameter space in which condensates form using qualitative arguments which we have checked numerically (see below). These arguments confirm and explain the results of [4.4, 4.5] but our conclusions are rather different because we have the additional requirement on the lifetime of the metastable current carrying state.

First, let us ask in which region of parameter space is it energetically favourable for a  $\chi$  condensate to form on the string. To do this we follow Witten [4.1] and look at the stability of the U(1)' string solution with  $\chi=0$  and  $A_\mu=0$  everywhere. The equation for small fluctuations in  $\chi$  in the presence of  $\phi$  is

$$\ddot{\chi} - \nabla^2 \chi + \lambda_3 (|\phi|^2 - m^2) \chi = 0 \quad (4.2)$$

We look for solutions of this equation of the form  $\chi(x,y,z,t) = e^{-i\omega t} \chi_0(x,y)$ . This reduces (4.2) to

$$\left( -\frac{\partial^2}{\partial x^2} - \frac{\partial^2}{\partial y^2} \right) \chi_0 + v(r)\chi_0 = \omega^2 \chi_0$$

$$V(r) = \lambda_3 (|\phi|^2 - m^2)$$

which is just a two dimensional Schrödinger equation. If a bound state solution with  $\omega^2 < 0$  exists then the string solution with  $\chi = 0$  is unstable and the  $\chi$  field will evolve to a lower energy state with  $\chi \neq 0$ . For  $m^2 = \eta^2$  the potential is negative definite and a bound state always exists [4.1, 4.6]. We shall discuss the solution in this special case later. For  $m^2 < \eta^2$  the situation is more complicated. The potential is a well of width  $W \approx m_\phi^{-1} \approx (\sqrt{\lambda_1} \eta)^{-1}$  and depth  $U = \lambda_3 \eta^2$ . If the dimensionless strength of the potential,  $UW^2 \approx \lambda_3/\lambda_1$ , is large then the potential is strong enough to localize the wavefunction  $\chi$ . In this case (adding  $\lambda_3 m^2$  to the energy) we can approximate the ground state energy to be just that of an harmonic oscillator with  $E_0 = (\lambda_1 \lambda_2)^{1/2} \eta^2$ . By subtracting  $\lambda_3 m^2$ , we find the ground state energy is negative if  $\mu^2 > (\lambda_1/\lambda_3)^{1/2}$  which is much less than unity. Thus for large  $\lambda_3/\lambda_1$  a wide range of  $m/\eta$  gives a condensate. If however,  $\lambda_3/\lambda_1$  is small we have the opposite limit in which we can treat the wavefunction as essentially constant across the potential. Subtracting  $\lambda_3(\eta^2 - m^2)$  from the energy so that we have a negative definite potential, by a standard result [4.6, page 163] for weak potentials the ground state energy is

$$E_0 \approx -e^{-1/(UW^2)} \frac{-2}{W} \approx -\lambda_1 \eta^2 e^{-\lambda_1/\lambda_3}$$

which is exponentially small. Adding back  $\lambda_3(\eta^2 - m^2)$  the ground state energy is only negative if

$$\mu^2 > 1 - (\lambda_1/\lambda_3)e^{-\lambda_1/\lambda_3},$$

which is very close to unity. So for  $\lambda_3 \ll \lambda_1$  there is very little  $\mu$  parameter space corresponding to a condensate (These results explain those of [4.5] especially their figure 4 where the allowed range of  $\beta = (\lambda_3/\lambda_1)$  is plotted for different values of  $\alpha = (\lambda_3\mu^2/\lambda_1)$  ).

The second condition in equation (4.1) restricts us to the region  $\lambda_3^2 \mu^4 < \lambda_1 \lambda_2$ , and requiring a reasonably large  $\mu$  parameter space means that  $\lambda_1 < \lambda_3 \mu^4$ . Hence  $\lambda_3 \mu^2$  is bounded above by  $(\lambda_1 \lambda_2)^{1/2}$  and below by  $\lambda_1/\mu^2$  (Figure 4.1). Using  $\mu^2 < 1$  we can exhibit a weak but convenient bound on the couplings:

$$\lambda_1 < \lambda_3 < \lambda_2 \tag{4.3}$$

Let us first assess the classical stability of the current carrying state. We shall construe an effective Hamiltonian for a loop of string of radius R carrying a constant current, from which the classical critical current is defined as the current at which the superconducting  $\chi \neq 0$  minimum disappears. If this happens



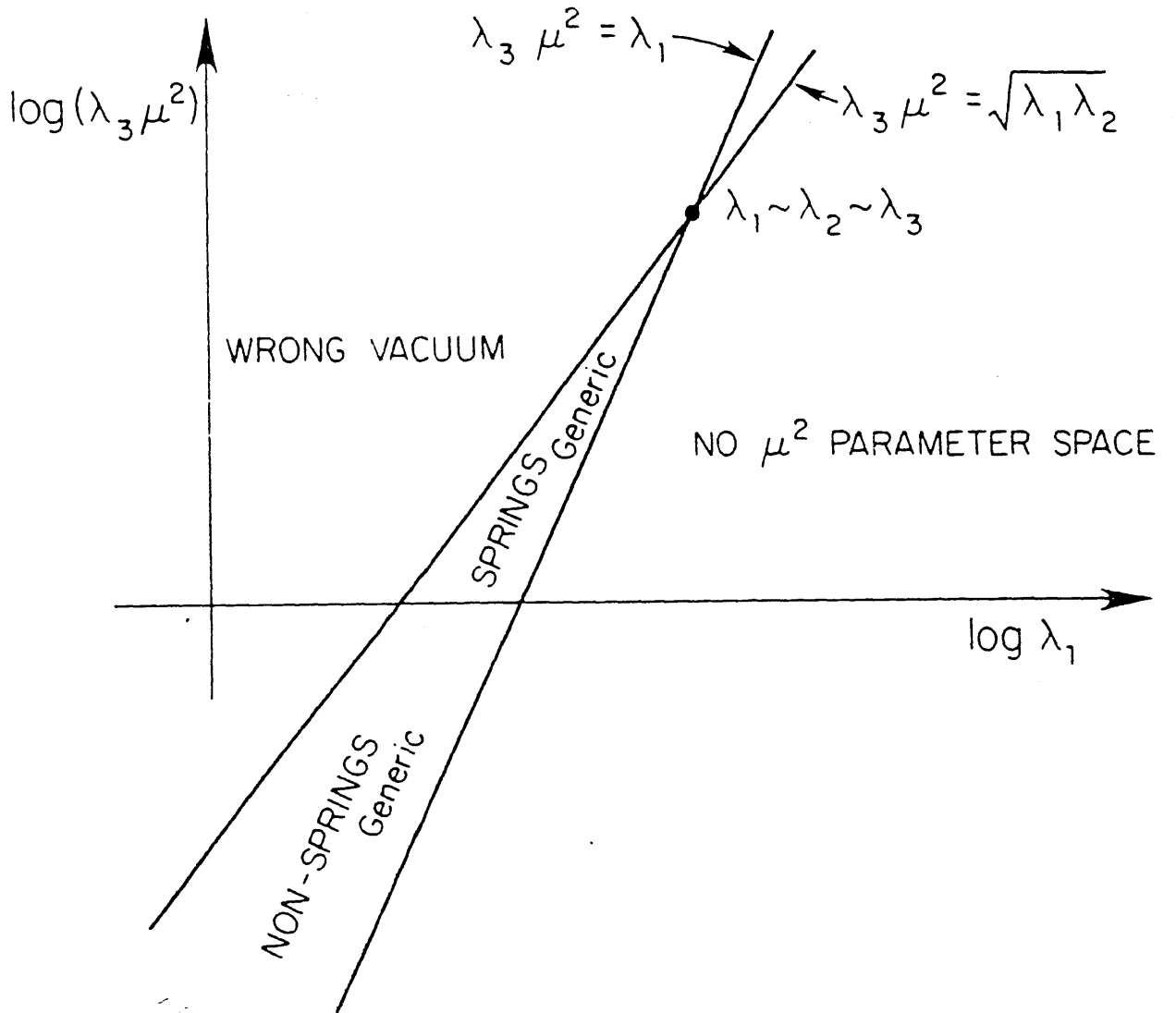


Figure 4.1 A diagram showing the region of parameter space in which a string will be superconducting.

above the 'spring current', where the pressure from the current and associated field balances the string tension, then springs are stable solutions to the classical field equations. We shall then estimate the quantum stability of such a configuration: it transpires that springs are extremely long lived.

The current carrying state corresponds to

$$\chi = \chi_0(\rho)e^{i\theta(\sigma)}$$

$$J_\alpha = 2e\kappa(\partial_\alpha\theta + eA_\alpha) = 2e\kappa_{\text{eff}}\partial_\alpha\theta \quad (4.4)$$

( $\alpha=0,1$ ) where (see chapter 3)

$$\kappa = \int d^2\rho \chi_0(\rho)^2 \quad (4.5)$$

$$\kappa_{\text{eff}} = \frac{\kappa}{1 + (e^2\kappa/\pi)\ln(R/W')} \quad (4.6)$$

Here,  $R$  is the radius of the string loop and  $W' \sim m_\chi^{-1}$  is the width of the condensate.

We shall assume that the  $\phi$  and  $A$  fields remain unchanged as the current increases, and that the  $\chi$  field can be written as  $\chi = \chi_0(\rho, J=0)a(t, \sigma)$  where 'a' includes a phase and an overall amplitude. This latter assumption is that the presence of the current does not affect the width. Numerically (see below) we found that this was a good approximation in regions of parameter where springs are formed. Indeed, it is only because the  $\chi$  field is

little affected by the current that springs can form at all.

Substituting this ansatz into the action, integrating over  $\rho$  and using the equation of motion of  $\chi_0$  to eliminate the radial gradient term we obtain the effective two dimensional lagrangian:

$$L_a^{(2)} = \kappa |D_\alpha a|^2 - (\lambda_2/2)\kappa_4 (|a|^4 - 2|a|^2) \quad (4.7)$$

with

$$\kappa_4 = \int d^2\rho \chi_0^4 \quad (4.8)$$

Next we must include the contributions of the gauge fields by solving for  $A_\alpha$  in terms of  $J_\alpha$ . The variation in  $A_\alpha$ ,  $\Delta A_\alpha \sim J_\alpha (\rho/W')^2$  is small compared to its value at the centre of the string [4.3] so we will treat it as constant across the string. Thus the gauge field contribution is

$$\begin{aligned} L_A^{(2)} &= (1/2) \int d^2\rho ( \underline{E}^2 - \underline{B}^2 ) \\ &\approx (1/4\pi) J_\alpha^2 \ln(R/W') \end{aligned} \quad (4.9)$$

So the full effective two dimensional Lagrangian for the field 'a' can be written as:

$$\begin{aligned} L^{(2)} &= \kappa (\partial_\alpha |a|)^2 - (\lambda_2/2)\kappa_4 (|a|^4 - 2|a|^2) \\ &\quad + \kappa |a|^2 \frac{(\partial_\alpha \theta)^2}{(1 + v^2 a^2)} \end{aligned} \quad (4.10)$$

where

$$v^2 = (e^2 \kappa / \pi) \ln(R/W') \quad (4.11)$$

Let  $p^2 = -(\partial_\alpha \theta)^2$ , which is positive for space-like current on the string. The contribution to the potential from the current is positive and flat above  $a \approx v^{-1}$ . Thus if  $\kappa$  is large, that is if  $v^2 \gg 1$ , the position of the minimum is affected very little by the current. In fact, in this limit, the superconducting minimum disappears only when

$$p^2 = p_c^2 = \left( \frac{4}{27} \right) \frac{\lambda_2 \kappa^4}{\kappa} \left[ \frac{e^2 \kappa}{\pi} \ln \left( \frac{R}{W'} \right) \right]^2 \quad (4.12)$$

The 'spring current' is determined by equating the energy per unit length in the current with the string tension  $T \sim \eta^2$  (see chapter 3). Hence

$$p_s^2 = \frac{T(1 + v^2 |a|^2)}{\kappa |a|^2} \quad (4.13)$$

Springs are not stable if  $p_s^2 > p_c^2$ . We estimate  $\kappa_4$  and  $\kappa$  by taking  $|\chi_0|^2 \sim (\lambda_3 m^2 / \lambda_2)$  and

$$W'^2 \sim \begin{cases} 1/\lambda_3 \eta^2 (1 - \mu^2), & \text{if } \lambda_1 > \lambda_3 (1 - \mu^2) \\ 1/\lambda_1 \eta^2, & \text{if } \lambda_1 < \lambda_3 (1 - \mu^2) \end{cases} \quad (4.14)$$

The width in the second case being determined by that of the vortex. Thus classically, for large  $\kappa$  there are no springs if

$$\lambda_3 \mu^2 \lesssim (1/v^2 \kappa) \quad (4.15)$$

Now suppose that instead  $\kappa$  is small so that  $v^2 \ll 1$ . In this case our approximation of treating the radial dependence of the fields as fixed is no longer valid. Nevertheless we can see in a rough way that springs do not exist in this region of parameter space. The minimum of the potential in (4.10) goes to zero when

$$p^2 = p_c^2 \approx \frac{\lambda_2 \kappa^4}{\kappa} \quad (4.16)$$

Comparing this with the spring current we find that for small  $\kappa$  springs do not exist anywhere.

Thus the conclusion from our analytic method is that springs generically exist <sup>classically</sup> when  $\kappa \gg 1$ , as long as  $\lambda_3 \mu^2$  is not too small. Since  $\kappa$  is roughly the inverse of a quartic coupling constant we can expect it to be substantially larger than unity in a perturbation theory.

So far our results have been very qualitative, and our arguments only approximate. We have therefore checked them numerically for some particular values of the coupling constants.

To do this we have used a simple 'relaxation method'. The energy per unit length is simply written as a function of the gauge and Higgs fields and the radial integral approximated numerically (we used the trapezium rule). Now we have the Hamiltonian of a mechanical system and we proceed to minimize it as follows. Consider adjusting the  $\phi$  field at site  $n$  ( $\phi_n$ ), while keeping all the other discretised field variables fixed. To minimize the energy one solves  $\partial H/\partial \phi_n = 0$ . This is a cubic equation and so its roots are easily found. In fact there is a unique solution provided the spatial step is small enough. One starts with an ansatz for the fields and, keeping the appropriate boundary values fixed, evolves the fields at each site in turn to minimize the Hamiltonian.

The electromagnetic gauge field is treated in a slightly different way. We solve for  $A_\sigma$  in terms of  $p$  and again treat it as constant across the string so that the current contributes a term

$$\frac{|\chi|^2 p^2}{(1+v^2 \int d^2 \rho' |\chi(\rho')|^2)} \quad (4.17)$$

to the Hamiltonian.

In the program distances are expressed in dimensionless units  $\xi = e\eta\rho$ , the fields are scaled by  $\eta$ , and the Hamiltonian depends on the couplings in the ratio  $\lambda_1/e^2 \dots$  etc. Thus the program uses and calculates  $e^2\kappa$  (rather than  $\kappa$ ), and the only extra parameter we have to

choose is the value of the logarithm which we take to be 100. This corresponds to GUT scale strings of radius about  $10^{12}m$ . The spring current is the current at which the energy per unit length in the current is exactly half the total energy of the string: since the current term contributes to the pressure with the opposite sign to the rest of the energy [4.3] this is the current at which the effective tension vanishes. The critical current is the current at which the condensate vanishes.

The algorithm converges very rapidly for ordinary local strings and gives an accuracy of better than one per cent for their energy if we have of order ten points per string width  $\sim(\lambda_1\eta^2)^{-1/2}$ . For the superconducting case a few minutes of VAX cpu time is needed for convergence. We ran this algorithm for various couplings to confirm the arguments stated before. We required that the condensate energy changed by less than one part in  $10^6$  in fifty 'time steps' (i.e. evolving each radial point fifty times) before we accepted the solution as having converged.

In Table 4.1 we have listed some results of our program. We display  $e^2\kappa$ ,  $p_S^2$  and  $e^2\kappa_S$  (where  $\kappa_S$  is defined as  $\int d^2\rho |\chi|^2$  at the spring current  $p_S$ ) for various values of the parameters  $\lambda_i/e^2$  ( $i=1,2,3$ ) and  $\mu$ . For example, the first entry is clearly a spring:  $e^2\kappa$  is large, so the effective Hamiltonian is flat above a small value of 'a', and even at the spring current  $e^2\kappa$  is hardly changed, showing that there is very little back reaction on the

condensate. The second entry has  $\lambda_3$  made sufficiently small to satisfy the bound (4.15): we find that the critical current is reached before the spring current. The third entry shows a situation where  $e^2\kappa$  is small. Our analysis suggests that this should not form a spring which we indeed find to be the case. The last entry with  $\mu = 1$  is a spring. This is discussed below.

Table 4.1: Some results from the numerical solutions of the string field equations.

$\mu$	$(\lambda_1/e^2)$	$(\lambda_2/e^2)$	$(\lambda_3/e^2)$	spring?	$e^2\kappa$	$e^2\kappa_s$
0.95	0.01	0.4	0.06	yes	23.9	22.8
0.90	0.02	2.0	0.20	no	4.5	-
0.90	0.10	1.20	0.40	no	2.6	-
1.00	2.00	4.0	2.00	yes	*	*

\* Note that with  $\mu=1$ ,  $e^2\kappa$  is logarithmically divergent.

The importance and meaning of  $\kappa$  becomes clearer when we study the stability of the current on the string against the tunnelling of flux through the condensate. This can happen when a quantum fluctuation takes 'a' to zero somewhere and an instanton electric flux tube appears in the worldsheet. The appropriate procedure to calculate the probability for such an event is to find the action of the instanton solution of the Euclidean equations of



motion [4.7]. This means minimising the Euclidean action  $S_E$  given by:

$$S_E = \kappa \int d^2\sigma (|D_\alpha a|^2 + (\lambda_2 \kappa_4 / 2\kappa) (|a|^2 - 1)^2) + \int d^2\sigma d^2\rho (1/2) (\underline{E}^2 + \underline{B}^2) \quad (4.18)$$

where we have shifted the potential so that the Lagrangian vanishes away from the instanton. The contribution from the electromagnetic field extends off the worldsheet; however, the main contribution comes from the centre of the Euclidean vortex near the string so we believe that a good approximation to  $S_E$  is obtained by cutting off the electric field beyond  $l \sim W'$ . Scaling the gauge field  $A_\alpha = \Omega \tilde{A}_\alpha$  and the coordinates  $\sigma_\alpha = \Omega^{-1} \tilde{\sigma}_\alpha$  with  $\Omega = (\kappa)^{1/2} / l\pi$ , we obtain:

$$S_E \approx \kappa \int d^2\tilde{\sigma} (|\tilde{D}_\alpha a|^2 + (1/2) \lambda_I (|a|^2 - 1)^2 + (1/2) \tilde{E}_\sigma^2) \quad (4.19)$$

where  $\lambda_I = \pi \lambda_2 \kappa_4 l^2 / \kappa^2$ . Apart from the factor  $\kappa$  this is just the action of a truly two dimensional vortex. Hence

$$S_E \approx 2\pi\kappa f(\lambda_I / e^2) \quad (4.20)$$

where  $f$  is a slowly increasing function well known from vortex studies [4.8, 4.5], and  $f(1)=1$ . A naive estimate gives  $\lambda_I \sim \lambda_2$ . Note however that  $S_E$  is relatively

insensitive to the precise value of  $\lambda_I$ .

In the usual way [4.7] the tunnelling rate per unit length is estimated as  $\Gamma \approx m_{\chi}^2 S_E e^{-S_E}$ , thus the larger  $\kappa$  is, the lower the tunnelling rate. Physically,  $\kappa$  is proportional to the square of the number of penetration depths across the superconducting string. This is easy to understand: in order to lose flux from a loop of string we must move it through the string in a vortex line of length  $W'$  and mass per unit length of about  $|\chi|^2$ . The action for this process is roughly  $|\chi|^2 W'^2 \approx \kappa$ .

This physical intuition gives us the confidence to extend this calculation to all currents. We expect the tunnelling action at winding  $p$  to be essentially  $2\pi \int d^2\rho |\chi(\rho)|^2 = 2\pi\kappa |a|^2$  where 'a' is the value of 'a' that minimises the effective Hamiltonian for a particular  $p$ . But we have seen that for large  $\kappa$ , that is in the classical spring regime,  $\kappa_S \approx \kappa$ , both analytically and in our numerical solutions. So we can say that when  $\kappa \gg 1$  the lifetime of the current on the string is the same whether it is a tiny fraction of its critical value or whether it is the spring current. Now suppose we require that small currents persist on the string long enough for astrophysical consequences. For example, the OTW [4.9] scenario conservatively requires a current of  $10^{-3}T$  ( $T \sim 10^{16} \text{GeV}$ ) on a string formed at decoupling ( $t \sim 10^{12} \text{s}$ ) to persist for at least one oscillation. If  $N \sim pR$  is the total winding of  $\theta$  on the loop,  $N$  tunnelling events are

required. So using the estimate of the tunnelling rate we require:

$$S_E - \ln S_E > \ln (m_\chi^2 L^2 / N) \sim 125 \quad (4.21)$$

Hence we need  $\kappa \gtrsim 20$ . This is the region of parameter space where classical springs are generic and in which we saw that  $\kappa_S \sim \kappa$ . We can therefore state an important conclusion, long lived currents for astrophysics tend to require theories in which springs are equally long lived. This is cosmologically disastrous [4.10, chapter 3]. Of course, we cannot rule out the superconducting string scenarios on this basis because we can always tune  $\lambda_3$  to smaller values so that condition (4.15) is satisfied. This also necessitates a tuning of either  $\lambda_1$  or  $\mu$ . It may be thought 'unnatural' to have quartic couplings of different orders of magnitude particularly if  $\phi$  and  $\chi$  belong to the same representation of a grand unified gauge group, and in this sense springs are a real problem.

Finally, we consider the case where  $\mu$  is very close to one, that is when  $m_\chi \ll m_\phi$  in the broken phase (assuming the ratio of  $\lambda_3$  to  $\lambda_1$  is not very small). We know that this is in a sense a 'natural' state of affairs because of the smallness of the weak scale relative to the GUT scale. From the arguments above a condensate exists for a wide range of  $(\lambda_3/\lambda_1)$  so we can say that, unless a symmetry ensures  $\lambda_3=0$ , a condensate nearly always exists. The value of  $\kappa$  will be large as the following argument makes clear. If we set  $m^2 = \eta^2$  exactly, as we pointed out the potential still has the correct minimum. However the  $\chi$

field is now 'massless' at infinity. What happens? The  $\chi$  field equation of motion becomes for large  $\rho$

$$\frac{1}{\rho} \frac{\partial}{\partial \rho} \left( \rho \frac{\partial \chi_0}{\partial \rho} \right) = \lambda_2 \chi_0^3(\rho) \quad (4.22)$$

which has the solution

$$\chi_0(\rho) = 1/(\sqrt{\lambda_2} \rho) \quad (4.23)$$

Thus the usual  $e^{-\sqrt{(\lambda_3(\eta^2 - m^2))\rho}$  dependence changes into a power law. We show a numerical solution in Figure 4.2 for a case in which we have verified the asymptotic behaviour.

Since the energy density falls off as a power law,  $\propto 1/\rho^4$ , the energy depends as  $1/\rho_c^2$  on the cutoff radius  $\rho_c$ . Therefore such strings would have a long range scalar attractive force  $F \propto 1/\rho^3$  (in addition of course to any electromagnetic force), and  $\kappa$  would be logarithmically divergent. However, if  $\chi$  has a small mass in vacuo then  $\kappa \sim \ln(m_\phi/m_\chi)/\lambda_2$  which for GUT and weak scales is roughly  $50/\lambda_2$ . Thus, contrary to our naive expectation, strings are generic when  $m_\chi \ll m_\phi$  unless the coupling between the fields are very small.

NOTE ADDED

It has recently been suggested (R.Davis and P.Shellard, private communication) that to obtain strings with current alone we depend strongly on taking a large

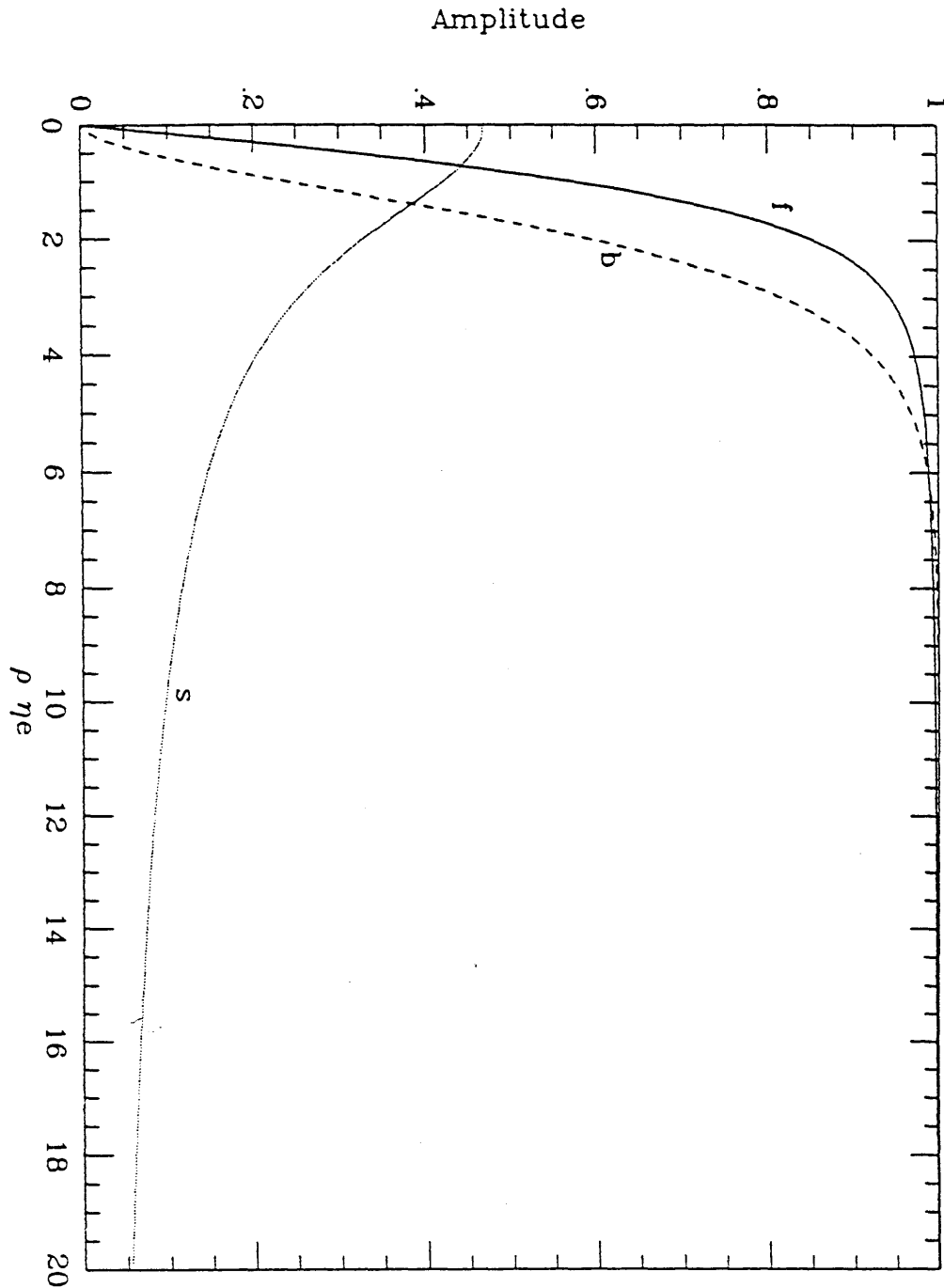


Figure 4.2 The field profiles for a string with  $\mu=1$ ; 'f' and 's' are the  $\phi$  and  $\chi$  scaled by  $\eta$ , while b is the azimuthal component of the gauge field scaled by  $\eta$  and multiplied by e .

logarithm. We have checked the spring solutions in the table and have found that they remain springs down to a log of 20, corresponding to a size of  $10^{-23}$ m.

CHAPTER 5: THE EFFECT OF TOPOLOGICAL  
DEFECTS ON PHASE TRANSITIONS  
IN THE EARLY UNIVERSE

## CHAPTER 5. The effect of Topological Defects on Phase Transitions in the Early Universe

It has previously been demonstrated by Weinberg and others [5.2], that at sufficiently high temperatures, it is possible to restore the full gauge symmetry of a spontaneously broken simple gauge group that could describe the interaction of particles. The big bang model suggests that the universe was once very hot and dense and at these high temperatures we would expect the full symmetry to be manifest. As the universe expanded and cooled it would have undergone a series of phase transitions at which the symmetry was broken. At these phase transitions topological defects may have been formed [5.3]. These may have been monopoles, strings, domain walls, or various combinations thereof, which could have been either superconducting or not [5.6, 5.26].

The presence of these defects in the early universe has intriguing consequences for cosmology. As already discussed, superconducting and 'ordinary' strings play central roles in two different scenarios of galaxy formation. To test these scenarios it is important to understand the properties of the defects and to be able to answer questions such as: At what temperature are they formed? What is their number density and distribution at formation? How does their distribution change as the universe expands?



In this chapter we attempt to answer these questions by developing an analytic description of a phase transition which leads to the formation of strings. We also derive the statistical properties of strings. Our results are in very good agreement with theoretical calculations based on an approach very different to our own [5.1, 5.3], and on computer simulations [5.7, 5.17].

The chapter is divided into four parts. In section 1 we consider one of the simplest theories that displays a phase transition, that of a real scalar field theory. In section 2 we derive the partition function describing the equilibrium properties of a U(1) gauge theory. In section 3 we consider the effects of string formation on the phase transition and show that the dominant contribution to the partition function at temperatures well below the critical temperature comes from the constant field configuration (i.e the mean field approximation is good in this regime). However, as the temperature is increased, the high density of states (entropy) available for the topological defects balances the energy required to form them, and they then make the dominant contribution to the partition function. In this section we also derive the statistical properties of strings and the effect that temperature has on their width and energy per unit length. The final section is devoted to a summary and discussion of our results and their cosmological significance.

Section 1. THE PARTITION FUNCTION FOR A REAL SCALAR  
FIELD THEORY

We shall start our discussion of phase transitions by considering one of the simplest theories that displays one; that of a real scalar field theory with Lagrange density

$$L = \frac{1}{2} (\partial_\mu \phi)(\partial^\mu \phi) + \frac{1}{2} m_0^2 \phi^2 - \frac{\lambda}{4!} \phi^4 \quad (5.1)$$

On taking  $m_0^2 > 0$ ,  $L$  possesses a double well potential which breaks the  $\phi \rightarrow -\phi$  symmetry of the theory.

The partition function of this theory in thermal equilibrium at temperature  $T$  has the path integral representation in terms of Euclidean fields

$$Z \propto \int D\phi \exp[-I_\beta(\phi)] \quad (5.2)$$

where [5.10]

$$I_\beta(\phi) = \int_0^\beta d\tau \int d^3x \left[ -\frac{1}{2} (\partial_\mu \phi)(\partial^\mu \phi) - \frac{1}{2} m_0^2 \phi^2 + \frac{\lambda}{4!} \phi^4 \right] \quad (5.3)$$

The sum over configurations of  $\phi(\tau, \underline{x})$  is restricted to fields periodic in  $\tau$  with period  $\beta$  and we shall take the

signature of our Euclidean space to be -4.

The standard approach to evaluating this partition function is to adopt the mean field approximation. One restricts the path integral to periodic configurations whose Euclidean space-time average is specified in advance to be:

$$\frac{1}{\beta V} \int_0^\beta d\tau \int d^3 \underline{x} \phi(\tau, \underline{x}) = \bar{\phi} \quad (5.4)$$

where  $V$  is the spatial volume of the system. The resulting expression [5.4]:

$$Z(\bar{\phi}) \propto \int D\phi \left[ \delta\left(\bar{\phi} - \frac{1}{\beta V} \int_0^\beta d\tau \int d^3 \underline{x} \phi(\tau, \underline{x})\right) \right] \exp(-I_\beta[\phi]) \quad (5.5)$$

has the following interpretation. Let us couple the field  $\phi(\tau, \underline{x})$  to a constant source  $j$ . The effect of this source is to enable the thermal average  $\langle \phi \rangle$  to take any value we wish (almost), ( $\langle \phi \rangle$  will be constant by virtue of the translational invariance of  $j$  for large  $V$ ). If we now write  $Z$  as

$$Z(\bar{\phi}) = e^{-\beta V V(\bar{\phi})} \quad (5.6)$$

then  $V(\bar{\phi})$  is the Helmholtz energy density (effective potential) of the system when  $j$  is chosen so that

$\langle \phi \rangle = \bar{\phi}$ . With  $V(\bar{\phi})$  satisfying

$$\frac{\partial V}{\partial \bar{\phi}} = 0 \quad (6.7)$$

in the absence of external sources, the thermal average  $\langle \phi \rangle$  for the original system is the value of  $\bar{\phi}$  for which  $V$  is minimised. In principle it is straight forward to compute  $\langle \phi \rangle$  by performing a saddle point expansion for  $Z(\bar{\phi})$  [5.5]. This is equivalent to performing a loop expansion for  $V(\bar{\phi})$ , the generating function for zero momentum Green functions. The existence of a phase transition is already present at the one-loop level and we shall restrict ourselves to this alone.

The calculation is so well known, we shall only quote the result that, at large  $T$ ,  $V(\bar{\phi})$  takes the form:

$$V(\bar{\phi}) = -\frac{1}{2} m_0^2 \left(1 - \frac{T^2}{T_c^2}\right) \bar{\phi}^2 + \frac{\lambda}{4!} \bar{\phi}^4 + \dots \quad (5.8)$$

where

$$T_c^2 = \frac{24m_0^2}{\lambda} \quad (5.9)$$

and one loop renormalisation has been implemented. Higher order terms are suppressed either by a factor  $\frac{\lambda T}{m} \sim \sqrt{\lambda}$ , (near  $T_c$ ) or by a factor of  $\lambda$  [5.2].

There is a possible problem in that  $V$  of (5.8) is not

concave, as the free energy must be [5.5]. We can however ignore this as our interpretation of  $V$  in the remainder of this section will be rather different from that above. Taking (5.8) at face value, we see that, as  $T$  increases from zero to  $T_c$ , so  $\langle \phi \rangle$ , satisfying

$$\langle \phi \rangle^2 = \frac{6m_0^2}{\lambda} \left( 1 - \frac{T^2}{T_c^2} \right) \quad (5.10)$$

decreases smoothly to zero, implying a second order phase transition.

Convexity apart, the picture implied by the effective potential is that the thermal average decreases uniformly across all of space. This is very unlikely to be true. The classical equation of motion derived from (5.1),

$$\left( \square - m_0^2 \right) \phi + \frac{\lambda}{6} \phi^3 = 0 \quad (5.11)$$

permits static domain wall solutions of the form

$$\phi_w(x,y,z) = \eta \tanh\left( \frac{m_0 z}{\sqrt{2}} \right) \quad (5.12)$$

[5.11], [where we have taken a wall in the  $x$ - $y$  plane as an example]. The field  $\phi$  flips value across this wall from  $-\eta$  to  $\eta$ , where  $\eta^2 = \frac{6m_0^2}{\lambda}$ . A much more likely scenario for the phase transition is that, as the temperature is

increased, more and more domain wall area will be formed until the whole of space is filled at which point the symmetric phase  $\langle \phi \rangle = 0$  is achieved. That is, the effective potential description corresponds to the averaging of a much more complicated structure. Until we are very close to the phase transition, however, we would expect the effective potential averaging to be reliable since the domains will be large (see later).

To evaluate the effect of this domain wall formation on the temperature and nature of the phase transition some care has to be taken. The thickness of a domain wall at zero temperature is  $\zeta = O(m_0^{-1})$  and its surface tension  $\sigma = O(\frac{m_0^3}{\lambda})$ . Calculations that rely on holding these fixed at finite temperature [5.12] will give the wrong answer. The long range correlations that are associated with a phase transition arise because the effective scalar mass  $m_{\text{eff}} = (\frac{\partial^2 V}{\partial \phi^2} \Big|_{\phi=\bar{\phi}})^{1/2}$  vanishes at  $T = T_c$ . The effect of non-zero temperature (to  $O(\lambda)$ ) on a domain wall will be to replace  $m_0$  in  $\zeta$  and  $\sigma$  by  $m_{\text{eff}}$ . In this way the surface tension of a single domain wall vanishes at  $T = T_c$ , enabling the creation of domain walls at no extra energetic cost.

There are two ways of seeing this from the functional representation of  $Z$ . One of the methods is outlined below, the other in Appendix A.

Since  $\phi(\tau, \underline{x})$  is periodic in  $\tau$  it permits the Taylor expansion:

$$\phi(\tau, \underline{x}) = \sum_{\mathbf{n}} \phi_{\mathbf{n}}(\underline{x}) e^{\frac{i2\pi\mathbf{n}\tau}{\beta}}, \quad \phi_{\mathbf{n}}^* = \phi_{-\mathbf{n}} \quad (5.13)$$

in terms of a denumerable set of three-dimensional fields. The action  $I_{\beta}$  of (5.3) then takes the form

$$I_{\beta}[\phi] = \beta \bar{I}_{\beta}[\{\phi_{\mathbf{n}}\}] \quad (5.14)$$

where  $\bar{I}_{\beta}$  can be decomposed into the contributions from  $\phi_0$  and  $\phi_{\mathbf{n}} (\mathbf{n} \neq 0)$  [termed as  $\phi'$ ] as

$$\bar{I}_{\beta}[\phi_0, \phi'] = H_0[\phi_0] + H_0[\phi'] + H_I[\phi_0, \phi'] \quad (5.15)$$

$$H_0[\phi_0] = \int d^3x \left[ \frac{1}{2} (\nabla\phi_0)^2 - \frac{1}{2} m_0^2 \phi_0^2 + \frac{\lambda}{4!} \phi_0^4 \right] \quad (5.16)$$

$$H_0[\phi'] = \sum_{\mathbf{n} \neq 0} H_0[\phi_{\mathbf{n}}] = \sum_{\mathbf{n} \neq 0} \int d^3x \frac{1}{2} [(\nabla\phi_{\mathbf{n}}^*)(\nabla\phi_{\mathbf{n}}) + \left(\frac{2\pi\mathbf{n}}{\beta}\right)^2 \phi_{\mathbf{n}}^* \phi_{\mathbf{n}}] \quad (5.17)$$

$$H_I[\phi_0, \phi'] = \frac{1}{2} \int d^3x \sum_{\mathbf{n} \neq 0} m_0^2 \phi_{\mathbf{n}}^* \phi_{\mathbf{n}} + \frac{\lambda}{4!} \sum_{\mathbf{p}+\mathbf{q}+\mathbf{r}+\mathbf{s}=0} \int d^3x \phi_{\mathbf{p}} \phi_{\mathbf{q}} \phi_{\mathbf{r}} \phi_{\mathbf{s}}$$

(excluding  $\phi_0^4$ )

$$= -\sum_{n \neq 0} \int d^3x \left( \frac{1}{2} m_0^2 \phi_n^* \phi_n - \frac{\lambda}{4} \phi_0^2 \phi_n^* \phi_n \right) + \text{terms containing } n \neq 2 \phi' \quad (5.18)$$

(to  $O(\lambda)$  these extra terms will not contribute to  $Z$ ) From (5.17) we see that the masses of the  $\phi_n$  ( $n \neq 0$ ) modes are large at high temperatures. We refer to  $\phi_0$  and  $\phi'$  as light and heavy modes respectively.  $Z$  now becomes:

$$Z \propto \int D\phi e^{-I_\beta} = \int D\phi_0 D\phi' e^{-\beta \bar{I}[\phi_0, \phi']} \quad (5.19)$$

$$= \int D\phi_0 e^{-\beta (H[\phi_0] + v[\phi_0])} \quad (5.20)$$

on integrating out the heavy modes, where

$$e^{-\beta v[\phi_0]} \propto \int D\phi' e^{-\beta H_0[\phi'] - \beta H_I[\phi_0, \phi']} \quad (5.21)$$

The 'effective' potential  $v[\phi_0]$  for the three-dimensional field  $\phi_0$  contains temperature dependent parameters. Most importantly, at high temperatures and to first order in  $\lambda$ ,  $v[\phi_0]$  is the spatial integral of a local density. This can be seen by expanding (5.21) to first order in  $\lambda$ :

$$e^{-\beta v[\phi_0]} \propto \int D\phi' e^{-\beta H_0[\phi']} (1 - \beta H_I[\phi_0, \phi'])$$

$$\approx 1 - \frac{\beta \lambda}{4} \int d^3x \phi_0^2 \sum_{n \neq 0} \int D\phi_n D\phi_n^* e^{-\beta H_0[\phi_n]} \phi_n^*(x) \phi_n(x) + \dots \quad (5.22)$$



$$= 1 - \beta \int d^3x \phi_0^2(x) \frac{\Delta m^2}{2} + \dots \quad (5.23)$$

where we have dropped terms down by at least a factor of  $(\lambda T/m)$  or  $\lambda$  and those independent of  $\phi_0$ . After performing the zero temperature renormalisation of the mass, we have [5.2]:

$$\Delta m^2 = \frac{\lambda}{2\beta} \sum_{n \neq 0} \int \frac{d^3p}{(2\pi)^3} \frac{1}{p^2 + (2\pi n/\beta)^2} \quad (5.24)$$

$$\approx (\lambda T^2/24) = m_0^2 (T^2/T_c^2) \quad (5.25)$$

Exponentiating (5.23) gives

$$v[\phi_0] = \int d^3x \frac{1}{2} \Delta m^2 \phi_0^2(x) + O((\lambda T/m), \lambda) \quad (5.26)$$

Diagrammatically the light-mode mass increment  $\Delta m^2$  has the representation shown in figure 5.1, where the solid line denotes  $\phi_0$ , the light mode, and the dashed line  $\phi'$ , the heavy modes.

Inserting the first term of  $v[\phi_0]$  in (5.26) gives  $Z$  as

$$Z \propto \int D\phi_0 e^{-\beta \bar{I}[\phi_0]} \quad (5.27)$$

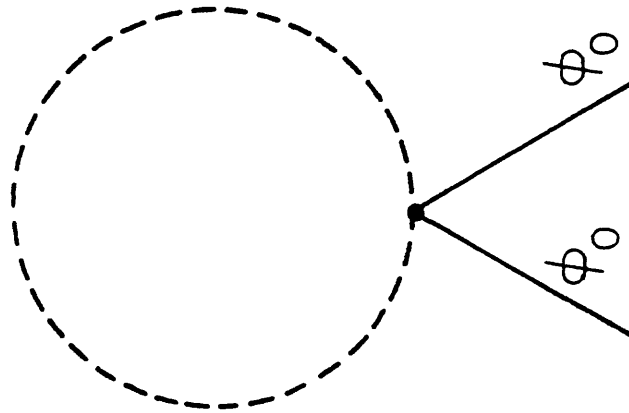


Figure 5.1 Diagrammatic representation of the lowest order mass correction. (Here dashed lines denote the heavy modes and the solid lines the light modes).

the vacuum functional for the three-dimensional field with 'action'

$$\bar{I}[\phi_0] = \int d^3x \left[ \frac{1}{2} (\nabla\phi_0)^2 - \frac{1}{2} m_0^2 \left( 1 - \frac{T^2}{T_c^2} \right) \phi_0^2 + \frac{\lambda}{4!} \phi_0^4 \right] \quad (5.28)$$

Equivalently in terms of the one-loop effective potential  $V(\phi)$  of (5.8)

$$\bar{I}[\phi_0] = \int d^3x \left[ \frac{1}{2} (\nabla\phi_0)^2 + V(\phi_0) \right] \quad (5.29)$$

Thus, as well as its definition for constant  $\phi$ ,  $V(\phi)$  plays the role of an 'effective' potential for the non-constant three-dimensional light mode  $\phi_0(x)$ . From this viewpoint, it is the vanishing of the scalar mass in the effective three-dimensional theory that triggers the long range correlations characterising a phase transition.

Now let us consider the nature of the phase transition. The dominant contribution to the partition function (5.27), will come from solutions to the semi-classical equation

$$\frac{\delta \bar{I}}{\delta \phi_0} = 0. \quad (5.30)$$

As well as the constant solution  $\bar{\phi}^2 = (6m_0^2/\lambda)[1-(T^2/T_c^2)]$ , there are domain wall solutions of the form (5.12), in

which  $m_0$  has been replaced by the effective scalar mass  $m(T)$ , where  $m^2(T) = m_0^2[1-(T^2/T_c^2)]$ . Away from the critical temperature the solution  $\phi = \text{constant}$ , being the minimum energy solution, makes the dominant contribution to the partition function and the mean field approach is a good approximation. As we approach the critical temperature however, the energy required to produce a section of domain wall becomes smaller and smaller. Eventually because of the large number of different configurations of domain walls of a given size it may be possible for their entropy to counterbalance the Boltzmann coefficient and they may come to dominate the partition function. They may then drive the system into undergoing a phase transition at a temperature slightly less than  $T_c$ .

We shall not bother to evaluate the effect of domain walls on the phase transition in any more detail. The reason for this is that theories that produce domain walls at a phase transition in the early universe can be ruled out as inconsistent with present day observations [5.11]. For example, they would produce large anisotropies in the microwave background. Instead we will perform our analysis for a more complicated, but cosmologically more interesting theory, that which would lead to the formation of cosmic strings.

SECTION 2. The Partition Function for a U(1) Scalar  
Gauge Theory

The simplest theory to possess vortex solutions is scalar QED, with Lagrange density:

$$L = -\frac{1}{4} F^{\mu\nu} F_{\mu\nu} + \frac{1}{2} \left| (\partial_\mu + ieA_\mu) \phi \right|^2 + \frac{1}{2} m_0^2 |\phi|^2 - \frac{\lambda}{4!} |\phi|^4 \quad (5.31)$$

where  $\phi$  is a complex scalar field. The partition function for this theory takes the form:

$$Z \propto \int D\phi D\phi^* DA (\det M) \exp(-I_\beta[\phi, A]) \quad (5.32)$$

where  $\det M$  describes the gauge fixing, and

$$I_\beta[\phi, A] = -\int_0^\beta d\tau \int d^3x L_E[\phi, A] \quad (5.33)$$

with  $L_E$  the Euclidean form of the Lagrangian (5.31)

As in section 1, the thermodynamic free energy for  $\langle \phi \rangle = \bar{\phi}$ ,  $V(\phi)$  is obtained by fixing the spatial average of  $\phi(\underline{x})$  to  $\bar{\phi}$  in (5.32).  $V(\phi)$  is necessarily a gauge-variant quantity, since it is the generator of zero momentum 1PI Green functions. However physical conclusions drawn from it should be gauge invariant. It is most convenient to calculate  $V(\phi)$  in the covariant gauge, for which, at high temperatures and to  $O(\lambda, e^2)$  [5.2],

$$V(\phi) = -\frac{1}{2} m_0^2 |\phi|^2 (1 - (T^2/T_c^2)) + \frac{\lambda}{4!} |\phi|^4 \quad (5.34)$$

$T_c^2$ , now takes the form  $T_c^2 = m_0^2 / ((\lambda/18) + (e^2/4))$ . To evaluate the partition function we shall adopt the same procedure as in section 1. An alternative approach is outlined in Appendix A. We first decompose the scalar  $\phi$  and vector  $A_\mu$  fields into light  $(\phi_0, A_{0\mu})$  and heavy  $(\phi', A'_\mu)$  modes. As before we can write  $Z$  as:

$$Z \propto \int D\phi_0 DA_0 \exp(-\beta \bar{I}[\phi_0, A_0]) \quad (5.35)$$

where

$$\exp(-\beta \bar{I}[\phi_0, A_0]) = \int D\phi' DA' (\det M) \exp(-I_\beta[\phi, A]) \quad (5.36)$$

Obtaining the mass corrections by keeping terms quadratic in  $\phi_0$  and  $A_{0\mu}$  is less simple than for the pure scalar case of the previous section. As in section 1, the heavy modes give rise to a temperature-dependent mass term,  $(\Delta m^2/2)|\phi|^2$ , for the scalar field. The contributions to  $(\Delta m^2/2)$  are shown diagrammatically in figure 5.2. The effect of this term is to replace  $m_0^2$  in the Euclidean time-independent effective action obtained from (5.31) by  $m_0^2 (1 - (T^2/T_c^2))$ , just as in (5.28).

There is a novelty here however, in that the heavy scalar modes also induce a vector mass  $(\Delta m^2/2)A_\mu A^\mu$  in the tadpole approximation (figure 5.3). This induced mass is of order  $e^2 T^2$ . Unfortunately, the tadpole diagram does not

Figure 5.2 Feynman graphs for the tadpole corrections to the scalar mass. (Here again dashed lines denote heavy modes, solid lines the light mode and wavy lines refer to the gauge field modes.)

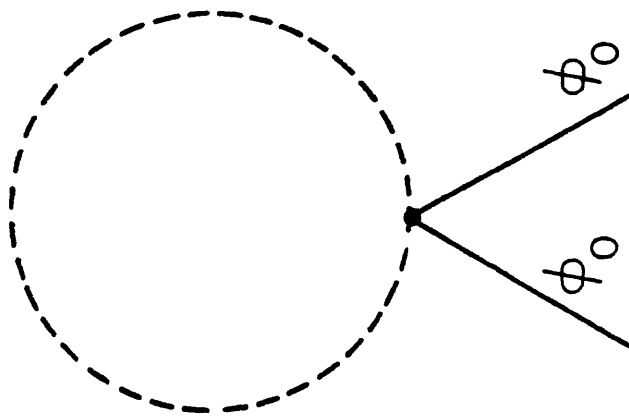
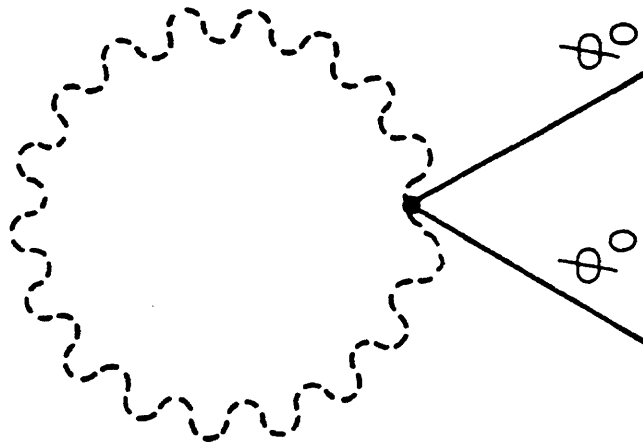
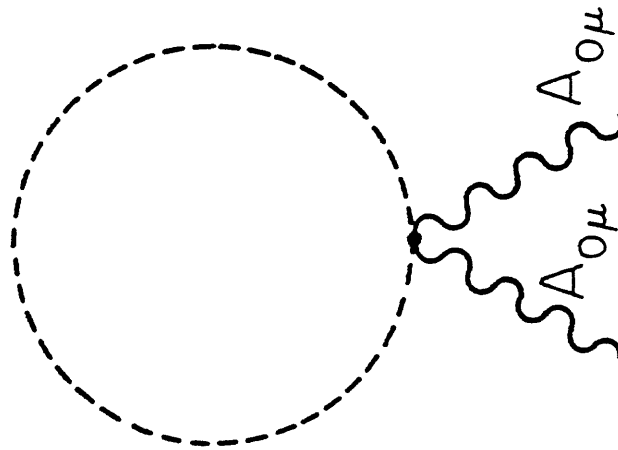


Figure 5.3 Feynman graph for the tadpole correction to the gauge field mass.

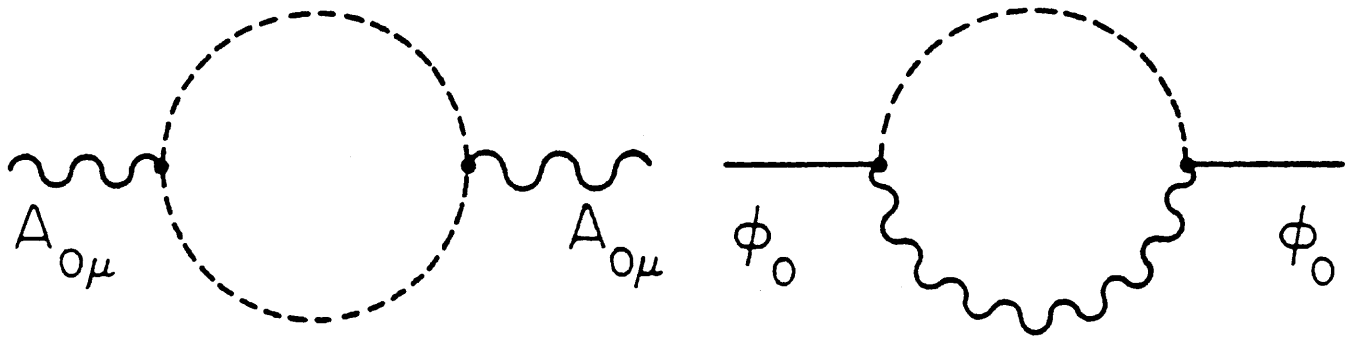




describe the total effects of the temperature-dependent self mass to our order of approximation. Non-local contributions like the photon self-energy have to be included as they also give terms  $O(e^2 T^2)$  for large  $T$ . The remaining one-loop diagrams which contribute to  $O(e^2 T^2)$  are shown in figure 5.4. Further problems arise because the heat bath gives a preferential inertial frame which leads to temporal and spatial components of  $A_\mu$  being decoupled, giving rise to two independent self-mass terms  $\Pi_L(k)$ ,  $\Pi_T(k)$  for momentum  $k$  [5.13]. The same preferential reference frame makes the  $\Pi$ 's non-analytic in  $k_0$ . The result is that depending on how one takes the zero momentum limit in the inverse fourier transforms different masses are obtained [5.13]. Only the tadpole term, with no momentum dependence is immune from this uncertainty. Yet another complication arises because (unlike the mean field calculations) the background fields are not constant. This means that the self-energy diagrams of figure 5.4 have to be evaluated with non-zero external momenta. These difficulties make it hard to explicitly evaluate the gauge mass, even to  $O(e^2 T^2)$ .

There is no easy way to resolve these problems. The simplest approach is to restrict ourselves to the regime,  $\lambda \gg e^2$ , in which the gauge field contributions cannot be large. (The qualitative details of our later discussions are not changed by introducing a gauge mass anyway.) Terms of order  $e^2 T^2$  are then constrained by  $e^2 \eta^2$  ( $e^2 m_0^2 / \lambda$ ) and the vector mass is approximately unchanged. At the same time the vector loop gives a small contribution to the

Figure 5.4 The remaining graphs of  $O(e^2)$ .



effective scalar mass. The effect is to replace  $\bar{I}$  of (5.36) by

$$\bar{I} = -\int d^3x L(\phi_0(\mathbf{x}), A_{0\mu}(\mathbf{x})) \quad (5.37)$$

where  $L$  is derived from (5.31) by :

- (i) going Euclidean
- (ii) removing Euclidean time dependence
- (iii) deleting the massive modes
- (iv) replacing  $m_0^2$  by  $m_0^2(1-(T^2/T_c^2))$
- (v) implementing gauge fixing.

Thus we finally obtain:

$$Z = \int D\phi_0 DA_{0\mu} \exp(-\beta \bar{I}[\phi_0, A_{0\mu}]) \quad (5.38)$$

where in the covariant gauge

$$\begin{aligned} \bar{I}[\phi_0, A_{0\mu}] = \int d^3x [ & \frac{1}{4} F_{0ij} F_0^{ij} - \frac{1}{2} (\partial_i \phi_0)(\partial^i \phi_0^*) \\ & - \frac{ie}{2} A_{0i} [\phi_0 \partial^i \phi_0^* - \phi_0^* \partial^i \phi_0] - \frac{1}{2} m_0^2 (1 - \frac{T^2}{T_c^2}) |\phi_0|^2 \\ & - \frac{1}{2} e^2 |\phi_0|^2 A_{0i} A_0^i + \frac{\lambda}{4!} |\phi_0|^4 + \frac{1}{\xi} (\partial_i A_0^i)^2 ] \quad (5.39) \end{aligned}$$

and the term  $\frac{1}{\xi} (\partial_i A_0^i)$  describes our gauge fixing.

**Section 3. The Statistical Properties of Strings**  
**around the phase transition.**

The time has now come to evaluate the partition function (5.38) in further detail. To do this we apply the saddle point method; the dominant contributions to the integral will come from the field configurations that satisfy the stationary equations:

$$\left. \frac{\delta I}{\delta \phi} \right|_{\phi = \phi_{\text{saddle}}, A^\mu = A^\mu_{\text{saddle}}} = 0$$

$$\left. \frac{\delta I}{\delta A_\mu} \right|_{\phi = \phi_{\text{saddle}}, A^\mu = A^\mu_{\text{saddle}}} = 0$$

that is, from the field configurations that satisfy the equations of motion:

$$\partial^i F_{ji} = \frac{1}{2} ie(\phi^* \partial_j \phi - \phi \partial_j \phi^*) - e^2 A_j |\phi|^2 \quad (5.40)$$

$$|\partial_i + ieA_i|^2 \phi = -m_0^2 \left(1 - \frac{T^2}{T_c^2}\right) \phi + \frac{\lambda}{3!} |\phi|^2 \phi \quad (5.41)$$

The contribution of any solution of these equations to the partition function can be found by substitution into (5.38). The solution  $\phi = \text{const}$ ,  $A = 0$  is the minimum energy solution and therefore gives the maximum contribution. Away from the critical temperature the partition function will be well approximated by this term alone. However, as we approach  $T_c$  this will no longer be the case.

We will now have to find all the maxima of the functional and sum their contributions. This becomes necessary because, although the secondary maxima will be individually weighted heavily against the constant field configuration, their sum, because of the large number of different non-constant configurations, will be larger.

In principle in evaluating the partition function (5.38) we should consider the contributions of all the different types of solutions to equations (5.40, 5.41). We will not do this, but instead will only consider the string like solutions. We do this because here we wish to consider the effect of the topologically stable defects on the phase transition.<sup>†</sup> Equations (5.41, 5.42) contain string-like solutions at temperatures  $T < T_c$ . The simplest string solution is an infinitely straight static string running for example, along the z-axis. This can be expressed as [5.14]:

$$\phi = |\phi(r)| e^{i\theta} \quad (5.42)$$

$$\underline{A} = \frac{r \underline{\Lambda} \underline{k}}{r} |\underline{A}(r)| \quad (5.43)$$

where  $\underline{k}$  is a unit vector in the z-direction. By imposing

-----  
<sup>†</sup>(The distribution of non-topologically stable field configurations we believe is not cosmologically interesting. They would have rapidly disappeared as the universe expanded and cooled. Only the trapped singularities would remain for a cosmologically interesting period.)

the gauge conditions ( $A_{0,0}(x)=0$ ,  $\nabla \cdot \underline{A}_0(x)=0$ ), and substituting (5.42, 5.43) into (5.40, 5.41) we obtain:

$$-\frac{1}{r} \frac{d}{dr} \left( r \frac{d}{dr} |\phi_0| \right) + \left[ \left( \frac{1}{r} - e|A_0| \right)^2 - m_0^2 \left( 1 - \frac{T^2}{T_c^2} \right) + \frac{\lambda}{3!} |\phi_0|^2 \right] |\phi_0| = 0 \quad (5.44)$$

$$-\frac{d}{dr} \left( \frac{1}{r} \frac{d}{dr} (r |A_0|) \right) - e \frac{1}{r} |\phi_0|^2 + |A_0| e^2 |\phi_0|^2 = 0 \quad (5.45)$$

Before continuing with the evaluation of the partition function we will first discuss the form of the thermal string solutions and how they vary with temperature. The solutions to (5.44, 5.45) are shown schematically in figure 5.5.

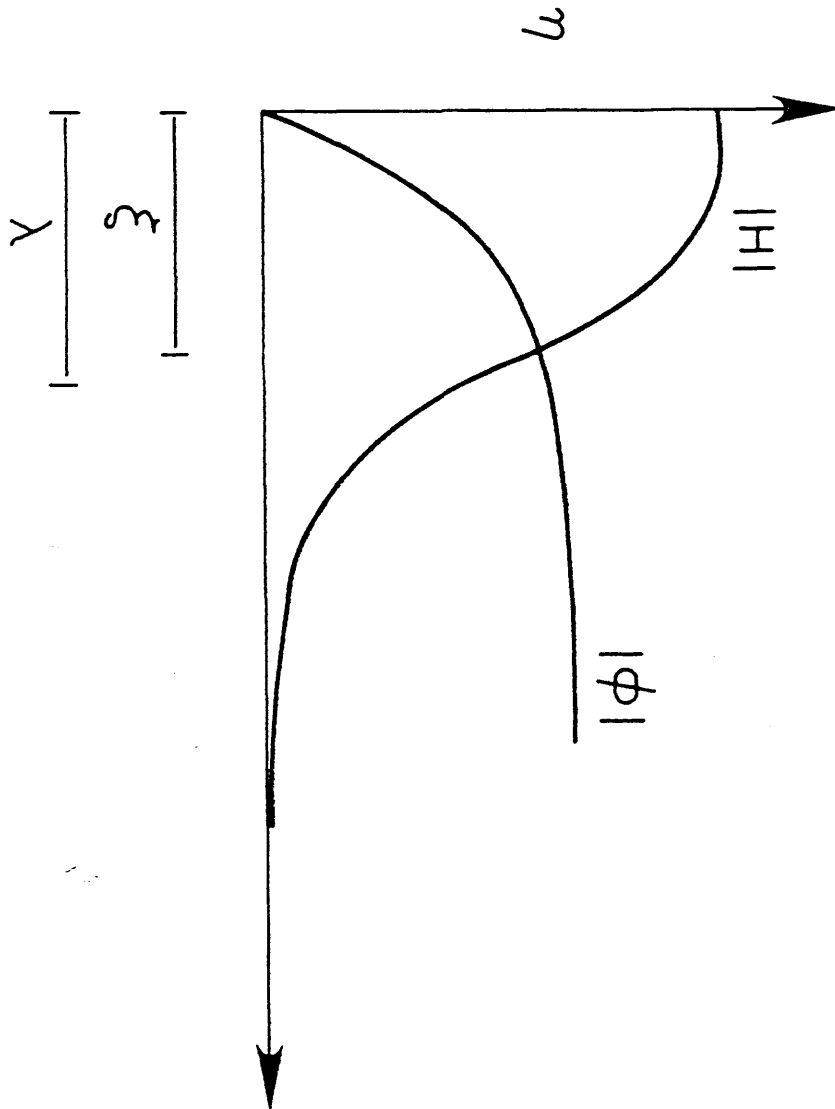
At large distances from the string

$$\lim_{r \rightarrow \infty} \phi(r) \rightarrow \eta$$

where  $\eta^2 = (3!m_S^2/\lambda)$  and  $m_S^2(T) = m_0^2(1-(T^2/T_c^2))$ . At the core  $|\phi|$  vanishes. The thickness of the core is determined by  $m_S^{-1}$ , the Compton wavelength of the Higgs particle. The magnetic field is restricted to the core, the skin depth being determined by  $m_V^{-1}$ , the inverse of the vector mass  $m_V$ ,

Figure 5.5 An example of the field configurations for a vortex solution at a temperature  $T$ .

$$\xi = O(m_S^{-1}) \quad \lambda = O(m_V^{-1}).$$



$$m_v = e\eta = \frac{e}{\sqrt{(\lambda)}} m_s.$$

The energy per unit length of the vortex has two separate components, one due to the scalar field,

$$\sigma_s = O(\eta^2(T))$$

and the other due to the vector field,

$$\sigma_v = O\left(\frac{e^2\eta^4}{m_v^2}\right) = O(\eta^2(T)) \quad (5.46)$$

Note that if we had found an additional  $\underline{A}_0$  mass term of the form  $\Delta\mu^2 = \alpha e^2 T^2$ , its effect would have been to replace  $\sigma_v$  of (5.46) with

$$\sigma_v = O\left(\frac{\eta^4(T)}{\eta^2(T) + \alpha T^2}\right) \quad (5.47)$$

Increasing the temperature causes  $\sigma_s$  and  $\sigma_v$  to decrease to zero reducing the energy per unit length of the string (this would be true even if we had found the  $\Delta\mu^2$  correction). The width of the strings also increases.

We now return to evaluating the contribution of the strings to the partition function (5.38). We can write the partition function as

$$Z \approx \int \exp(-\beta I_{st}[\phi_s, A_s]) \quad (5.48)$$



where we have restricted the sum to field configurations satisfying (5.40, 5.41) that are nodal lines. Equation (5.44, 5.45) gives the field configurations for an infinite string; string solutions that are not straight, but curved so smoothly that any segment of length of order the width will appear to be straight, are, to a very good approximation, also solutions of the equations (5.40, 5.41), whose energy per unit length is approximately the same as the infinitely straight string. Next we note that since, in this chapter, we are interested in the effect of the topologically stable strings on the phase transition, the strings (in the absence of monopoles) must be either in loops or 'infinite' in length. To proceed further in evaluating the partition function it will be necessary to neglect the interaction energy of the strings when they are more than a distance  $l$  ( $l$  = width of string) apart, and include it inside that distance as an infinite repulsive/attractive force<sup>+</sup>. We do this by restricting our strings to be non-self-intersecting. Placing the strings in the volume  $V$  on a cubic lattice (for convenience only) of spacing  $l$ , we can write:

$$Z = \sum_n W(n) \exp(-\beta \sigma l n) \quad (5.49)$$

-----  
(<sup>+</sup>This is effectively what occurs in the numerical simulations. When two strings come within a distance  $l$  of each other, they intercommute. We are really replacing an exponential force by a step function force which acts over a distance  $l$ .)

where  $W(n)$  denotes the number of different configurations of a string of length  $nl$  with the above properties and  $\sigma = \sigma_v + \sigma_s$  the total energy per unit length.

Let us first consider the contribution of loops. At high string segment density, non-self-intersecting random walks will be approximately Brownian walks [5.18]. The case of non-self-intersecting walks at very low densities has been studied by polymer physicists (see [5.19] for example). If  $P(t)$  denotes the fraction of walks of length  $nl$  which start and end at the same point, it follows from these studies that (for large  $n$ ):

$$P(n) = Cn^{-q} \quad q = \frac{3}{2} \text{ at high density}$$

$$= \frac{7}{4} \text{ at low density}$$

where  $C$  is a normalisation factor. This results in the number of distinct configurations of a single loop of size  $nl$  being:

$$W_1(n) = \frac{1}{2} C n^{-q-1} a^n \quad (a = 5 \text{ on a cubic lattice})$$

(5.50)

The extra divisor of  $2n$  in (5.50) arises from the fact that an  $n$ -step loop is both non-orientable and has  $n$  possible starting points. The contribution of single loops to the partition function  $Z$  is, from (5.49) and (5.50)

$$Z_1 = \frac{1}{2} \frac{CV}{l^3} \sum_{n=1}^{\infty} n^{-q-1} \exp(-\beta n l \sigma_{\text{eff}}) \quad (5.51)$$

where

$$\begin{aligned} \sigma_{\text{eff}} &= \sigma - \frac{\ln(a)}{\beta l} \\ &= \sigma - \frac{T}{l} \ln(a) \\ &= \sigma \left(1 - \frac{T}{T_{\text{st}}}\right) \end{aligned} \quad (5.52)$$

and

$$T_{\text{st}} = \frac{\sigma l}{\ln(a)} \quad (5.53)$$

The  $n$  steps need not constitute a single loop but two or more loops. Because of the lack of interaction energy the partition function for a 'gas' of loops is:

$$\begin{aligned} Z_{\text{loop}} &= 1 + Z_1 + \frac{1}{2!} Z_1^2 + \frac{1}{3!} Z_1^3 + \dots \\ &= \exp(Z_1) \\ &= \exp\left[ \frac{1}{2} \frac{CV}{l^3} \sum_{n=1}^{\infty} n^{-q-1} e^{-\beta n l \sigma_{\text{eff}}} \right] \end{aligned} \quad (5.54)$$

From these weights we can calculate the average number of loops.

$$\begin{aligned} \bar{N}_{\text{loops}} &= \left[ \sum_{n=0}^{\infty} \frac{n(Z_1)^n}{n!} \right] / Z_{\text{loop}} \\ &= Z_1 \end{aligned} \tag{5.55}$$

Similarly the mean number of loops of size  $n_1$  is (for large  $n$ ):

$$R(n_1) = \frac{1}{2} \frac{CV}{l^3} n^{-q-1} \exp(-\beta n_1 \sigma_{\text{eff}}) \tag{5.56}$$

Note that this is in agreement with the numerical simulations of [5.7]. It also agrees, if we neglect string interactions completely, with the statistical properties of strings derived using the rather different approach of Mitchell and Turok [5.1]. At high temperatures, for which  $\sigma_{\text{eff}} \approx 0$ ,  $R$  appears to be a scale invariant distribution whilst at lower temperatures, loops of large length are exponentially suppressed.

Now let us consider the contribution of 'infinite' strings to the partition function<sup>+</sup>. Since for large  $n$

$$a^n - Cn^{-q-1} a^n \approx a^n \tag{5.57}$$

-----  
 (+By infinite we mean strings which are as large as the box in which our calculations are being performed.)

we can write the partition function as:

$$\begin{aligned}
 Z_{\infty} &= \lim_{n \rightarrow \infty} \sum_k \left[ \frac{V}{l^3} \right]^k \exp(-\beta n l \sigma_{\text{eff}}) \frac{1}{k!} \\
 &= \lim_{n \rightarrow \infty} \exp\left( \frac{V}{l^3} \exp(-\beta n l \sigma_{\text{eff}}) \right) \quad (5.58)
 \end{aligned}$$

We can see immediately that when  $\sigma_{\text{eff}} \gg 0$ , these strings make a negligible contribution. As  $\sigma_{\text{eff}}$  tends to zero however, the contribution of the infinite strings will become increasingly important.

We note that  $Z_{\infty}$  and  $Z_{\text{loop}}$  both diverge at temperatures greater than  $T_{\text{st}}$ . Above this temperature there are large fluctuations in the  $\phi$  field and it is no longer appropriate to describe the fields in terms of string-like configurations. Thus we can think of  $T_{\text{st}}$  as the temperature at which strings are formed. This temperature (neglecting the  $\ln(a)$ ) is:

$$T_{\text{st}} \approx \sigma(T) l(T) \approx \gamma \eta^2 m^{-1} \quad (5.60)$$

where  $\gamma \sim O(1)$  and  $m = \min(m_s, m_v)$  (in our case  $\lambda \gg e^2$ ,  $m = m_v$ ). Since the right hand side of (5.60) vanishes at  $T = T_c$ , it follows that:

$$T_{\text{st}} < T_c \quad (5.61)$$

as it must be. The difference between  $T_{st}$  and  $T_c$  is small. Explicitly,

$$1 - \frac{T_{st}^2}{T_c^2} = O(\lambda), \quad m=m_s \quad (5.62)$$

or

$$1 - \frac{T_{st}^2}{T_c^2} = O(e^2), \quad m=m_v \quad (5.63)$$

In each case we have ignored terms  $O((e^2/\lambda))$  in the coefficients on the right hand side, but even if  $e^2=\lambda$  the coefficients only change by a factor of order unity. As so many other coefficients are uncertain it serves no purpose to be more specific.

At  $T_{st}$  most of the string length is in infinite strings and equation (5.49) implies that the loops have a scale invariant distribution. This is in complete agreement with the numerical simulations of Vilenkin and Vachaspati [5.17].

We can calculate the width of the strings at formation (this will be of the same order as their mean separations). By substituting (5.62) and (5.63) into  $m_s$  we obtain

$$m_s(T_{st}) = O(\sqrt{\lambda}m_s(T=0)), \quad m=m_s,$$

$$m_s(T_{st}) = O(em_s(T=0)), \quad m=m_v,$$

and

$$m_v(T_{st}) = O(\sqrt{\lambda}m_v(T=0)), \quad m=m_s,$$

$$m_v(T_{st}) = O(em_s(T=0)), \quad m=m_v;$$

That is, the network of strings at the phase transition has the separation of the centres of the flux tubes scaled up by a factor  $O(1/e)$ , (recall  $e^2 \ll \lambda$ ), compared to the closest packing of cold strings. The factor  $O(1/e)$  can be obtained by other considerations [5.3], and this reinforces our belief in the validity of the chain of approximations given above.

At temperatures below  $T_{st}$  it is thermodynamically less favourable to have infinite strings and more favourable to have small loops.

From a cosmological point of view the most interesting question to address is 'what happens as the universe cools through  $T_{st}$ ?'. Our calculations were for flat space but they would seem to suggest that, when the universe was very hot, we would be unable to recognize any string configurations. As it cools through  $T_{st}$  strings

would be formed. Initially most of the string length would be in infinite strings, but as the universe cooled further strings would chop themselves up as fast as possible into the smallest loops they could. Eventually the strings would no longer be able to chop themselves up fast enough to remain in thermal equilibrium. We still expect most of the string length to be in small loops. This picture, if true, makes the string domination scenario of Kibble [5.15] and Bennett [5.16] seem unlikely. The simulations of Albrecht and Turok [5.18] and those of Bennett and Bouchett [5.19] seem to confirm our picture.

#### Section 4. Summary and Discussion

In this chapter we have attempted to develop an analytic description of a phase transition that results in the production of topologically stable defects. Although for most of the chapter we have restricted ourselves to a discussion of scalar QED (which possesses Nielsen-Olesen string like solutions) it is clear that using similar techniques the description could be extended to encompass other more complicated theories.

Previously the mean field approach has been used as a basis for models of symmetry restoring phase transitions. In these models the system is described by constant fields of optimal strength. For example for scalar QED this approach would approximate the partition function (5.38) to its absolute maxima only. At low temperatures this is a valid approximation, we have showed however that as the



temperature approaches  $T_{st}$  this is no longer the case. Ideally to improve on the approximation one would like to find all the maxima of the functional and sum their various contributions to  $Z$  but unfortunately in practice this is not really practical. In this chapter we have assumed (ad hoc!) that string like field configurations make the dominant contribution to the partition function and that contributions from other non-constant field configurations can be neglected. This assumption seems much more plausible however when it is realised that the independent vortex model of the  $\lambda$  transition in superfluid helium includes the same assumption with no further justification than our own and yet gives good quantitative agreement with experimental observations.

Our stringy model predicts that the phase transition is second order and occurs at a temperature  $T_{st}$  which is below that calculated using the mean field model. The model can be thought of as picturing the restoration of symmetry as being due to overlapping strings filling the whole of space.

It is clear that our model is still a fairly crude description of the phase transition and it is premature to rule out the possibility that in practice the phase transition may be first order. A laboratory system that undergoes an analogous phase transition to the restoration of a spontaneously broken  $U(1)$  gauge symmetry is the superconductor. The mean field approach predicts

that the phase transition from superconducting to normal state is second order. In practice it is probably weakly first order. The first order transition being induced by the large fluctuations present at temperatures close to  $T_c$ . I hope to address the problem of whether or not this is true for our system in a future publication.

Even neglecting the implications of topologically stable field configurations for understanding the nature of the phase transition it is still of interest to know when they formed and what their statistical properties are. This is because they can last an astrophysically interesting period of time and have interesting cosmological consequences. Strings for example, might have provided the initial density perturbations about which galaxies formed [5.3, 5.6]. Our model suggests that they were formed when the temperature was  $T_{st}$ . Above  $T_{st}$  one would be unable to recognise string like configurations. It is interesting to note that  $T_{st} = O(T_{Ginzburg})$ , the string formation temperature suggested by Kibble [5.3]

We have seen that Nielsen-Olesen strings develop a temperature dependent tension and width. The width of a string at the phase transition is scaled up by a factor  $O(1/e)$  that of a cold string. At the phase transition this width is also the typical string-string separation. This length scale is the same as that obtained using Kibble's picture of the formation of strings [5.3]. We therefore believe our analysis lends support to his estimates of

initial string densities etc.

From the partition function for the string solutions we have evaluated the equilibrium distribution of strings. We have discovered that as  $T_{st}$  is approached most of the string length goes into infinite strings and that there is a scale invariant distribution of loops, both with approximately Brownian trajectories. If we had neglected string-string interactions completely we would have predicted that the string trajectories were exactly Brownian. This agrees with the results obtained by the rather different approach of Mitchell and Turok [5.1]. A simulation of string formation in two dimensions has recently confirmed that the trajectories are only approximately Brownian [5.23]. At lower densities the difference between neglecting string interactions completely and incorporating them to some degree by modelling the string trajectories by non-self-intersecting random walks becomes more noticeable. It would be interesting to discover whether the simulations of Vilenkin and Smith [5.7] can detect this difference.

At first glance the above comments might seem paradoxical. Surely string interactions should be more important at high densities. In our simple model this is not true because at high densities the excluded volume to a non-self-intersecting walk becomes approximately homogeneous and so the probability for a walk to go in any direction becomes very nearly equal [5.18]. This result might of course be a consequence of our over simplified

model of string string interactions and we are presently investigating this [5.27].

The relevance of our high temperature results to the early universe are obvious. What might not be so clear is the relevance of our low temperature results. Shortly after the universe cooled through  $T_{st}$  the string network would no longer be in thermal equilibrium. Our results indicate that the system would like to evolve to a state with an exponentially suppressed distribution of large loop sizes. This makes the string domination scenarios of Kibble [5.15] and Bennett [5.16] seem unlikely but only detailed simulations of the string dynamics in an expanding universe could rule out their scenario altogether.

A model of monopoles connected by strings in which the monopole mass was of the same order of magnitude as the string tension would be well approximated by open strings [5.1]. If we allow the possibility of having open as well as closed strings we can also estimate the distribution of these. The result is an exponentially suppressed distribution of open strings, (i.e. the longest ones are suppressed). This agrees well with the numerical simulations of such models [5.20].

One might be worried about our use of the canonical ensemble in a description of a phase transition because there are large fluctuations in some of the thermodynamic quantities. As an example consider the mean energy density

due to loops of string. This is finite right up to the phase transition. The rms fluctuations in this quantity however diverges as  $(T-T_{st})^{-1/2}$ . The mean energy density in loops is therefore not a sensible quantity to discuss at temperatures close to  $T_{st}$ . Note however that not all interesting quantities have such large fluctuations about their mean values. For example, consider the rms fluctuations in the mean number of loops of size  $nl$  ( $R(nl)$ ). This is proportional to  $R(nl)^{1/2}$  which allows us to sensibly discuss  $R(nl)$  even at temperatures very close to  $T_{st}$ . The point to note is that if you wish to use the canonical ensemble in a description of a phase transition you should check that the mean quantities you wish to discuss do not have large fluctuations about their mean values.

We would like to make one comment about the imaginary time formalism. At high temperatures we were lead to investigate  $\tau$ -independent solutions for the fields. This was a good approximation because at high temperatures the width of the string  $\zeta \gg \beta$ , so to a good approximation the variation of the fields over the interval  $\beta$  can be taken to be zero. At lower temperatures neglecting the  $\tau$  dependence of the solutions is no longer justifiable. It is unclear what the interpretation of the  $\tau$ -dependent solutions would be in terms of the real time  $t$ , because we can not perform a Wick rotation to re-obtain the real-time theory.

The results obtained have applications outside cosmic strings and the early universe. Patel has used some of the formalism of section 3 in investigating confinement in QCD [5.21]. Similar methods have also been used to investigate the lambda transition in liquid  ${}^4\text{He}$  [5.22, 5.19] (for further references see [5.19]).

The calculations presented in this chapter were in flat space. The next step is to consider curved spacetime to see how this affects the distribution of strings. This work is currently in progress [5.24].

## Appendix A

Here we present an alternative derivation of the partition functions of sections 1 and 2. We start by deriving that of the scalar field theory of section 1.

As in section 1 we start from the path integral representation of the partition function:

$$Z = \int D\phi \exp[I_\beta(\phi)]$$

This time we split  $I_\beta$  into two parts,  $I_{\text{ren}}$  the finite temperature renormalized action and  $I_{\text{count}}$  the part containing the counterterms. To  $O(\lambda)$  for example:

$$I_{\text{ren}} = \int_0^\beta d\tau \int d^3x \left[ \frac{1}{2} (\partial_\mu \phi)(\partial^\mu \phi) + \frac{1}{2} m^2 (\mathbb{T}) \phi^2 - \frac{\lambda}{4!} \phi^4 \right] \quad (5.64)$$

$$I_{\text{count}} = \int_0^\beta d\tau \int d^3x \frac{\lambda}{2} A \phi^2$$

We now evaluate the partition function by expanding  $I$  about a field configuration  $\phi_0$  that satisfies the equation of motion derived from  $I_{\text{ren}}$ . We obtain:

$$I = I[\phi_0] + \frac{1}{2} \left\langle \frac{\delta^2 I_{\text{ren}}}{\delta \phi_1 \delta \phi_2} \eta_1 \eta_2 \right\rangle_{1,2} + \dots$$

$$+ \left\langle \frac{A\lambda}{2} \phi_0^2 \right\rangle_1 + A\lambda \eta_1 \phi_0 + \left\langle \frac{A\lambda}{2} \eta^2 \right\rangle_1$$

where

$$\eta = \phi - \phi_0, \quad \phi_1 = \phi(x_1)$$

and  $\langle \dots \rangle_{1, \dots, N}$  means integrate over  $d^3x_1 d\tau_1 \dots d^3x_N d\tau_N$ . This expansion is then substituted into the partition function. The resulting functional is evaluated by introducing a current  $j$  coupled to the field  $\eta$ . To  $O(\lambda)$  one obtains:

$$Z = \exp(I[\phi_0]) \exp\left(\left\langle \frac{\lambda}{4} \phi_0^2 D_{11} + \frac{A\lambda}{2} \phi_0^2 \right\rangle_1\right)$$

where

$$D_{12} = - \int \frac{d^3p}{(2\pi)^3} \frac{1}{\beta} \sum_n \frac{e^{i(x_1 - x_2)p}}{(2\pi/\beta)^2 + p^2}$$

is the finite temperature propagator. Now 'm' in (5.64) was chosen to be the finite temperature mass and so:

$$\frac{A\lambda}{2} = - \frac{\lambda}{2} D_{11}$$

Thus we obtain the contribution of one saddle point to the partition function as:

$$Z \propto \exp(I_{\text{ren}}[\phi_0])$$

This is the contribution of one saddle point. If we make a 'dilute gas' approximation we obtain:

$$Z = A \sum_{\phi_0} \exp(I_{\text{ren}}[\phi_0])$$

where A is a normalisation constant and the sum is over all field configurations satisfying the equation of motion derived from  $I_{\text{ren}}$ . At high temperatures it is a good approximation to neglect the  $\tau$  variation of our solutions. This is because the solutions have to be periodic in  $\beta$  and at high temperatures  $\beta$  will be much smaller than the spatial width of the solutions [5.25]. Thus we have re-obtained the results of section 2.



It is straight forward to apply this scheme to evaluating the partition function for scalar QED and re-obtain the results of section 2.

REFERENCES

REFERENCES

Chapter 1

(1.1) For a review on the standard model see for example M.Turner, 'Cosmology and Particle Physics', in Les Houches, Session XLIV, 1985 Architecture of Fundamental interactions at short distances, [Elsevier Science Publishers](1987)

A.Albrecht, 'Cosmology for High Energy Physicists', FERMILAB-conf-87/206-A

(1.2) For a review of nucleosynthesis see for example A.M.Boesgaard and G.Steigman, Ann. Rev. Astron. Astrophysics 23, 319(1979)

(1.3) For a review on inflation see for example S.Blau and A.Guth, 'Inflationary Cosmology' in 300 years of Gravitation, eds. S.Hawking and W.Israel, [Cambridge University Press](1987)

(1.4) For a review on cosmic strings see for example A.Vilenkin, Phys. Rep. 121, 263(1985)

(1.5) J.Pati and A.Salam, Phys. Rev. D8, 1240(1973)  
H.Georgi and S.Glashow, Phys. Rev. Lett. 32, 438(1974)

H.Georgi, H.Quinn and S.Weinberg, Phys. Rev. Lett. 33, 451(1974)

(1.6) P.Higgs, Phys. Rev. Lett. 12, 132(1964), Phys. Rev. Lett. 13, 508(1964)

P.Englert and R.Brout, Phys. Rev. Lett. 13, 321(1964)

T.W.B.Kibble, Phys. Rev. 155,1557(1967)

(1.7) see for example D.Olive, 'Lectures on Gauge Theories and Lie Algebras', Imperial College Preprint

(1.8) D.A.Kirhnitz, JETP Lett 15, 529(1972)

D.A.Kirhnitz and A.D.Linde, Phys. Lett. 42B, 471(1972)

S.Weinberg, Phys. Rev. D9, 3357(1974)

L.Dolan and R.Jackiw, Phys. Rev. D9, 3320(1974)

see also chapter 6.

(1.9) T.W.B.Kibble, J.Phys. A9, 1387(1976); Phys. Rep. 67, 183(1980)

(1.10) Y.Zel'dovich, I. Kobzarev and L.Okun, JETP 40, 1(1975)

(1.11) E.Witten, in '13th. Texas Symposium on Relativistic Astrophysics', Ed. M. Pulmer, [World Scientific](1987)

(1.12) A.Vilenkin, Phys.Rev.D23, 852(1981)

(1.13) N.Kaiser and A.Stebbins, Nature 310, 391(1984)

(1.14) A.Vilenkin, Phys. Rev. Lett 46, 1169(1981)

N.Turok, Phys. Lett 126B, 437(1983)

N.Turok and R.Brandenberger, Phys. Rev. D33, 2175(1986)

R.Brandenberger and P.Shellard, Brown preprint.

(1.15) L.Cowie and E.Hu, Ap. J. Lett. 318, 33(1987)

(1.16) E.Witten, Nucl. Phys. B249, 557(1985)

(1.17) E.M.Chudnovsky, G.Field, D.Spergal and A.Vilenkin, Phys. Rev. D34, 944(1986)

E.Copeland, M.Hindmarsh and N.Turok, Phys. Rev. Lett. 58, 1910(1987)

(1.18) T.Vachaspati, Bartol preprint, (1987)

- (1.19) G.Field and A.Vilenkin, Nature 326, 772(1986)
- (1.20) P.Goddard and D.Olive, Rep. Prog. Phys. 41,  
1357(1987)
- (1.21) R.Callen, Phys. Rev. D25, 2144(1982), D26,  
2058(1982)
- V.Rubakov, JETP Lett. 33, 644(1981), Nucl. Phys.  
B203, 311(1982)
- (1.22) E.N.Parker, Astrophys. J. 160, 383(1970)
- G.Lazarides, Q.Shafi and T.Walsh, Phys. Lett.  
100B, 21(1981)
- M.Longo, Phys. Rev. D25, 2399(1982)
- (1.23) For a review see E.Kolb and M.Turner, Astrophys.  
J. 286, 702(1984)
- (1.24) E.Weinberg, Phys. Lett. 126B, 441(1983)
- (1.25) G.Volvik and V.Mineev, JETP 45, 1186(1977)
- R.Davis, Phys. Rev. D35, 3705(1987)

## Chapter 2

- (2.1) D.Mitchell and N.Turok, Nucl. Phys. B294,  
1138(1987)
- (2.2) E.Weinberg, Phys. Lett. 126B, 441(1983)
- (2.3) K.Lee and E.Weinberg, Nucl. Phys. B246, 354(1984)
- (2.4) A.Everett, T.Vachaspati and A.Vilenkin, Phys. Rev.  
D31, (6) 1925(1985)
- (2.5) T.Vachaspati and A. Vilenkin, Phys. Rev. D30,  
2036(1984)
- (2.7) G.'t Hooft, Nucl. Phys. B79, 276(1984)
- A.Polyakov, JETP Lett 20, 194(1974)
- (2.7) P.Goddard, J.Nuyts and D.Olive, Nucl. Phys. B125,

1(1977)

(2.8) F.Bais, Phys. Lett. 98B, 437(1981)

(2.9) A.Vilenkin, Phys. Rep. 121, 263(1985)

(2.10) A.Vilenkin, Nucl. Phys. B196, 240(1982)

(2.11) F.A.Bais and P.Langacker, Nucl. Phys. B197,  
520(1982)

(2.12) A similar procedure was adopted in T.W.B.Kibble,  
Phys. Lett. 166B, 311(1986)

(2.13) E.Copeland, D.Haws and R.Rivers,  
Fermilab-pub-88/30-A, March 1988.

(2.14) J.P.Preskill, Phys. Rev. Lett. 43, 1365(1979)

(2.15) Y.Zel'dovich and M.Khlopov, Phys. Lett. 79B,  
239(1976)

### CHAPTER 3.

(3.1) E.Witten, Nucl. Phys. B249, 557 (1985).

(3.2) T.W.B. Kibble, J.Phys. A9,1387(1976).

A.Vilenkin, Phys. Rep. 121, 263(1985).

(3.3) J.Ostriker, C.Thompson and E. Witten, Phys. Lett.  
B180 231 (1986).

(3.4) E.M.Chudnovsky, G.Field, D.Spergel and A.Vilenkin,  
Phys. Rev D34, 944(1986).

(3.5) A.Vilenkin and G.Field, Nature 326, 772(1987).

(3.6) C.Hill, D.Schramm and T.Walker, Phys. Rev. D36,  
1007(1987).

(3.7) T.Vachaspati, Bartol Preprint (1987).

(3.8) E.Copeland, M.Hindmarsh and N.Turok, Phys. Rev.  
Lett. 58, 1910(1987).

- (3.9) D.Haws, M.Hindmarsh and N.Turok, Los Alamos preprint LA-UR-88-727 (to appear in Phys. Lett.)
- (3.10) A.Vilenkin and T.Vachaspati, Phys. Rev. Lett. 58, 1041(1987).
- (3.11) N.Turok, Nucl. Phys. B242, 520 (1984).
- (3.12) H.Nielsen and P.Olesen, Nucl. Phys. B61, 45(1978)  
D.Forster, Nucl. Phys. B81, 84(1974)
- (3.13) F.Lund and T.Regge, Phys. Rev. D14, 1524(1976)
- (3.14) C.Hill, H.Hodges and M.Turner, Phys. Rev. D37, 263(1988)  
A.Babul, T.Piran and D.Spergel, Princeton University preprint.
- (3.15) N.K.Nielsen and P.Olesen, Nucl. Phys. B291, 829(1987)
- (3.16) D.Garfinkle and T.Vachaspati, Phys. Rev. D36, 2229(1987).
- (3.17) I.S.Gradshiteyn and I.M.Ryzhik, Tables of Integrals, series and products., (Academic Press, New York, 1981)
- (3.18) J.D.Jackson, Classical Electrodynamics, (John Wiley & Son Inc., New York, 1965)
- (3.19) E.Copeland and D.Haws, Fermilab preprint (in preparation)
- (3.21) D.Spergal, private communication,
- (3.22) C.Hill, H.Hodges and M.Turner, Phys. Rev. Lett. 59, 2493(1987)
- (3.23) A.Albrecht and N.Turok, Phys. Rev. Lett. 54, 1868(1985)
- (3.24) A.Vilenkin and T.Vachaspati, Phys. Rev. D35, 1138(1987)

Chapter 4.

- (4.1) E.Witten, Nucl. Phys. B249, 557(1985).
- (4.2) T.W.B.Kibble, J. Phys. A9, 1387(1976).
- (4.3) E.Copeland, D.Haws, M.Hindmarsh and N.Turok,  
Imperial College preprint IC/TP/86-87/30 (to appear in  
Nucl.Phys. B).
- (4.4) A.Babul, T.Piran and D.Spergal, Princeton University  
Preprint (1987).
- (4.5) C.Hill, H.Hodges and M.Turner, Phys. Rev. D37,  
263(1988).
- (4.6) L.D.Landau and E.M.Lifshitz, 'Quantum Mechanics -  
Non Relativistic Theory', [Pergamon, Aberdeen] (1977).
- (4.7) S.Coleman, Phys. Rev. D15, 2929(1977).  
C.Callen and S.Coleman, Phys. Rev. D16, 1762(1977).
- (4.8) L.Jacobs and C.Rebbi, Phys. Rev. B19, 4486(1979).
- (4.9) J.Ostriker, C.Thompson and E.Witten, Phys. Lett.  
B180, 231(1986)
- (4.10) E.Copeland, M.Hindmarsh and N.Turok, Phys. Rev.  
Lett. 58, 1910(1987).

Chapter 5.

- (5.1) D.Mitchell and N.Turok, Nucl. Phys. B294,  
1138(1987)



- (5.2) S.Weinberg, Phys. Rev. D9, 3357(1974)  
L.Dolan and R.Jackiw, Phys. Rev. D9, 3320(1974)
- (5.3) T.W.B.Kibble, J.Phys. A9, 83(1976), Phys. Rep. 67,  
183(1980)
- (5.4) R.Funkuda, E.Kyriakopoulos, Nucl. Phys. B85,  
354(1987)
- (5.5) R.Rivers, Zeit Fur Phys. C22, 137(1984)
- (5.6) A.Vilenkin, Phys. Rep. 121, 263(1985)
- (5.7) G.A.Smith and A.Vilenkin, Tufts University preprint  
TUTP 87-3-a
- (5.8) A.Albrecht and N.Turok, Phys. Rev. D30, 2036(1984)
- (5.9) D.Bennett and F.Bouchett, Fermilab preprint,  
'Evidence for a scaling solution in cosmic string  
evolution', (1987)
- (5.10) D.J.Amit, 'Field Theory, the Renormalisation Group  
and Critical Phenomena', [McGraw-Hill, New York](1978)
- (5.11) Y.Zel'dovich, I.Kobzarev and L.Okun, JETP 40,  
1(1975)
- (5.12) C.Aragao de Carvalho, D.Bazeia, O.Eboli, G.Marques,  
A.da Silvia and I.Ventura, Phys. Rev. D31, 1411(1985)
- (5.13) K.Kajantie and J.Kapusta, Ann. Phys. 160,  
477(1985)
- (5.14) H.B.Nielsen and P.Olesen, Nucl. Phys. B61,  
45(1973)
- (5.15) T.Kibble, Nucl. Phys. B252, 227(1985)
- (5.16) D.Bennett, Phys. Rev. D33, 872(1986); D34,  
3592(1986)
- (5.17) T.Vachaspati and A.Vilenkin, Phys. Rev. D30,  
2036(1984)
- (5.18) J.Scherrer and J.Frieman, Phys. Rev. D33,

3556(1986)

(5.19) F.W.Wiegel, 'Introduction to Path-Integral methods in Physics and Polymer Science', [World Scientific](1986)

(5.20) E.Copeland, D.Haws, T.W.B.Kibble, D.Mitchell and N.Turok, Nucl. Phys. B298, 445(1988)

(5.21) A.Patel, Nucl. Phys. B243, 411(1984)

(5.22) M.Cohen and R.Feynman, Phys. Rev. 107, 13(1957)

(5.23) The fact that the trajectories are only approximately brownian and not exactly has been confirmed in two dimensions by D.Haws, C.McNeil and P.Salmon (private communication)

(5.24) E.Copeland, D.Haws, R.Rivers work in progress

(5.25) We thank Neil Turok for pointing this out to us

(5.26) E.Witten, Nucl. Phys. B249, 557(1985)

(5.27) D.Haws, S.Holbaard and R.Rivers, work in progress